INFORMATION TO USERS

The most advanced technology has been used to photograph and reproduce this manuscript from the microfilm master. UMI films the original text directly from the copy submitted. Thus, some dissertation copies are in typewriter face, while others may be from a computer printer.

In the unlikely event that the author did not send UMI a complete manuscript and there are missing pages, these will be noted. Also, if unauthorized copyrighted material had to be removed, a note will indicate the deletion.

Oversize materials (e.g., maps, drawings, charts) are reproduced by sectioning the original, beginning at the upper left-hand corner and continuing from left to right in equal sections with small overlaps. Each oversize page is available as one exposure on a standard 35 mm slide or as a 17″ × 23″ black and white photographic print for an additional charge.

Photographs included in the original manuscript have been reproduced xerographically in this copy. 35 mm slides or 6″ × 9″ black and white photographic prints are available for any photographs or illustrations appearing in this copy for an additional charge. Contact UMI directly to order.

Accessing the World's Information since 1938

300 North Zeeb Road, Ann Arbor, MI 48106-1346 USA

Order Number 8816447

Transport of carbon dioxide in perfluorosulfonate membranes enhanced by relative humidity and ethylenediamine content

Dunkley-Timmerman, Terry, Ph.D.

The University of Texas at Austin, 1988

U·M·I
300 N. Zeeb Rd.
Ann Arbor, MI 48106

TRANSPORT OF CARBON DIOXIDE IN PERFLUOROSULFONATE MEMBRANES ENHANCED BY RELATIVE HUMIDITY AND ETHYLENEDIAMINE CONTENT

by

TERRY DUNKLEY-TIMMERMAN, B.S. ChE

DISSERTATION

Presented to the Faculty of the Graduate School of

The University of Texas at Austin

in Partial Fulfillment

of the Requirements

for the Degree of

DOCTOR OF PHILOSOPHY

THE UNIVERSITY OF TEXAS AT AUSTIN

MAY, 1988

TRANSPORT OF CARBON DIOXIDE IN PERFLUOROSULFONATE MEMBRANES ENHANCED BY RELATIVE HUMIDITY AND ETHYLENEDIAMINE CONTENT

APPROVED BY

SUPERVISORY COMMITTEE:

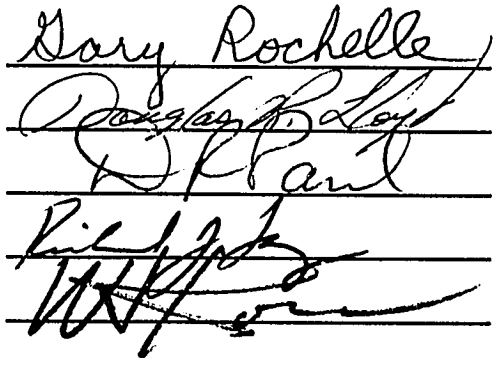

To Scott

Acknowledgements

I would like to express my sincere appreciation to all of my committee members for their helpful suggestions and advice. I especially would like to thank Dr. W. Koros, whose positive attitude helped me get through the difficult times, as well as the good.

A special thanks is offered to the primary sponsor of this research, the Separations Research Program at The University of Texas at Austin.

Most of all, I would like to thank my husband, Scott Timmerman, whose unending love and attention made my life and work so much easier. His continuous interest and helpful suggestions were invaluable to this research effort. Thanks also to my father for his guidance.

Terry Dunkley-Timmerman

The University of Texas at Austin

May, 1988

TABLE OF CONTENTS

Acknowledgements v

Table of Contents vi

List of Tables ix

List of Figures x

Chapter 1. Introduction 1

Chapter 2. Background 12

2.1. Facilitated Membranes 12

2.2. Literature Review 14

Chapter 3. Experimental Apparatus and Procedure 17

3.1. Preparation of Nafion 117 with H^+ (Nafion 117, H^+) 17

3.2. Preparation of Nafion 117 with Ethylenediamine (EDA) 18

3.2.1. Loading in High Concentrations of EDA 19

3.2.2. Leaching To Determine EDA Content 19

3.3. The Equilibrium Loading of EDA in Nafion 117 20

3.3.1. Loading in Low Concentrations of EDA 20

3.3.2. Equilibrium Determination 23

3.4. Quantitative Analysis: pH Titration of Solutions 26

3.5. Restoring Nafion 117, EDA to H^+ Form 28

3.6. Water Content, Ion Exchange Site Content, and Swelling....28
3.7. Flux and Permeability of CO_2....35
3.7.1. Definition of Permeability....35
3.7.2. Flow System and Procedure....36
3.7.3. Permeation Cell Design....44
3.8. Diffusion Coefficient of CO_2....46
3.9. CO_2 Solubility....50
3.10. Equilibrium Constants of CO_2-$EDAH^+$ and CO_2-EDA-$EDAH^+$ Reactions....51

Chapter 4. Results and Discussion 54
4.1. Solution - Membrane Equilibrium: EDA and Water Content . 54
4.2. Effect of Relative Humidity on Water Content 58
4.3. Effect of Relative Humidity on Swelling....61
4.4. Transport Measurements in the H+ Form of Nafion....62
4.4.1. Effect of CO_2 Concentration in Feed Gas....62
4.4.2. Effect of Relative Humidity....68
4.5. Transport Measurements in the EDA Form of Nafion....72
4.5.1. Effect of CO_2 Concentration in Feed Gas....72
4.5.2. Effect of Relative Humidity....85
4.6. Reaction Chemistry....86
4.7. Modeling....91
4.7.1. Flux with $EDAH^+$....91
4.7.2. Flux with $EDAH^+$ and EDA....95

4.7.3. Predicting Effect of Sweep Side Concentrations.....99

Chapter 5. Conclusions and Recommendations.....104

5.1. Conclusions.....104

5.2. Recommendaions.....106

Appendix A. Experimental Data.....109

Appendix B. Acid Titrations.....136

Appendix C. Cell Design.....140

Appendix D. Sample Calculations.....143

Appendix E. Error Analysis and Equipment Calibration.....146

Glossary.....149

Bibliography.....152

List of Tables

		page
Table 1-1:	Major Industrial Processes That Need Gas Treating	2
Table 3-1:	Saturated Salt Solutions Used In Relative Humidity Cell	34
Table 4-1:	EDA Loading and Water Activity in Nafion 117 Equilibrated With Solution (25°C)	57
Table 4-2:	Permeability, Diffusion and Solubility Data for CO_2, O_2 and H_2 in Nafion, H^+ form and in water at 25°C	67
Table 4-3:	Normalized CO_2 Solubility in Nafion 117	76
Table 4-4:	Effect of $\pm$ 5% Experimental Error on The Prediction of CO_2 Flux From Equilibrium Theory. Membrane Loading=0.928 gmol EDA/ gmol site	96
Table 4-5:	Accuracy of Equilibrium Model: Prediction versus Actual Driving Force	103

List of Figures

Figure 1-1: Schematic of Nafion Structure in Acid Form. For Commercial Use, m=1, n=5 to 12 (Grot, 1972) 9

Figure 2-1: Schematic of CO_2 Facilitated Transport by Reversible Reaction With Carrier, R, To Form RCO_2 Complex 13

Figure 3-1: Relative Humidity Cell For Water Content Measurements. Operated at Room Temperature and Pressure 31

Figure 3-2: Experimental Apparatus For Permeation Measurements 37

Figure 3-3: Schematic of Permeation Cell 38

Figure 4-1: Equilibrium Loading of Nafion 117 with Ethylenediamine, Total Exchange Sites per membrane=0.0016 gmol, Equivalent Weight, H^+=1100 g/gmol exchange sites 55

Figure 4-2: Water Desorption Isotherm of Nafion 117, H^+ Form and With EDA, 25°C, 1 atm. 59

Figure 4-3: Swelling of Nafion 117, H^+ Form and With EDA, 25°C, 1 atm 60

Figure 4-4: Effect of CO_2 Concentration, Loading and Series on Flux in Nafion 117, H^+ Form and With EDA, 100% Relative Humidity, 25°C, 1 atm 63

Figure 4-5: Effect of Decreasing Relative Humidity on Permeability of Nafion 117, H^+, 25°C, 1 atm, 3-100% CO_2 64

Figure 4-6: Effect of Decreasing Relative Humidity on CO_2 Diffusion Coefficient in Nafion 117, H^+, 25°C, 1 atm, 3-100% CO_2 65

Figure 4-7: Effect of Decreasing Relative Humidity on CO_2 Solubility in Nafion 117, H^+, 25°C, 1 atm, 3-100% CO_2 66

Figure 4-8: Effect of CO_2 Concentration, Loading and Series on CO_2 Diffusion Coefficient with Nafion 117 With EDA, 100% Relative Humidity, 25°C, 1 atm 73

Figure 4-9: Effect of Decreasing Relative Humidity and Loading on Permeability of Nafion 117, H+ Form andWith EDA 25°C, 1 atm, 100% CO_2 74

Figure 4-10: Effect of Decreasing Relative Humidity and Loading on CO_2 Diffusion Coefficient with Nafion 117 With EDA, 25°C, 1 atm, 100% CO_2 75

Figure 4-11: Effect of CO_2 Concentration, Loading and Series on CO_2 Solubility in Nafion 117 With EDA, 25°C, 1 atm, 100% Relative Humidity 78

Figure 4-12: Effect of Decreasing Relative Humidity and Loading on CO_2 Solubility in Nafion 117 With EDA, 25°C, 1 atm, 100% CO_2 79

Figure 4-13: Modeling of CO_2 Flux With EDA Loaded Membranes. Membrane Loading = 0.928 gmol EDA/gmol site 92

Figure 4-14: Modeling of CO_2 Flux With EDA Loaded Membranes. Membrane Loading = 1.455 gmol EDA/gmol site 97

Figure 4-15: Prediction of Equilibrium CO_2 Solubility in EDA Loaded Membranes: A Means To Determine Driving Force. Keq_1=245 atm^{-1} , Keq_2 = 50 atm^{-1} 101

Chapter 1

Introduction

1.1 Importance of Gas Separations with Membranes

Membrane gas separations have received recent attention because of their applications in industrial bulk CO_2 removal, energy efficiency and gas selectivity. Table 1-1 lists various industrial processes which require removal of CO_2, as well as other acid gases, and their cleanup concentration levels. Industry has used solid polymer membranes successfully for bulk CO_2 removal in natural gas processing (Stookey, 1985; Grey and Mazur, 1984; Miller, 1984; Cooley, 1984), enhanced oil recovery projects (Schendel, 1984) and landfill gas processing (Kimura, 1982). In these cases, conventional amine and hot potassium carbonate treating are too energy intensive at CO_2 concentrations greater than 15 to 20%. Conventional distillation techniques become economical only at much higher CO_2 concentrations. Economic studies of integrating solid polymer membranes with conventional techniques (Schell, 1985) have shown increased efficiencies of up to 50% (Chowdhury, 1987) and capital savings of up to 25% (Schendel, 1984). These significant savings are possible with the membrane process because no phase changes occur; therefore, it is not an energy intensive process. This advantage is very important when one

Table 1-1: Major Industrial Processes that Need Gas Treating (Astarita et al., 1983)

Process	Acid Gas to be Removed	Cleanup Concentration (% acid gas)
Hydrogen Manufacture	CO_2	<0.1% CO_2
Petroleum desulfurization	CO_2+H_2S+COS	10 ppm H_2S
Natural Gas Purification		
Pipeline Gas	CO_2,H_2S,COS	<4 ppmH_2S;<1% CO_2
Syn Gas for Chemicals(H_2/CO)	CO_2,H_2S	<500 ppm CO_2;<0.01 ppm H_2S
Coal Gasification		
SNG(high Btu gas)	CO_2,H_2S,COS	500 ppm CO_2; 0.01 ppm H_2S
Low Btu Gas		100 ppm H_2S
Ammonia Manufacture	CO_2	<16 ppm CO_2+CO
(H_2/N_2 mixture)	CO_2+H_2S+COS	0.01 ppm H_2S
Refinery Fuel Gas	H_2S,CO_2,COS	100 ppm H_2S

considers that more than half of the energy expense and capital for conventional processses is spent for the separation and concentration steps (Anon, 1980).

Current research has shown that greater selectivities and permeabilities for CO_2 can be achieved with liquid membranes (Ward, 1972; Matson et al., 1983; Kimura, 1982; Onda et al., 1968; Meldon et al., 1977, 1982; Kimura et al., 1979; and Sharma and Danckwerts, 1963) versus solid polymer membranes. Better energy efficiencies should also result. The liquid membranes achieve high selectivities by the incorporation of a reagent which is selective to the permeant on a chemically reactive basis. The CO_2 complex which results from this reaction greatly augments or "facilitates" the transport of CO_2 by diffusing in parallel with the free CO_2. This process is often called facilitated transport. The selectivity of solid polymer membranes is limited because they separate gases by size and or shape. They cannot, therefore, separate such gases as CO_2 and H_2, which separation is important in synthesis gas preparation. Permeabilities two to three orders of magnitude greater are obtained in the liquid membranes due to the higher diffusivities and chemical solubilities of the permeant in the liquid phase. Furthermore, the greater permeabilities afford them the ability to make thicker membranes of greater mechanical stability than the thin solid polymers while still providing similar fluxes. For the same reason, no large pressure gradients are required to provide industrially significant fluxes. However, the carrier-solvent solution in the liquid membrane is contained by only surface tension forces and is therefore subject to loss due to evaporation or pressure forces.

Ion exchange membranes hold promise to overcome this problem because the CO_2 carriers within are ionically bound to the membrane and not easily removed or lost through evaporation or pressure forces (LeBlanc et al., 1980). Secondly, the solvent is not easily lost due to pressure forces because, unlike the liquid membrane, it is nonporous. The solvent is contained within the interstitial volume of the membrane. However, evaporative forces will cause the loss of solvent as was described in the case of the liquid membrane. Yet, the interstitial volume of the ion exchange membrane will reduce accordingly with the loss of solvent, thereby maintaining the integrity of the support. The porous support of the liquid membrane cannot adjust in this manner which results in negatively affecting the integrity. These advantages may afford the ion exchange membrane longer operating lifetimes over that of liquid membranes under industrial conditions.

A final important advantage of ion exchange membranes is that they have the potential for higher carrier loadings than that in liquid membranes because the solubility of the carrier in the membrane is only determined by the ion exchange site density, which can be increased or decreased during formation. Conversely, the carrier loading in the liquid membrane is limited by the solubility of the carrier in the solvent phase.

Ion exchange membranes achieve higher selectivities and permeabilities over that of solid polymer membranes in the same way as the liquid membranes. This behaviour is an exception to the general rule of solid polymer membranes that high

membrane selectivity correlates with low permeability of the desired product through the membrane (Chern et al, 1984).

1.2 Previous Work on CO_2 Separation with Ion Exchange Membranes

Previous studies on CO_2 separation with ion exchange membranes are few. Permeability measurements have been made with fully hydrated membranes at 100% relative humidity. LeBlanc et al. (1980) demonstrated the feasibility of CO_2 removal with a cation exchange membrane with exchange sites fully loaded with ethylenediamine (EDA) cations which reacted reversibly with CO_2. An estimate of the diffusion coefficient of the CO_2 complex was made from conductance measurements on the EDA loaded membrane. Way et al. (1987) also measured CO_2 removal with a cation exchange membrane, Nafion 117, with EDA cations. They studied the effects of loadings below or equal to 1 gmol EDA per gmol ion exchange site. Although no measurement of the diffusion coefficient or solubility of CO_2 was made, an estimate of the diffusion coefficient was made by assuming pure solution values of CO_2 solubility for the Na^+ form of the membrane. Another assumption in estimating the diffusion coefficient was that the diffusion coefficient of CO_2 in the Na^+ form was the same as that in the EDA loaded membrane.

The validity of these two assumptions is questionable. Leiber and Lewis (1985) showed that the rate and activation parameters for complexation reactions within the high ionic strength environmment of the perfluorosulfonic acid membrane, such as Nafion, were very different from those in solution. This

environment may also affect the transport parameters of CO_2 in the membrane even under nonreactive conditions. Secondly, Weiland and Trass (1971) showed that the diffusion coefficient of CO_2 was significantly less in amine solutions because of the effects of increased solution viscosity. This behaviour should also be expected in the EDA loaded membrane.

Way et al. and LeBlanc et al. prepared the EDA loaded membranes from the Na^+ form and then rinsed them with water to remove any neutral species. However, the degree of this rinsing may have affected the final loading of the membrane since the equilibrium loading of ion exchange membranes has been shown to vary with the concentration of the contacting solution (King, 1988).

The form of the membrane and its water content have been shown to have significant effects on the transport properties of other gases. The permeability and diffusion coefficient of O_2 and H_2 in Nafion have been shown to be higher in the H^+ form versus the K^+ form (Sakai, et al., 1985). Large differences of permeability and diffusion coefficient were shown between the fully hydrated and dried form of Nafion 117, H^+ at ambient conditions (Sakai et al., 1985; Sakai et al., 1986).

Swelling of Nafion with uptake of water (Sondheimer et al.,1986; Yeager, 1982) is significant and has been measured for the Na^+, K^+ and Cs^+ forms. This behaviour should affect the diffusion pathway (Crank and Park, 1968).

1.3 Objective

The objectives of this study were (1) to examine the transport of CO_2 in Nafion 117 enhanced by relative humidity and EDA content and (2) to model the CO_2-EDA system based on equilibrium considerations. This was to be accomplished by determining the diffusion coefficient and permeability, in situ. Loadings greater than one and conditions drier than 100% relative humidity were investigated. The goal was to clarify the diffusion process and the reaction chemistry between CO_2 and EDA.

The H^+ form was equilibrated in aqueous solutions of EDA to effect EDA loadings from 0 (H^+) to 1.45 gmol EDA/gmol ion exchange site. The membranes were not rinsed after equilibration so that the loading would not be affected. Diffusion coefficients and permeabilities of CO_2 were measured in all membranes under conditions from 0 to 100% relative humidity and 0.005 to 1 atm CO_2. The effect of relative humidity on membrane water content and swelling was measured. The transport results are discussed in terms of EDA loading, water content, swelling and published data on the internal structure of Nafion. Implied solubilities of CO_2 determined from the measured diffusion coefficients and permeabilities are used to discuss the reaction chemistry between CO_2 and EDA.

1.4 Ion Exchange Membrane Nafion 117

Nafion 117 is a cation exchange membrane composed of a polytetrafluoroethylene backbone and branches terminating with sulfonic acid groups (Grot, 1975) (Figure 1-1). Nafion was developed in the early 1970's for use in electrochemical applications, especially in the chlor-alkali industry (Grot, 1972). The equivalent weight of our sample was 1100 g per gmol of ion exchange sites. The ion exchange capacity (IEC = 1000/EW) was therefore 0.91 meq/g.

The microstructure of Nafion has been examined by previous authors by means of various methods such as NMR (Komoroski and Mauritz, 1982), infrared spectra (Falk, 1982) and small-angle and wide-angle x-ray scattering and light scattering (Hashimoto, 1982). The generally accepted model of Nafion structure postulates that the ionic sites and water are clustered and separated either completely or partially from the fluorocarbon backbone (Yeager, 1982; Gierke et al., 1981).

1.5 CO_2-Ethylenediamine Chemistry

Ethylenediamine (EDA) is a primary amine which reacts reversibly and instantaneously with CO_2 (Weiland and Trass, 1971). EDA was chosen for the ion exchange system because its bifunctionality allowed for one end to be protonated, associated with the ion site, while leaving the other end free to react with CO_2. In the membrane, the portion of the EDA unassociated with the sites will remain as

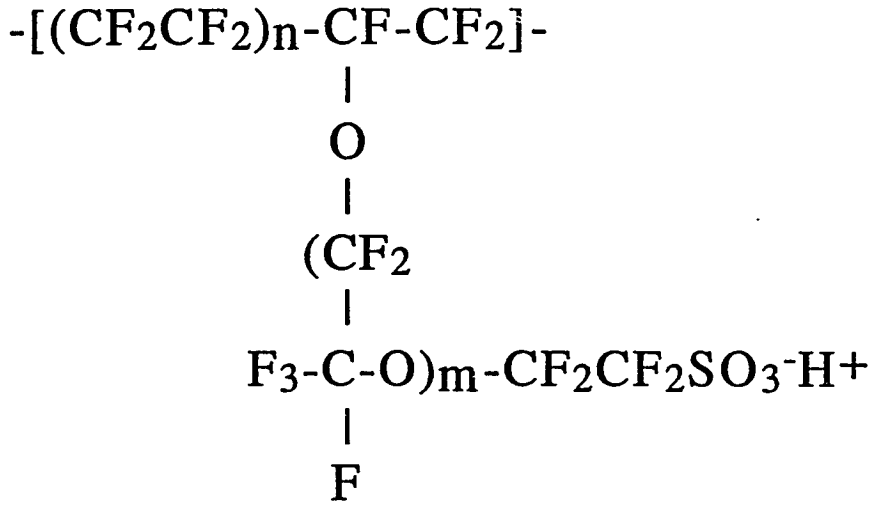

Figure 1-1: Schematic of Nafion Structure in Acid Form. For commercial use, m=1, n=5 to 12 (Grot, 1972).

free EDA. The overall reaction of CO_2 with EDA in solution is second order (Weiland and Trass, 1971; Jensen and Christensen, 1955):

$$CO_2 + H_2N\text{-}(CH_2)_2\text{-}NH_2 \Longleftrightarrow (^+H_3N\text{-}(CH_2)_2\text{-}NHCOO^-)^\circ \qquad (1\text{-}1)$$

Although EDA is bifunctional, only one of the two amino groups can be relied on to firmly bind the CO_2 (Jensen and Christensen, 1955; Swick et al., 1954). Carbamate is the dominant form of CO_2 in aqueous EDA solutions (Jensen and Christensen, 1955).

The cation associated with an ion exchange site under the conditions of this study is most probably the monopositive form of EDA. The reaction of the monopositive form of EDA with CO_2 is also instantaneous and reversible (Jensen and Christensen, 1955):

$$CO_2 + 2(H_2N\text{-}(CH_2)_2\text{-}NH_3^+) \Leftrightarrow (^+H_3N\text{-}(CH_2)_2\text{-}COO^-)^\circ + (+H_3N\text{-}(CH_2)_2\text{-}NH_3^+)^{+2} \qquad (1\text{-}2)$$

This chemistry differs significantly from that for CO_2 facilitated transport in liquid membranes containing basic aqueous solutions, such as bicarbonate, which is represented by the following reaction sequence (Ward and Robb, 1967):

$$Base + H_2O \Longleftrightarrow Base^+ + OH^- \qquad (1\text{-}3)$$

$$CO_2 + OH^- \Longleftrightarrow HCO_3^- \qquad (1\text{-}4)$$

In the ion exchange membrane, the contribution of bicarbonate to the flux of CO_2 is assumed negligible because the formation or diffusion of the bicarbonate anion is electrically prohibitive (Gierke and Hsu, 1982). The formation of other anions, such as dicarbamate, should also be thermodynamically inhibited in the cation exchange resin.

Chapter 2

Background

2.1 Facilitated Transport Membrane

A facilitated transport membrane contains a reagent or "carrier" which complexes with a desired component "permeant" in the gas stream. The carrier remains in the membrane phase. A schematic of the transport process involved is shown in Figure 2-1 for the permeant CO_2 and a carrier, R. At the interface with the upstream gas phase, the carrier reacts with the permeant to form a carrier-permeant complex. This establishes a gradient in the concentration of complexed CO_2. The complex diffuses to the opposite boundary in parallel with CO_2 which diffuses down the concentration gradient maintained by the sweep gas. At the downstream surface, the lower CO_2 concentration causes the complex to dissociate which releases the CO_2 to the sweep gas. This process creates a counter-gradient in carrier concentration. A biological example of facilitated transport is the transfer of oxygen through hemoglobin solutions (Scholander, 1960). The reaction between CO_2 and hemoglobin has been shown to be near chemical equilibrium (Wittenburg, 1966).

Three different methods for containing the solution have been reported in the literature. In the simplest case, the solution is immobilized in a thin, porous

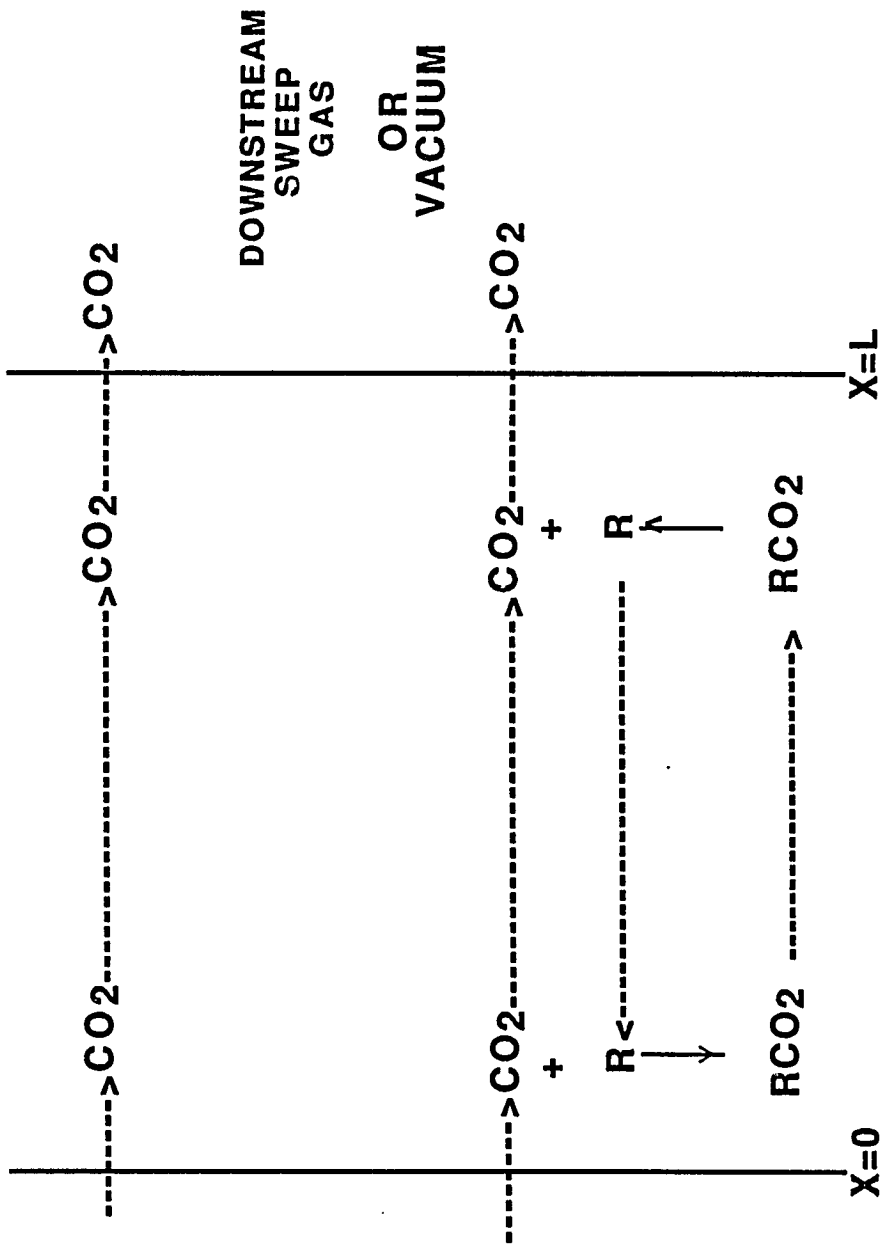

Figure 2-1: Schematic of CO_2 Facilitated Transport by Reversible Reaction With Carrier, R, To Form RCO_2 Complex

polymeric support (Enns, 1967; Ward and Robb, 1967). The solution within the membrane is held by surface tension forces. One modification on this method is to place the solution between two plates in which are drilled a series of holes (Otto and Quinn, 1971; Meldon et al., 1977). A third method is to bind ionically the carrier in an ion exchange membrane (LeBlanc et al., 1980; Way et al., 1986, 1987). The nonporous, ion exchange membrane swells to incorporate the solvent. These three cases are associated with what is defined in the literature as "immobilized liquid membrane", (ILM), "immobilized liquid film", (ILF), and "ion exchange membrane", (IEM).

2.2 Literature Review

Studies of the facilitated transport of CO_2 were spurred in the late 1960's in an attempt to increase the rate of CO_2 absorption into carbonate solutions. The absorption of CO_2 into carbonate solutions alone, is in general, not very great (Onda et al., 1968). Early experiments showed that the hydrolysis of CO_2 was the rate limiting step and that the absorption rate was catalyzed by the addition of anions of Bronsted bases (Sharma and Danckwerts, 1963), amino acids (glycine, sodium glutamate) or arsenious acid (Onda et al., 1968) and the enzyme carbonic anhydrase (Enns, 1967). Ward and Robb (1967) found that carbonic anhydrase and arsenite catalyzed the absorption of CO_2 while enhancing its selectivity over O_2.

The work by Ward and Robb and Enns represented two of the first works of facilitated CO_2 transport in immobilized liquid membranes. Most of the liquid

membranes were prepared with aqueous solvent. However, Ward and Neulander (1969) and Kawami et al. (1982) measured CO_2 permeability in a solvent of polyethylene glycol.

While most of the above studies were at room temperature and pressure, Kimura et al. (1979) and Matson et al. 1977) examined facilitated CO_2 transport at the industrially significant conditions for coal gasification of 300 psi and 90 to 130°C.

Donaldson and Quinn (1975) showed that studies in immobilized liquid membranes of CO_2 facilitated transport offered an attractive technique for the study of reaction kinetics by using tracer species. A disadvantage to using ILM's was that reproducibility between membranes was difficult and determination of the transfer area was unclear because the porous environment was not homogeneous.

A few later studies were performed in immobilized liquid films, which offered greater reproducibility of results because of the defined diffusion pathway and cross-sectional area for diffusion. Otto and Quinn (1971) give an experimental and mathematical treatment to the catalytic effect of carbonic anhydrase on the facilitated transport of CO_2 through bicarbonate solutions. Meldon et al. (1977) showed that non-catalytic weak acid additives (phosphoric acid, pyrophosphoric acid, boric acid and silica acid) increased the absorption of CO_2 by acting as a buffer, decreasing the pH gradient across a NaOH liquid film.

The remaining studies returned to the inherent simplicity of using the immobilized liquid membrane and focused on clarifying the mechanisms of amine reactions with CO_2. Donaldson and Nguyen (1980) found that at low concentrations of mono- and diethanolamine (DEA) the reaction with CO_2 proceeds via reversible carbamate formation. Triethanolamine catalyzed CO_2 hydration and triethylamine acted as a weak base to produce free OH^- which then reacted with CO_2. Meldon et al. (1986) also found that particularly high CO_2 fluxes in membranes containing DEA indicated facilitated transport of CO_2 by the formation of carbamates.

The use of amines to remove CO_2, as well as H_2S, has been long used in scrubbers (Astarita et al., 1983) due to their high capacity for CO_2. Several authors have studied CO_2 absorption with amines (Emmert et al., 1962; Astarita et al., 1964; Jeffreys et al., 1964) in stirred cells, wetted wall columns or laminar jets.

LeBlanc et al. (1980) extended the technology to the ion exchange membrane. He demonstrated the feasibility of facilitated transport of CO_2 with a cation exchange membrane loaded with the monopositive form of EDA. Permeabilities up to 34 times that of free CO_2 diffusion alone was achieved. Way et al. (1986, 1987) measured very high selectivities of CO_2 over methane and H_2S in a mixed gas stream with the cation exchange membrane, Nafion 117. The potential industrial importance of the ion exchange membrane system for CO_2 removal was stressed in these three studies.

Chapter 3

Experimental Apparatus and Procedure

3.1 Preparation of Nafion 117 with H^+ (Nafion 117, H^+)

Samples of Nafion 117 measuring 8 1/2" by 11" were obtained from Du Pont representative Warren Van Scoyoc at the Wilmington, Delaware site in August, 1984 and December, 1986. The results obtained with the first membrane were inconsistent and are not addressed here. The following procedure applies to the second membrane obtained. Four squares measuring 8 cm by 9 cm were cut from a given sample and rinsed repeatedly with distilled water and then with acetone to remove any organic impurities. The membranes were then boiled in distilled water for an hour to restore the membrane to the fully hydrated condition. After rehydrating the membranes, all four membranes were placed into excess solutions of HCl, approximately 1 liter of 2 N HCl, and boiled for one hour in order to ensure that all exchange sites were of H^+ form. The 2 N HCl was prepared from Fisher Scientific reagent A.C.S. Hydrochloric Acid, Lot 737040 and distilled water. After boiling, the membranes were allowed to come slowly to room temperature over 24 hours. A second boiling in distilled water ensured that any excess hydrogen ions were removed and that the membrane was fully hydrated.

The membranes were always allowed to come to room temperature slowly after each boiling so that their history of treatment was the same. When not in use, the membranes were stored in distilled water. Each hydrated membrane was trimmed to measure approximately 8.8 cm by 8 cm, which left smaller samples measuring approximately 15 cm^2. These smaller samples were stored with the larger membranes they were cut from when not in use. The density of ion exchange sites for each sample was determined by the procedure described in Section 3.6.

3.2 Preparation of Nafion 117 with Ethylenediamine

Two of the Nafion 117 membranes in the H^+ form, prepared as above, were equilibrated in 0.15 M EDA and 1.5 M EDA. The amount of EDA loaded in each case could not be determined by simple solution analysis because the difference to be measured was too small to be accurately measured. In this case, the amount of EDA loaded was determined by first leaching the membranes so that equilibration at a lower solution EDA concentration was effected. The membrane loading at the lower EDA solution concentration was determined separately by loading separate membranes in H^+ form into EDA solutions of low enough concentration so that the amount loaded could be determined accurately by solution analyses. These two methods are described in Sections 3.2.1, 3.2.2 , 3.3, and 3.3.1.

3.2.1 Loading in High Concentrations of EDA

Solutions of 0.15M and 1.5M EDA were prepared from mixtures of reagent grade EDA (MCB, Lot C 6M02, 10/80, Quality Control Code EX 510) and distilled water. Nafion 117, H^+ membranes described in Section 3.1 were placed into 1 liter volumes of these solutions, one in each volume. The solutions were stirred continuously and heated from 25°C to 50°C over a 1 hour period. The solutions were then removed from the heat and stirred for four days. Lastly, the membranes were taken out of the solutions, blotted dry and used in permeation experiments, described in Section 3.7.

3.2.2 Leaching To Determine EDA Content

After the permeation experiments, the EDA loadings of the membranes loaded in 0.15 M EDA and 1.5 M EDA were determined. The membranes were leached separately in 30 mL test tubes containing exactly 25 mL of distilled water. They were stirred continuously over several days until the solutions reached equilibrium which was determined from conductivity and pH measurements described in Section 3.3.2. Quantitative analyses of the molarity of the EDA in the leachates were determined from pH titrations described in Section 3.4. The membrane loading in the leached membrane was read off an experimentally determined graph of membrane loading versus equilibrium solution concentration. The method used to determine this graph is described in Section 3.3. The loadings of EDA present in the membranes, L_m (gmol EDA/gmol exchange sites) which

were equilibrated in the EDA solutions were calculated by material balance as follows:

$$L_m = \left\{ \frac{\left[\left(\begin{matrix}\text{Membrane} \\ \text{Loading}\end{matrix} \right)_{\substack{\text{Leached} \\ \text{Membrane}}} \left(\begin{matrix}\text{gmol} \\ \text{exchange sites}\end{matrix} \right) + \left(\begin{matrix}\text{gmol} \\ \text{EDA}\end{matrix} \right)_{\substack{\text{Leached} \\ \text{Solution}}} \right]}{\text{gmol exchange sites}} \right\} \quad (3\text{-}1)$$

where the gmol of exchange sites was determined as described in Section 3.6.

The "effective" EDA concentration, C_m (gmol EDA/liter water) in the membrane is defined as:

$$C_m = \frac{L_m 1000 \rho_w}{(EW)\text{Water Content}} \quad (3\text{-}1A)$$

where the water content (g/100g dry membrane) is referenced to the dry state (see Section 3.6), ρ_w is the density of water and 1000 is a conversion factor for cm^3 to liters.

3.3 The Equilibrium Loading of EDA in Nafion 117, H^+

3.3.1 Loading in Low Concentrations of EDA

Two Nafion 117, H^+ membranes described in Section 3.1 were placed separately into 30 mL test tubes containing 25 mL of a known solution of EDA and

distilled water. The concentrations of these loading solutions were determined such that the equilibrium values reached after loading would span closely the range of equilibrium concentrations of the leachates from the membranes loaded in the high concentrations of EDA. The amount of EDA that would be loaded into the membrane was estimated from ion exchange site density considerations. The membrane loadings were done one at a time. As a first membrane estimate, the initial concentration of the loading solution required to attain the concentration of the leachate from the 1.5 M EDA equilibrated membrane was calculated based on an estimated membrane loading of 1.5 gmol EDA/gmol exchange sites. The following equation was used to calculate the initial concentration of the loading solution:

$$\text{Solution Loading(M)} = \left\{ \frac{\left[(\text{EDA(M)})_{\text{Leachate}} \; (\text{V(l)})_{\text{Loading Solution}} + \left(L_{m_{\text{predicted}}} \right) \left(\frac{\text{gmol exchange}}{\text{sites}} \right) \right]}{\text{V (l)}_{\text{Loading Solution}}} \right\} \quad (3\text{-}2)$$

After equilibrium of the membrane in this solution had been attained, as determined by pH and conductivity measurements (see Section 3.3.2), the concentration of EDA in the solution was determined by pH titration (see Section 3.4). An equilibrium solution loading value of 0.08375 M EDA was attained from an initial solution loading of 0.15 M EDA. The equilibrium solution value, 0.8375 M EDA, was greater than the target value, 0.0388 M EDA. The membrane loading was lower than predicted. Therefore, the initial concentration of the second loading solution, which was required to attain the leachate concentration of the 0.15 M EDA equilibrated membrane, was calculated based on a lower predicted loading of 0.7

gmol EDA/gmol exchange sites. The equilibrium solution value attained, 0.0057 M EDA, was lower than the target value, 0.00985 M EDA. Both equilibrium solution concentrations from the loading experiments spanned closely the range of the concentrations of the leachates. The values of the membrane loadings of the membranes used in the loading experiments were determined by material balance on the EDA in solution before and after loading:

$$\text{Membrane Loading} = \frac{\left\{\left(\text{EDA(M)}_{\substack{\text{Initial}\\ \text{Loading Sol'n}}} - \text{EDA(M)}_{\substack{\text{Equilibrium}\\ \text{Loading Sol'n}}}\right)\left(\text{Volume(l)}\right)_{\substack{\text{Loading}\\ \text{Sol'n}}}\right\}}{\text{gmol exchange sites}} \quad (3\text{-}3)$$

A graph of membrane loading versus equilibrium solution loading was used to determine membrane loadings at other equilibrium solution loading concentrations (Figure 4-1). The loading value of the membrane equilibrated in 1.5M EDA was higher than the value which would be predicted based on a linear log extension of the lower portion of the curve. Additional measurements at higher solution loadings were taken to ascertain the shape of the curve in this region. Additional membranes in the H^+ form were equilibrated in 30 mL test tubes filled with approximately 25 mL of a concentration greater than 1.5 M EDA. The methods of solution preparation, membrane leaching, and determination of membrane loading were the same as previously described for the 0.15M EDA and 1.5M EDA equilibrated membranes. After the four membranes available had been

loaded with EDA, they were returned to their H+ form, as needed, by the procedure outlined in Section 3.5.

3.3.2 Equilibrium Determination

When the membranes were loaded into solutions of EDA, or leached, the point at which the process was complete was determined by measuring the solution conductance. At equilibrium, the conductance was expected to attain a constant value. Corresponding pH measurements were made to assist in analyzing the meaning of conductance values, as explained below.

Solution conductance was measured by a YSI Model 32 Conductance Meter with a YSI conductivity cell. The cell was conditioned in distilled water for two days before use. The meter was calibrated at 25°C with 0.1 M, 0.01 M and 0.001 M NaCl prepared from reagent grade NaCl, Fisher Scientific Certified A.C.S. Sodium Chloride, Lot 7.327.38. 20 mL samples of each of these solutions were poured into separate, covered 30 mL beakers and placed into a temperature controlled water bath at 25°C. The temperature of the samples was measured with a thermometer until it reached 25°C. The cell was placed into each sample at 25°C and the conductance measured. In between conductance measurements of each solution, the cell was rinsed with distilled water until the meter read approximately 3 micro-ohm, the measured conductance of distilled water. This procedure minimized any interference due to traces of solution on the cell from previously measured solutions. The cell constant, K, was calculated from these measured values of

conductance and published values of NaCl solution conductivity, k (Weast, 1973),using the following equation:

$$K\ (1/cm)=\frac{k(ohm/cm)}{conductance(ohm)} \qquad (3\text{-}4)$$

The cell constant was found to be 0.99/cm $\pm$ 1% fs, compared to the factory calibrated value of 1.0/cm $\pm$ 1% fs.

After calibration, the conductance of EDA was measured as a function of EDA concentration. Standard solutions of EDA were prepared from reagent grade EDA and distilled water. The same procedure for measuring the conductance of the NaCl samples was followed for measuring the conductance of the standard solutions of EDA.

Measurements of the conductance of the low EDA concentration loading solutions and of the leaching solutions followed this same procedure. The 25 mL samples were transferred into 30 mL beakers, covered and placed into a temperature-controlled water bath at 25°C. Transferring the solutions to beakers was necessary for accurate placement of the conductance probe into the sample. At least 1/4" spacing around the probe was required in order to minimize interference with the measurements.

After completing the conductance measurements, the samples, kept in beakers, were transferred to a stirring plate and their pH was measured. The solutions were then poured back into their original test tubes with the membranes and stirring of the solutions was continued. The conductance and pH of the solutions were measured approximately every 24 hours. The changes in EDA concentration associated with changes in conductivity were estimated from linear interpolations between values of conductivity squared versus EDA concentration. These estimated concentration changes were compared with pH measurements.

Ideally, equilibrium was reached at the point where no significant changes in estimated EDA concentration occurred. However, if the conductance of the solution increased without an associated increase in pH, i.e., pH remained constant or decreased, it was assumed that the solution had already reached equilibrium in EDA concentration and was absorbing CO_2 from the air. This assumption was checked by two methods. First, the estimated concentration determined from the measurement of conductance before the unexplained increases occurred was compared with the actual concentration determined from pH titration, as described in Section 3.4. Second, a microliter sample of the solution was injected into a total carbon analyzer to determine the concentration of carbon in the solution. Ionic products from the reaction between CO_2 and EDA would cause the solution conductivity to increase above the equilibrium conductivity value associated with the EDA concentration. Based on the stoichiometry associated with the possible reactions between CO_2 and EDA, a concentration of ion pairs (reaction products) was estimated. The conductivity of these ions was estimated as that which would

be measured in an NaCl solution of the same concentration. This conductivity was compared with the unexplained increase in the sample conductivity.

3.4 Quantitative Analysis: pH Titration of Solutions

A Corning pH Meter 130 and a Corning Combination X-EL pH probe were used to measure the pH of solutions. The meter was calibrated with Fisher Scientific Certified Buffer Solutions of pH 4.00±0.01 at 25°C, Lot 850934-24; pH 7.00±0.01 at 25°C, Lot 860458-24 and pH 10.00±0.02 at 25°C, Lot 851596-24. 40 mL samples of each buffer were placed into 50 mL Erlenmeyer flasks. The probe was first placed into the pH 7 buffer and allowed to equilibrate. All solutions were continuously stirred while their pH was being measured. After equilibration at pH 7, the probe was removed from the pH 7 buffer and placed into the pH 4 buffer and allowed to equilibrate. The calibration knob on the pH meter was adjusted so that a reading of pH 4.000, a "set-point", was displayed. Before the next pH measurement was taken, the probe was removed to a separate pH 7 buffer/rinse solution which was used only for equilibrating the probe at approximately pH 7 between measurements. pH measurements were taken of the additional pH buffer solutions, without any further adjustment of the calibration knob, to complete the calibration of the pH meter. When not in use, the probe was rinsed with distilled water and stored dry. The aforementioned calibration procedure was performed before each titration of an unknown. The titration procedure is presented in the following paragraph.

A 10 mL aliquot was pipetted from the solution to be quantified into a 30 mL beaker. The concentration of the titrant to be used was estimated such that the total equivalents in an equal volume of titrant would match approximately that of the sample. Solutions of acid titrant were prepared from Fisher Scientific Certified Hydrochloric Acid 1 N Solution (1.005-0.995 N), Lot 863738-24 and distilled water. A 10 mL burette was filled with the titrant and suspended over the sample which was being continuously stirred on a stirring plate. The pH probe was removed form the buffer/rinse of pH 7 and placed into the sample. pH readings of the sample were recorded before any titrant was added and after each addition of 0.25 mL to 0.5 mL of titrant. Readings were recorded after smaller additions of titrant when the changes in pH increased to approximately 0.5 to 1 pH unit between each addition of titrant. Titration of the sample was continued until the pH of the solution approached the pH of the titrant. After the titration was complete, the sample was poured into an erlenmeyer flask, stoppered and stored for future reference. The concentration of the unknown in the sample, for a solution of one unknown, was determined from the mL of titrant that had been added at the equivalence point using the following equation:

$$\text{Unknown Concentration(M)} = \left(\frac{\text{titrant added (ml)}}{\text{sample volume (ml)}}\right)\left(\frac{\text{no. equivalents of unknown}}{\text{no. equivalents of titrant}}\right)\text{titrant (M)} \quad (3\text{-}5)$$

3.5 Restoring Nafion 117, EDA to H+ Form

An EDA loaded membrane, described in Section 3.2, was placed into a 30 mL test tube. A solution of sodium hydroxide (NaOH) was prepared from Fisher Scientific Certified Sodium Hydroxide Solution, 2N, Lot 746170-24 and distilled water. The concentration of the NaOH solution prepared was estimated based on an excess of NaOH remaining in solution after the reactions between NaOH and EDA occurred. 25 mL of the prepared solution was pipetted into the test tube which was then stoppered and continuously stirred for 4 days. After the fourth day, the membrane was removed from the solution and repeatedly rinsed in distilled water. It was then soaked 24 hours in approximately 1 liter of distilled water. After the membrane was soaked, the same treatment procedures described in Section 3.1 beginning with boiling the membrane in excess solutions of 2N HCl were followed to reload the ion-exchange sites with H^+.

3.6 Water Content, Ion Exchange Site Content and Swelling

The water content (g water/g dry membrane), ion exchange site content (gmol ion exchange sites) and swelling (volume increase of swollen membrane/volume dry membrane) of representative samples of each of the different types of membranes used in the permeation experiments in their fully hydrated conditions and under 100% RH to vacuumed dry conditions were determined. Water content, ion exchange site content and swelling are defined by the following equations:

$$\text{Water Content (\%)} = \frac{(W(g)_{\text{membrane}} - W(g)_{\text{dry membrane}})*100}{W(g)_{\text{dry membrane}}} \qquad (3\text{-}6)$$

where W(g) = weight of the membrane in grams, and

$$\text{Ion Exchange Site Content} = \frac{\text{Wt(g) dry Nafion 117 } H^+}{\text{MW eq Nafion 117 } H^+} \qquad (3\text{-}7)$$

and

$$\text{Swelling (\%)} = \frac{(V(cc)_{\text{membrane}} - V(cc)_{\text{dry membrane}})*100}{V(cc)_{\text{dry membrane}}} \qquad (3\text{-}8)$$

where V(cc) = (surface area (cm^2))*(thickness(cm))

and V is the volume of the membrane in cubic centimeters.

The weight and volume of the fully hydrated membrane were determined first. A fully hydrated sample measuring approximately 8 cm by 2 cm was removed from the solution in which it was stored, blotted dry and placed into a plastic bag which was then sealed. A paper ring was constructed and placed around the plastic bag and membrane to facilitate weighing. The three items were placed upright and weighed in a tared, top loading balance (Sartorius, 1602 MP, max 160 g, div = 0.1 mg). The weight of the membrane was determined by subtracting the weight of the bag and paper, which was measured in a separate step in the same way. Next, the thickness and surface area of the membrane was measured with a

micrometer (Mitutoyo 0-1", div = 0.0001") and a ruler (0-300 mm, div = 1 mm), respectively. After these measurements, the membrane was replaced into its solution until the weighing at various relative humidities was started, as explained below.

Secondly, the weight of the membrane was measured at 11 to 100% relative humidity with the apparatus shown in Figure 3-1. It consisted of a balance (Mettler. Type H4, cap. 160 g, div=10 mg) with a hanging clip and an 800 mL glass beaker with a rubber stopper in which a 1/2" hole had been drilled through the center. In the weighing position, the bottom portion of the clip was suspended about mid-way into the beaker.

The first phase of the weighing procedure was the same for every sample. The beaker was filled with approximately 200 cm^3 of distilled water and covered with the rubber stopper with the clip positioned through the hole. Unless otherwise noted, the clip was always positioned through the hole in the rubber stopper. The entire assembly was placed into the balance where the top of the hanging clip was hung onto the weighing pin of the balance. The scale was turned on and manually tared. While taring and weighing, care was taken to make sure that the clip and any sample hung freely and did not touch any of the sides of either the stopper, the beaker or the solution. After taring, the balance was turned off before removing the entire assembly from the balance. After removing the stopper and clip from the beaker, parafilm was used to cover the beaker which remained covered for approximately 24 hours.

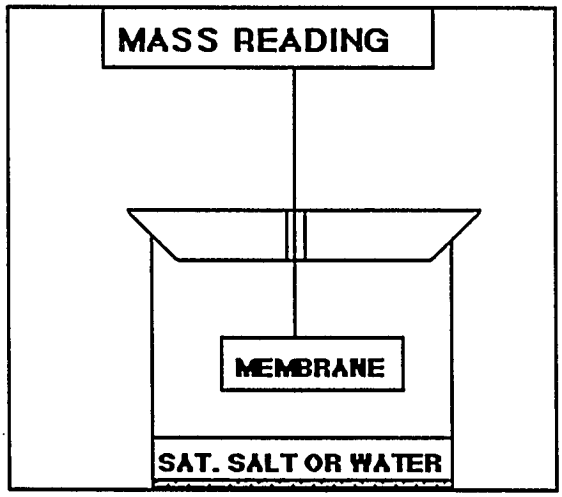

PAN BALANCE

FIGURE 3-1: Relative Humidity Cell. Operated at Room Temperature and Pressure

After this time, the same fully hydrated sample was removed from the solution in which it was stored and blotted dry. The membrane was attached in the horizontal, sideways position to the bottom portion of the clip. The rubber stopper, hanging clip and membrane assembly was placed quickly onto the uncovered beaker. This entire assembly was then placed into the balance and hooked up for weighing. This completed the first phase of the relative humidity-weighing experiments.

Phase two involved recording the weight of the membrane either to obtain the rate of liquid desorption and the weight at equilibrium or to obtain the weight at equilibrium without rate data. Different procedures were followed in each case. In the first case, the weight of the membrane was recorded at time zero and every few seconds to every few hours until the changes in weight between measurements approached zero. After the weight at equilibrium was attained, the balance was turned off before removing the beaker and clip assembly. After the membrane was removed form the clip, its volume was quickly measured. The same procedure previously described in this section for measuring the volume of the fully hydrated membrane was followed.

Next, the membrane was rehydrated for each successive relative humidity-weighing experiment. The procedure for hydrating the membrane, described in

either Section 3.1 for Nafion 117, H^+ or Section 3.2 for Nafion 117, EDA was followed. The procedure for the first phase of weighing and the procedures for weight and volume measurements, previously described in this section, were repeated with salt solutions in the beaker instead of distilled water. The salt solutions used, in the order in which they were used, are listed in Table 3-1 .

In the case when the weight at equilibrium without rate data was obtained, the procedure for the first phase of weighing was the same as that which was previously described in this section. In phase two, the weight of the membrane was recorded at time zero and every few hours to every day until the weight at equilibrium was attained. After the membrane was removed from the balance and its volume measured, it was used "as is", i.e., without rehydration, for the successive relative humidity-weighing experiment. The remaining steps in the procedure remained the same as that for the previous case.

Finally, the weight and volume of the dry membrane was determined. After the last relative humidity-weighing experiment of the type previously described in this section was completed, the membrane was placed into a vacuum oven at 25 °C and 29 in. Hg vacuum. Its weight was measured every few days over a period of about 1 to 2 weeks until it reached a steady state value. This value was its dry weight, except for the case when the membrane was loaded with EDA. In this case, the dry weight was calculated using the following equation:

$$Wt._{\text{dry Nafion 117, EDA}}\,(g) = Wt._{\text{dry Nafion 117, H}^+}(g) + Wt._{\text{EDA}}\,(g) \qquad (3\text{-}9)$$

Table 3-1: Saturated Salt Solutions Used in Relative Humidity Cell

SATURATED SOLUTIONS	%RH VAPOR SPACE (25°C) (Weast, 1974)
WATER	100
$CuSO_4$	96
KNO_3	94
$NH_4H_2PO_4$	92
$ZnSO_4*7H_2O$	88
KCl	85
NaCl	75
$Mg(NO_3)_2$	54
$MgCl_2$	33
LiCl	11

where $Wt._{EDA}$ (g) is the grams of EDA loaded into the membrane based on the titration experiments. The EDA membranes were also vacuum dried and the weight obtained did not vary significantly from that calculated by this procedure.

Next, the previously described procedure in this section for determining the volume of the membrane was followed. Values of the weights of the larger dry Nafion 117, H^+ membranes, used to determine the ion-exchange content, were calculated using the following equation:

$$Wt._{\substack{\text{larger membrane}\\ \text{dry Nafion 117H}^+}} = \left(\frac{Wt._{\text{larger membrane (g)}}}{Wt._{\text{sample}}}\right)_{\substack{\text{fully hydrated}\\ \text{Nafion117 H}^+}} \left(Wt._{\substack{\text{sample}\\ \text{dry Nafion 117 H}^+}}\right) \qquad (3\text{-}10)$$

where all weights are in grams. For a given membrane, the ion-exchange content (gmol) measured for the H^+ form was the same for the EDA form.

3.7 Flux and Permeability of CO_2

3.7.1 Definition of Permeability

The permeability, P, of a membrane to a permeant is defined by the following equation, where N is the flux of the permeant and p_2 and p_1 are the

upstream and downstream pressures of the component acting across the effective membrane thickness, L,

$$P = \frac{NL}{(p_2 - p_1)} \tag{3-11}$$

P is determined by the mobility and solubility of the permeant. Defining P in terms of these parameters can be accomplished by substituting N = -D(dC/dx), where x is a measure of L, into Equation (3-11) to obtain the following equation:

$$\int_0^1 \frac{P}{I}\,dx = \int_0^{C_2} \left(\frac{DdC}{C_2}\right)\left(\frac{C_2}{p_2}\right) = \overline{DS} \tag{3-12}$$

where $\overline{D} = \dfrac{\int_0^{C_2} DdC}{\int_0^{C_2} dC}$ defines an average measure of the permeant's mobility in the membrane between the upstream concentration, C_2, and downstream concentration, C_1, is approximately equal to 0. The parameter, $\overline{S} = C_2/p_2$ is a measure of the solubility of the permeant in the membrane.

3.7.2 Flow System and Procedure

The apparatus used to measure the flux and permeability of CO_2 is shown in Figure 3-2. The first phase of the permeation experiment was the same for all

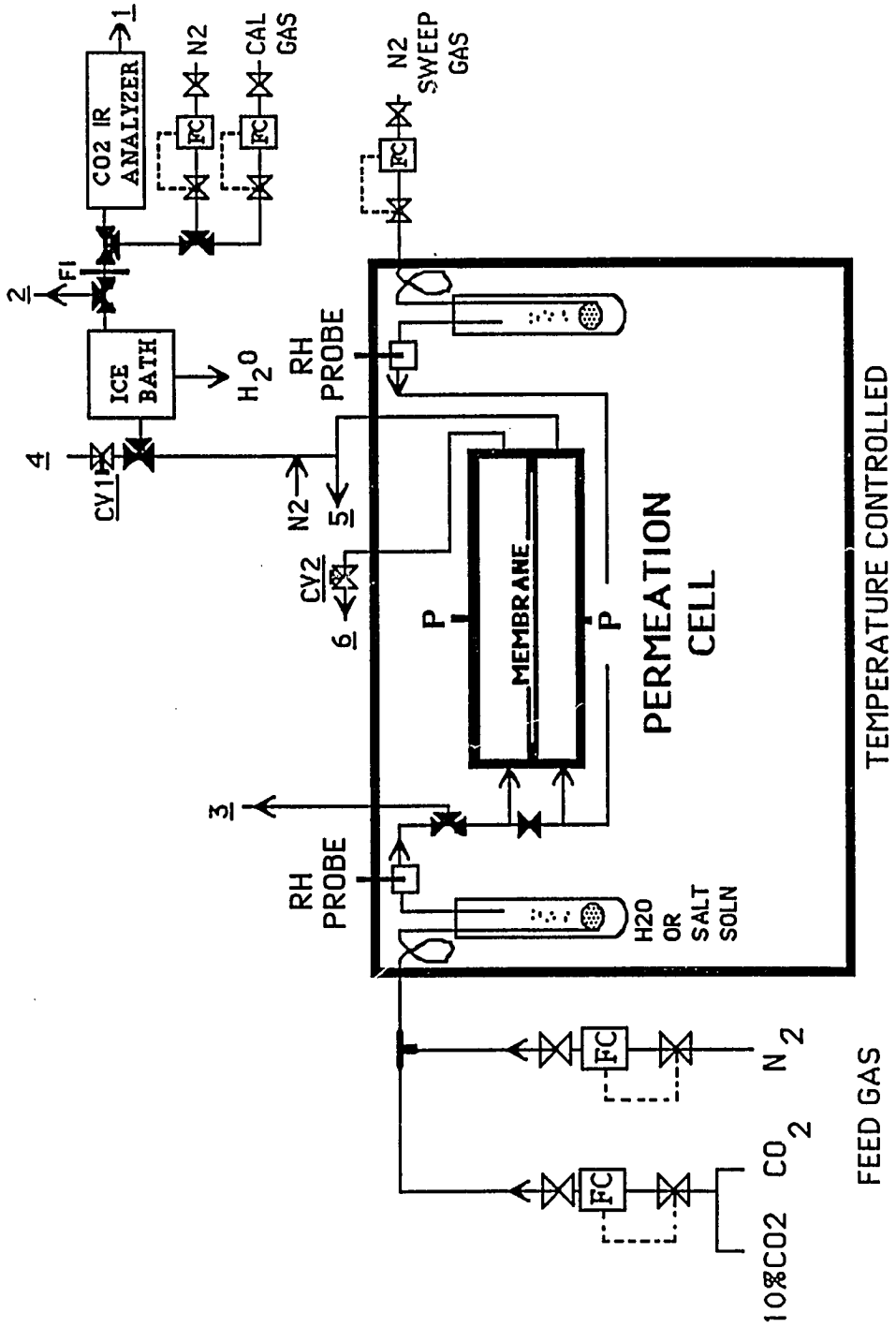

Figure 3-2: Experimental Apparatus For Permeation Measurements

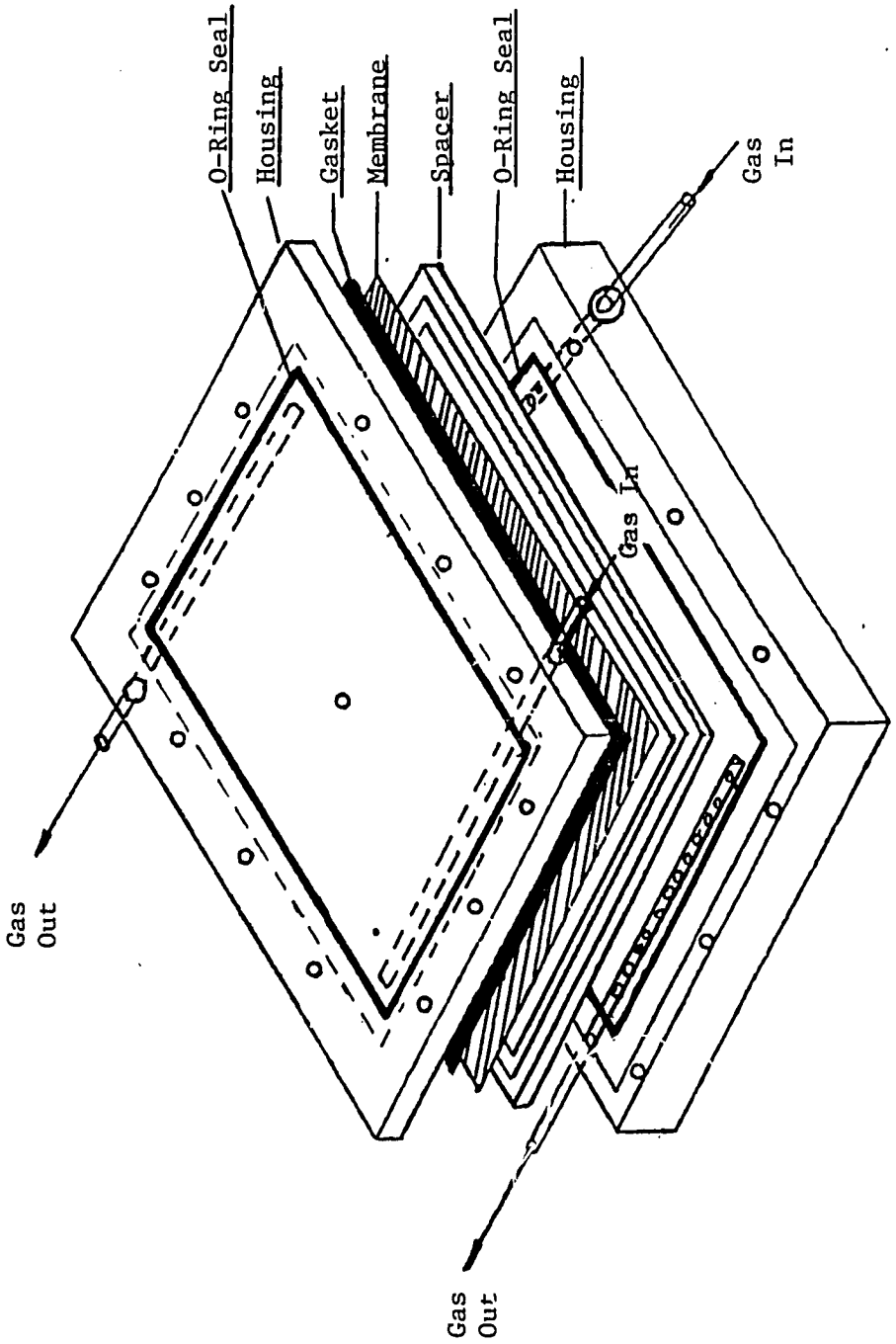

Figure 3-3: Schematic of Permeation Cell

membranes. A fully hydrated Nafion 117 membrane of approximately 70 cm^2 which had been prepared according to the procedure presented in either Section 3.1 or Section 3.2.1 was removed from the solution in which it was stored and blotted dry. The permeation cell, shown in Figure 3-3 (details are in Appendix C), was prepared for the membrane by applying a thin coat of stop-cock grease to the outer edges of all gaskets. The membrane was placed quickly onto the spacer in the cell, covered with gaskets and enclosed in the cell housing, whose screws then were tightened. The cell was placed horizontally into the experimental apparatus shown in Figure 3-2.

The next two steps were to ice down the product knock-out vessel and to replace the magnesium perchlorate (Fisher Scientific, reagent grade, anhydrous, Code M-54, E41, UN 1475) in the product drying tube, if required. These two steps helped to insure that only dry gas would enter the CO_2 Infrared Analyzer (Horiba PIR-2000, 3 range, max range 0-1% CO_2, with digital readout in $\%CO_2$). This analyzer is the most expensive and important part of the system. Water was an undesirable component in the gas to be analyzed because (1) part of the infrared absorption spectra of water overlaps that of CO_2 which interferes with an accurate reading of the amount of light absorbed by the CO_2 alone and (2) any condensation of water on the windows in the analyzer damages them which results in an inaccurate amount of light passing through them to be measured.

Next, the gas spargers were filled with distilled water to a height of approximately six inches. The inner tubes of these spargers were tipped with

medium density fritted glass when being used in distilled water. In the case when salts were used, the salts precipitated out onto the inner surfaces of the inner glass tube which partially clogged the tube during the experiment. The clogging was minimized by using an open-ended 1/4" tube for these experiments.

After the gas spargers were filled, the water bath (Blue M, "MagniWhirl" Constant Temperature Bath, Model MW-1130A-1, maximum capacity = 14.1 gal) was filled completely with distilled water. All apparatus within the bath, which included the gas spargers and knock-out vessels for the inlet gas streams, knock-out vessels for the outlet gas streams and the permeation cell, were covered completely with water. The dial on the bath was set at the temperature specified for the upcoming experiment. A mercury thermometer located within the bath was used to measure the temperature.

While the water bath temperature was stabilizing, the flow path of the sweep gas and both halves of the permeation cell were purged with N_2 (departmental) at 1 atm. With the N_2 source pressure set at 50 psig, the N_2 sweep gas was controlled at 100 std cm^3/min with a N_2 flowmeter/controller (Brooks 5850 Series with Model 5878-A1B1, 4 channel power supply). All flowmeter/controllers were operated with an upstream pressure of 50 psig, unless otherwise noted.

Approximately 50 std cm^3/min of this sweep gas was by-passed to the feed side of the permeation cell and discharged through port 6 (Figure 3-2). The rotameter, (FI), (Lab Crest, Div. F & P. Co., Meter Tube Cat. No. 448-035 with

1/16" SS float) and control valves 1 (CV 1) and 2 (CV 2) (Figure 3-2) were used to adjust this rate and, at the same time, to maintain a back-pressure of approximately 1" of water on the feed side of the membrane. Unless otherwise noted, under flow conditions, this back-pressure was maintained. Application of this pressure effectively forced the entire surface of the membrane onto the teflon cross support, which divided the two halves of the cell, thereby eliminating any tendency of the membrane to flex against either side of the cell.

The remaining 50 std cm^3/min, after being used to purge the sweep side of the system, was passed through the CO_2 analyzer, whose output signal was relayed to a chart recorder (Soltec Model 1242, 2 channel). The CO_2 concentration of the N_2 purge gas was continuously monitored for at least one hour. During this period of time, the recording would show a drop in the CO_2 concentration of the purge gas from approximately 330 ppm to 50 ppm. When the recording indicated the latter CO_2 concentration, the flow of the purge gas was diverted through port 2, an exit port located immediately upstream of the analyzer.

The purging of the system, described in the preceding two paragraphs, was continued for at least one day up to several days until the membrane reached equilibrium with the purge gas. This period of time was approximated as the period during which representative membrane samples would reach equilibrium after being exposed to the same changes in relative humidity. The experimental procedure used to determine these periods of time was previously described in Section 3.6.

The remaining steps in the experimental procedure involved the continuous flow of the feed gas but were not started until after the aforementioned time required for equilibration of the membrane had passed because of the relatively small amount of time, 30 minutes to 1 hour, required to complete them. While the nitrogen purge gas continued to flow through the system, the ice bath was refilled and the drying tube was replaced, if necessary. Next, the flowmeter/controllers were used to measure either 100% CO_2 gas (departmental) or to mix streams of N_2 (departmental) with 100% CO_2 gas, 10% CO_2 or 1420 ppm CO_2 gas. The CO_2 concentration and flowrate of this feed gas was equal to that which was required in the current experiment. The gas was passed through the feed gas sparger and knockout vessel and then was discharged through port 3.

The aforementioned gas was continually discharged through port 3 until its relative humidity reached a steady state value at which time it was ready to be used in the experiment. An in-line relative humidity probe (Vaisala Model HMP 32 UT Probe with HMI 32 Indicator and HMS 13A Selector), which was permanently located in the feed gas knock-out vessel, measured the relative humidity of this gas. The output signal from the probe was relayed to the second channel of the chart recorder which was previously described in this section. Similarly, the relative humidity of the purge gas was measured with another of the same type in-line relative humidity probe, which was permanently located in the sweep gas knock-out vessel.

The final step to be completed before the membrane was exposed to the feed gas was to determine the base CO_2 concentration in the system. The flow through port 2 was redirected to flow through the analyzer and out through port 1. The total sweep gas flowrate was increased to the rate required in the experiment while CV1 and CV2 were adjusted until a flowrate of approximately 100 std cm^3/min was indicated on the rotameter. The CO_2 concentration in the sweep gas and its relative humidity was monitored for approximately 30 minutes until a new lower base equilibrium CO_2 concentration value, C_{base}, of approximately 5 ppm to 30 ppm, and a constant relative humidity value was shown by the recordings.

After steady state conditions of the system were noted, the system was prepared for exposure to the feed gas. The chart recorder speed was set at a rate that enabled an accurate recording of the elapsed time and was run for about a minute before the experiment was started. The following steps were completed in 15 to 30 seconds. A starting point was marked on the chart while simultaneously noting the time in seconds. The bypass valve was closed before opening the inlet valve to the feed side of the cell. Finally, port 3 was closed while simultaneously noting the time in seconds. The time elapsed between marking the chart and closing port 3 is defined as the feed lag time, t_{lag}. CV1 and CV2 were immediately adjusted, if necessary, to maintain the original flowrate through the analyzer and to maintain the original feed side pressure.

The CO_2 concentration of the sweep gas was continuously recorded until it reached a steady state value, C_{ss}, at which time the chart speed was reduced. The

measured values of concentration, C_{ss} and C_{base}, were used in the following equation to calculate the flux of the permeant, N:

$$N(\text{std cm}^3/\text{s-cm}^2) = \frac{Qsweep(scc/s)*(C_{ss}-C_{base})(\%CO_2)}{A(cm^2)} \qquad (3\text{-}13)$$

where Q is the volumetric flowrate of the sweep gas, which was the value shown on the flowmeter/indicator. The surface area, A, is the area of the inner open portion of the membrane spacer. The flux of nitrogen (N_2) compared to that of CO_2 was assumed negligible based on the 50 times greater solubility of CO_2 in water versus nitrogen and the relatively large volume of N_2 sweep gas. The N_2 flux through a similar cation exchange membrane was negligible compared with that of CO_2 (LeBlanc et al., 1980). The remaining step in the permeation experiment is described in Section 3.8.

3.7.3 Permeation Cell Design

The cell (Figure 3-3) was designed by the author and constructed by in-house Science Instrument Maker II, Larry Larson. Mass transfer calculations were made to determine the dimensions of the cell required to ensure that gas phase mass transfer resistances would be negligible. The dimensions of the mass transfer volume on each side of the cell are 2.25 in wide by 3 in long by 0.125 in deep. The permeation area is 32 cm^2. The cell inlet and outlet distribution system each consists of 9 - 1/8 inch holes to aid thorough mixing of the gases. Initial experiments with

the cell confirmed that gas phase mass tranfer resistance was negligible under the flow conditions of 100 std cm^3/min for the feed and sweep gas for experiments with the H+ form membrane and flowrates of 1000 std cm^3/min for the feed and 100 std cm^3/min for the sweep gas for experiments with the EDA loaded membranes. These flowrates were constant for each type of experiment.

The membrane is sandwiched between two gas-tight Viton gaskets. A teflon "cross" 0.03125 in thick with solid surface area 2 cm^2 provides support for the membrane.

All tubing was of 1/4 " I. D. teflon of 1/4 " stainless steel, except for the exiting and entering lines to the gas spargers and knock-out vessels which were of 1/4" I.D. tygon tubing connected to 1/4" O.D. glass tubing. All teflon to teflon, teflon to stainless steel or teflon to tygon tubing connections were made with "Swagelok" fittings. "Swagelok" connections on glass tubing used teflon ferrules. Whitey valves were used only as general block valves and not as positive shut-off valves because they leaked. Glass "Pyrex" stop-cock valves were used to provide positive shut off of gas streams. The CO_2 analyzer, flow controllers, chart recorder, relative humidity probes and water bath were calibrated periodically. The calibration procedures are presented in Appendix A. The calibration of the instruments, whose procedure is described in the aforementioned section, was checked at the start of each experiment.

3.8 Diffusion Coefficient and Apparent Diffusion Coefficient

After the last procedure described in Section 3.7, whereby the steady state of CO_2 concentration of the sweep gas measured, was completed, the diffusion coefficient of CO_2, D_{CO_2}, was measured. The case of unsteady state diffusion has been solved for a flat membrane, assuming Henry's Law type sorption, constant D, i. e. independent of concentration, and a linear concentration distribution for the steady state (K. D. Ziegel, et al. 1969), to give the following equation:

$$\overline{D} = \frac{L^2}{7.199 t_{1/2}} \qquad (3\text{-}14)$$

The half-time, $t_{1/2}$, is defined as the time at which the value of the permeant concentration in the gas which is emerging from the permeation cell reaches half of its steady state value. This equation applies equally well to both the case of the nonreactive, sulfonic acid form and the reactive EDA form. In the latter case, the reaction between EDA and or $EDAH^+$ and CO_2 is instantaneous and reversible (Weiland and Trass, 1971; Jensen and Christensen, 1955). Therefore, equilibrium exists at all points within the membrane and the diffusing species are not affected by the concentration. CO_2 has also been shown to follow Henry's Law type sorption in both water (Weast, 1974) and EDA (Weiland and Trass, 1971).

The half-time, is corrected for the feed lag time, t_{lag}, and the half-time of the system, $t_{1/2,ss}$, such that

$$t_{1/2} = t_{1/2,exp} - t_{1/2,ss} - t_{lag} \quad (3\text{-}15)$$

The measurement of t_{lag} was previously described in Section 3.7. $t_{1/2,exp}$ is defined as the time elapsed in the unsteady state experiment between the recording of 1/2 of (C_{ss}+C_{base}) and the start of the experiment. $t_{1/2,ss}$ is associated with the analyzer response time and the time elapsed between when the sweep gas exits the permeation cell and enters the analyzer.

To obtain the value of $t_{1/2,ss}$, the following procedure was performed after the last step described in Section 3.7. First, the sweep gas was diverted through port 5. The portion of the product line located downstream of port 5 was purged by introducing approximately 100 std cm^3/min of 100% N_2 (industrial grade, 99% N_2) into the line at a point located immediately downstream of port 5. This purging was continued until the CO_2 concentration of the purge gas exiting the analyzer reached a value which was slightly less than the original value of C_{base}. After this value was noted, with the chart speed reset at a rate which enabled an accurate recording of the elapsed time, the port for the N_2 purge gas was closed before redirecting the sweep gas through the analyzer. The CO_2 concentration of the sweep gas was recorded continuously until the recording showed a steady state value. After this value was noted, the chart speed was reduced again. The time elapsed between the recording of 1/2 of (C_{ss} + C_b) and the original value of C_{base} in the steady state experiment is defined as the half-time of the system, $t_{1/2,ss}$.

The system was put back into the purge mode before the next phase of the experiment was started. The feed entrance port to the permeation cell was closed while simultaneously diverting the feed gas through port 3. The feed gas concentration and flowrate was set at 100% N_2 (industrial grade, 99% N_2) and 50 std cm^3/min, respectively. The sweep gas flowrate was set at 100 std cm^3/min. Approximately 50 std cm^3/min of this sweep gas was by-passed to the feed side of the permeation cell and discharged through port 6. The remaining 50 std cm^3/min, after being used to purge the sweep side of the system, was passed through the analyzer. The CO_2 concentration of the N_2 purge gas was continuously monitored for at least one hour. During this period of time, the recording would indicate a CO_2 concentration of at most 50 to 100 ppm. When the recording indicated this value, the flow of the purge gas was diverted through port 2. A separate stream of 100 std cm^3/min of 100% N_2 (industrial grade, 99% N_2) was used to rezero the analyzer. The purging of the system, described in this paragraph, and periodic measurements of the CO_2 concentration in the sweep purge gas were continued until the CO_2 concentration of the sweep purge gas reached a new base value of 5 to 30 ppm.

When the recording indicated the aforementioned CO_2 concentration, the second phase of the permeation experiment, described in this paragraph, was started. The procedures followed were those which were described previously in this section beginning with the setting of a new or repeated CO_2 concentration and flowrate of the feed gas which was equal to that which was required in the current experiment and ending with putting the system back into the purge mode. The

procedures in this phase were repeated every time the effects of a different CO_2 concentration or a repeated CO_2 concentration was studied.

After the effect of CO_2 concentration of the feed gas was studied for a given membrane and relative humidity condition, the third phase of the permeation experiment was started. With the system in the purge mode, the liquids in the feed and sweep gas spargers were replaced with a different solution. The solutions, listed in Table 3-1 in Section 3.6, are shown in the order in which they were used. The remaining procedures followed were those described previously in this section beginning with purging the system over a period of time during which the membrane reached equilibrium under the new relative humidity condition and ending with putting the system back into the purge mode. The procedures in phase two were repeated every time the effects of a different CO_2 concentration or of a repeated CO_2 concentration of feed gas were studied. The procedures described in this paragraph were repeated when the effects of a different condition of relative humidity was studied.

After the effects of CO_2 concentration and relative humidity were studied for a given membrane, the system was shut down. The shut down procedures were to stop the gas flows, to turn off and drain the water bath and to remove the permeation cell from the system, in that order.

3.9 CO_2 Solubility

From the measurements of permeability and diffusion coefficient previously described, an implied solubility was calculated as follows. The solubility, S, was determined from the relation P=DS (Crank and Park, 1968). Rearranging this relation gives

$$S=\frac{P}{D} \tag{3-16}$$

where P is determined under conditions where the downstream CO_2 partial pressure is approximately zero.

A normalized CO_2 solubility per ion exchange site, S_{site} (gmol CO_2/gmol site), was calculated from:

$$S_{site}=\frac{P(p_2)(EW)}{D(\rho_p)(\nabla)_{ID}} \tag{3-17}$$

where ρ_p is the density of the dry membrane (g/cm^3) and ∇_{ID} is the molar volume of the permeant (cm^3/gmol). In the case of the EDA loaded membrane, the normalized CO_2 per gmol of EDA, S_{EDA}, was calculated by dividing Equation (3-17) by the membrane loading, L_m (Equation 3-1), and using the measured densities of the respective membranes:

$$S_{EDA} = \frac{P(p_2)(EW)}{D(\rho_p)(V)_{ID}L_m} \qquad (3\text{-}18)$$

3.10 Equilibrium Constants of CO_2-$EDAH^+$ and CO_2-EDA-$EDAH^+$ Reactions

The reaction between CO2 and EDA and or EDAH+ (Weiland and Trass, 1971; Jensen and Christensen, 1955) is an instantaneous, reversible reaction. In this case, the bulk of the liquid will be at equilibrium (Danckwerts, 1970). Therefore, equilibrium theory can be applied to the data obtained in this study.

The most probable reactions involved for each of the EDA loaded membranes are those shown in Equation 1-2 with 0.928 gmol EDA/gmol site and Equation 1-1 and 1-2 with 1.455 gmol EDA/gmol site.

The simplest case is that with 0.928 gmol EDA/gmol site. The EDA is essentially loaded in the monopositive form. Therefore, only one reaction need be considered. For this reaction in solution, the equilibrium data of Jensen and Christensen can be used to obtain an equilibrium constant of 2.435 atm^{-1} at 25 °C.

In the case of the membrane environment, the assumption of equilibrium can be made and an equilibrium constant for Equation 1-2, Keq_2, can be calculated from the follwing relation:

$$Keq_2=\frac{[^+H_3N(CH_2)_2NHCOO^-][EDAH_2^+]}{[EDAH^+]^2[pCO_2]} \qquad (3\text{-}19)$$

The total concentration of carbamate in the membrane is approximately equal to the solubility of CO_2. The remainder of the concentrations can be obtained by material balance. The values of Keq for the reaction in liquid solution and in a solution filled membrane can be compared.

After solving for Keq_2 at a measured solubility of CO_2 and CO_2 pressure, this equation can be used to predict the solubility of CO_2 at other CO_2 concentrations. These solubility values can then be used in Equation 3-12 with the measured value of diffusion coefficients to obtain predictions of permeability and/or flux.

The more complicated case is that with 1.455 gmol EDA/gmol site. The EDA is loaded in both free EDA and monopositive EDA. Therefore, the equilibria of Equation 1-1 and 1-2 needs to be considered. The equilibrium relation for Equation 1-2 is shown in Equation 3-19. The equilibrium constant for Equation 1-1, Keq_1, can be calculated from the follwing relation:

$$Keq_1=\frac{[^+H_3N(CH_2)_2NHCOO^-]}{[EDA][pCO_2]} \qquad (3\text{-}20)$$

In order to determine the concentration of EDA, the equilibria of Equation 1-1 and 1-2 are solved simultaneously. By defining reaction coordinates, e_1 for Equation 1-1 and e_2 for Equation 1-2, the concentrations (gmol/gmol total EDA) of all species can be defined by the following set of relations:

$$[^{+}H_3N(CH_2)_2NHCOO^{-}] = e_1+e_2 \quad (3\text{-}21)$$

$$[H_2N(CH_2)_2NH_2] = 0.34-e_1 \quad (3\text{-}22)$$

$$[^{+}H_3N(CH_2)_2NH_3^{+}] = e_2 \quad (3\text{-}23)$$

$$[H_2N(CH_2)_2NH_3^{+}] = 0.66-2e_2 \quad (3\text{-}24)$$

The concentration of EDA (gmol EDA/gmol total EDA) is equal to the initial concentration of free EDA (gmol /gmol total EDA) minus an amount e_1 . The amount e_1 is the reaction coordinate for Equation 1-1. For a measured value of total solubility, (e_1+e_2), and the value of K_{eq2}, e_2 can be solved for from Equation 3-19. e_1 can then be determined by difference and used in Equation 3-20 to solve for the value of K_{eq1}. The equilibrium constant for Equation 1-1 is then known and can be used to predict the solubility of CO_2 at any CO_2 concentration. These solubility values can then be used in Equation 3-12 with the measured value of diffusion coefficients to obtain predictions of permeability and/or flux.

Chapter 4

Results and Discussion

4.1 Solution - Membrane Equilibrium : EDA and Water Content

Equilibrium loading experiments were performed to provide an estimate of the EDA concentration in the membranes used in the permeability studies. The data (Figure 4-1) are correlated empirically by:

$$L_m = 0.967 + 0.102 \log C_s + 0.3 C_s \qquad (0 < C_s \leq 2.11) \qquad (4\text{-}1)$$

$$= 1 + 0.3\, C_s \qquad (C_s > 2.11) \qquad (4\text{-}2)$$

where

L_m=membrane EDA loading, gmol/gmol site

C_s=solution EDA concentration, gmol/l

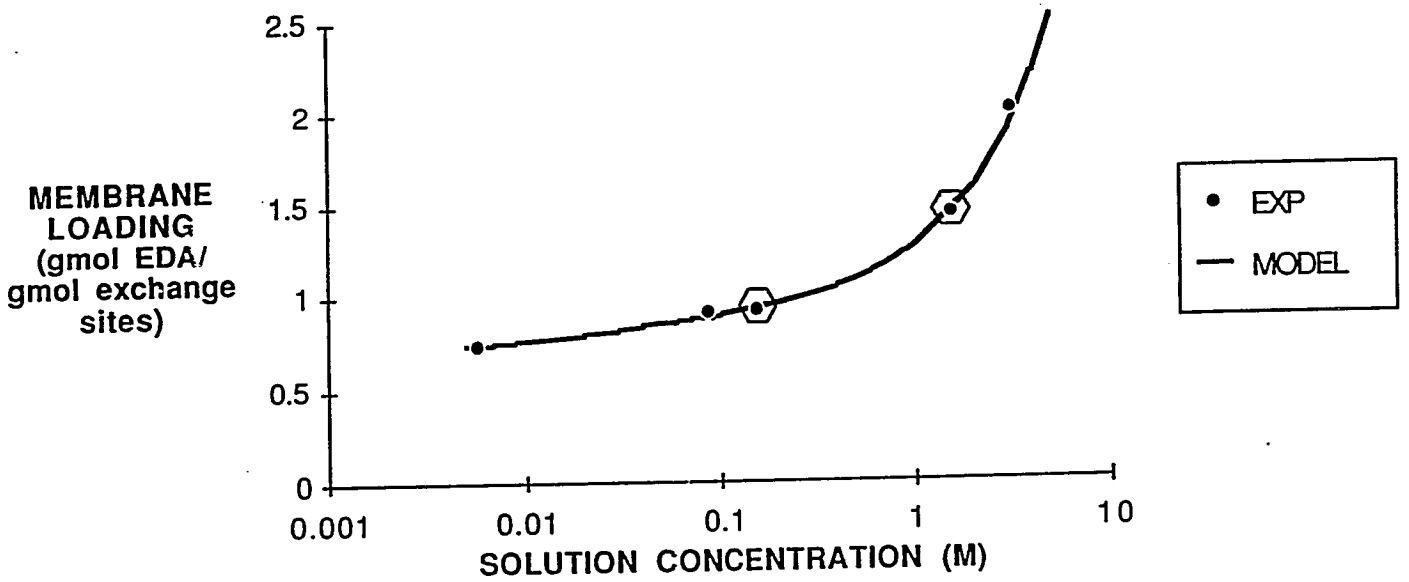

Figure 4-1: Equilibrium Loading of Nafion 117 with Ethylenediamine, Total Exchange Sites per membrane=0.0016 gmol, Equivalent Weight, H^+=1100 g/gmol exchange sites

A possible interpretation of this result is that the third term of Equation (4-1) represents free EDA in the membrane while the first two terms represent EDA cations, such as $EDAH^+$, associated with ion exchange sites.

The total EDA loadings for the membranes used in the CO_2 transport studies are shown in Table 4-1 with calculated values of free EDA loading, water content and membrane "effective" EDA concentration. The water content of the membrane decreased by 25% as the solution EDA concentration increased from zero to 1.5 M EDA. Sata et al. (1983) showed comparable effects of NaOH solution on a similar perfluorsulfonate, Na^+ ionomer membrane.

The water content, 36 wt%, in the H^+ form compares with that of 34 wt% measured by Gierke et al. (1981) for 1200 EW Nafion, H^+. The water content is greater for the H^+ form than for membranes with EDA. Greater water content is expected when the membranes are contacted with solutions of greater water activity, i. e. pure water.

Table 4-1. EDA Loading and Water Activity in Nafion 117 Equilibrated with Solution (25°C)

Solution		Membrane				
EDA Concentration (M)	Water Activity[b]	EDA Concentration ($gmol/kgH_2O$)	(gmol /site) Total	Free	Water (g/100g dry)	"Effective" Water Activity
0[a]	1	0	0	0	36	1
0.15	0.999	3.40	0.928	0.046	28	0.999
1.50	0.999	5.33	1.455	0.455	27	0.997

[a] Boiled 1 hour in distilled water, H^+ form

[b] Calculated from VLE data for H_2O-EDA (Schmelzer et al., 1973)

4.2 Effect of Relative Humidity on Water Content

Water desorption experiments (Figure 4-2) were performed in order to correlate the internal changes of the membrane with the effects on transport parameters of the membranes used in the permeability studies at reduced relative humidities.

When fully hydrated hydrated membranes were exposed to 100% relative humidity, the H^+ form and the membrane with 0.928 gmol EDA/gmol site lost water while the membrane with 1.455 gmol EDA/gmol site gained water. A solution layer was evident on the surface of this membrane. When patted dry it had the same weight as in the fully hydrated state.

The water content of each membrane followed similar trends at the higher relative humidities, decreasing 60% to 70% from the water in the fully hydrated state as the relative humidity was decreased to 80% relative humidity. Between 80 to 33% relative humidity, the water content in the H^+ form membrane decreased by 80%, whereas the water content in the membrane with 0.928 gmol EDA/gmol site decreased by only 25%. Below 33 to 0% relative humidity, the water content of all membranes decreased to zero. The H^+ form membrane contained <1% water at 11% relative humidity.

The desorption isotherm for the H^+ form (Figure 4-2), analyzed with BET adsorption theory (Brunauer, 1943), implies a surface area of 141 m^2/g dry

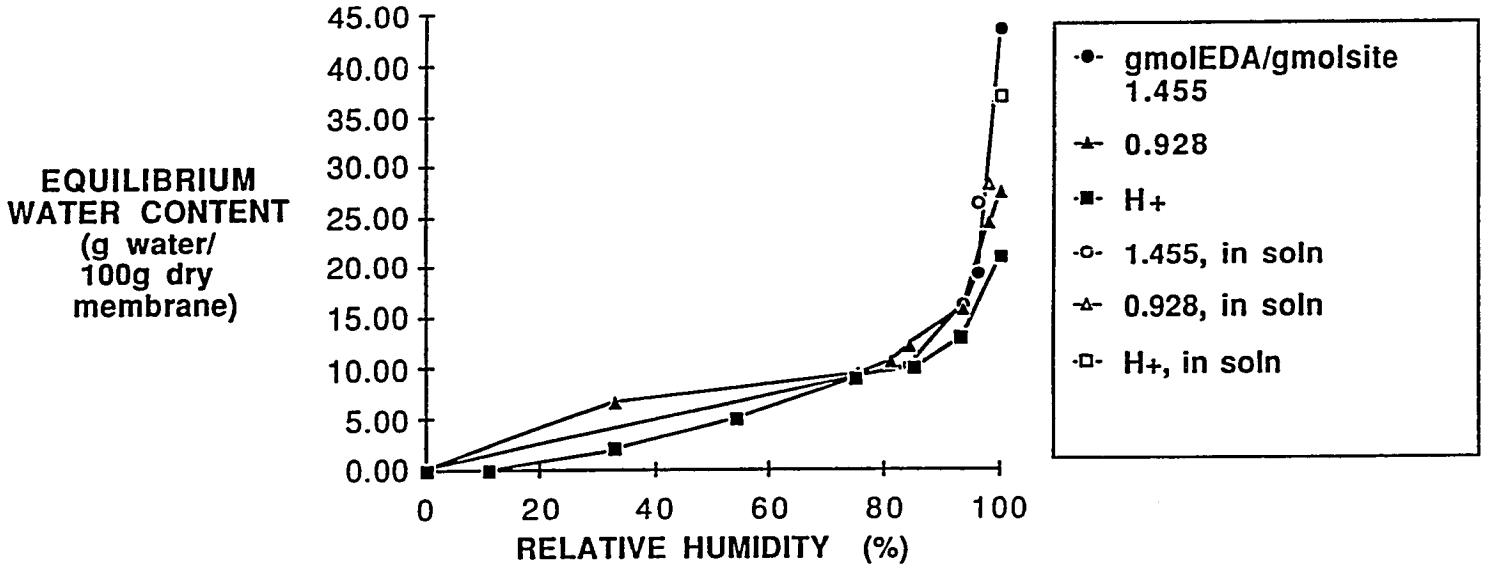

Figure 4-2: Water Desorption Isotherm of Nafion 117, H^+ Form and With EDA, 25°C, 1 atm.

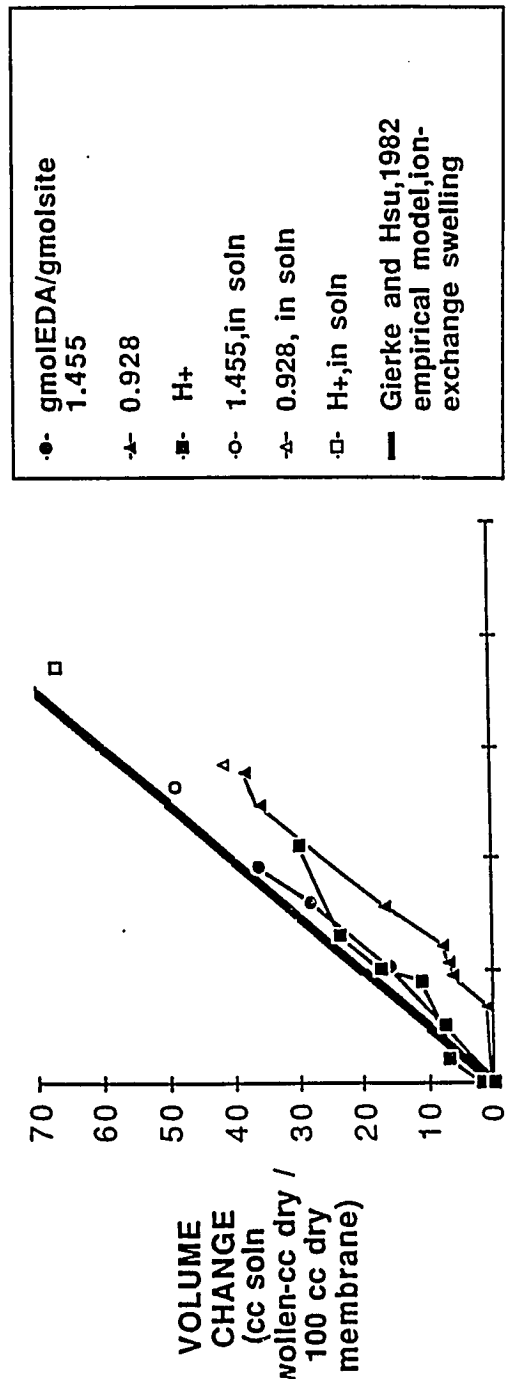

Figure 4-3: Swelling of Nafion 117, H^+ Form and With EDA, 25°C, 1 atm

polymer. We obtained a second estimate of 265 m^2/g dry polymer by calculating the total surface area of the ionic clusters. For this calculation, the diameter and density of the ionic clusters of dry 1200 EW Nafion were obtained from Gierke and Hsu (1982) and corrected for 1100 EW.

4.3 Effect of Relative Humidity on Swelling

For each measurement of water content (Figure 4-2), the change in volume was measured in order to correlate any density changes in the membranes. The correlation of volume change, ΔV (cc), with water content, Δm (g), is given in Figure 4-3. The volume change increased for all three membranes with increasing water content. A $\Delta V/\Delta m$ ratio of approximately 1.95 was obtained with 1.455 gmol EDA/gmol site over the entire range of water content.

The ratio for the H^+ form membrane alternated between 1.9 and 1 in different regions of water content. The membrane with 0.928 gmol EDA/gmol site behaved in a similar manner to the H^+ form, except that no significant increase in volume occurred between water contents of 0 and 7.5%.

In the fully hydrated case, the H^+ form swelled the most because of its larger water content. The volume increase of 68% is very close to that measured by Gierke and Hsu (1982) of 70% for 1200 EW Nafion.

At 100% relative humidity, the H^+ form swelled the least. This may occur because the smaller H^+ cations can hydrate a larger number of water molecules, effectively preventing them from participating in osmotic swelling effects (Komoroski and Mauritz, 1982).

The observed behaviour of the H^+ form and the membrane with 1.455 gmol EDA/gmol site is very close to the model of Gierke and Hsu (1982) which assumes that each increment of water will add the equivalent volume of pure water. This model gives a line with a slope of 1.95 on Figure 4. However, the offset in water content for the membrane with 0.928 gmol EDA/gmol site cannot be predicted by this simple model.

4.4 Transport Measurements in the H^+ Form of Nafion

The flux, permeability and effective diffusion coefficient of CO_2 in the H^+ form of Nafion 117 were measured at 0 to 100% relative humidity and 0.03 to 1 atm CO_2 in the feed gas (Figures 4-4, 4-5 and 4-6) at 25°C. The implied solubility derived from these measurements is given in Figure 4-7. The results with fully hydrated Nafion are compared in Table 4-2 with previous work on O_2 and H_2.

4.4.1 Effect of CO_2 Content

The CO_2 permeability and diffusion coefficient were basically independent of the CO_2 driving force. The CO_2 flux was directly proportional to the CO_2

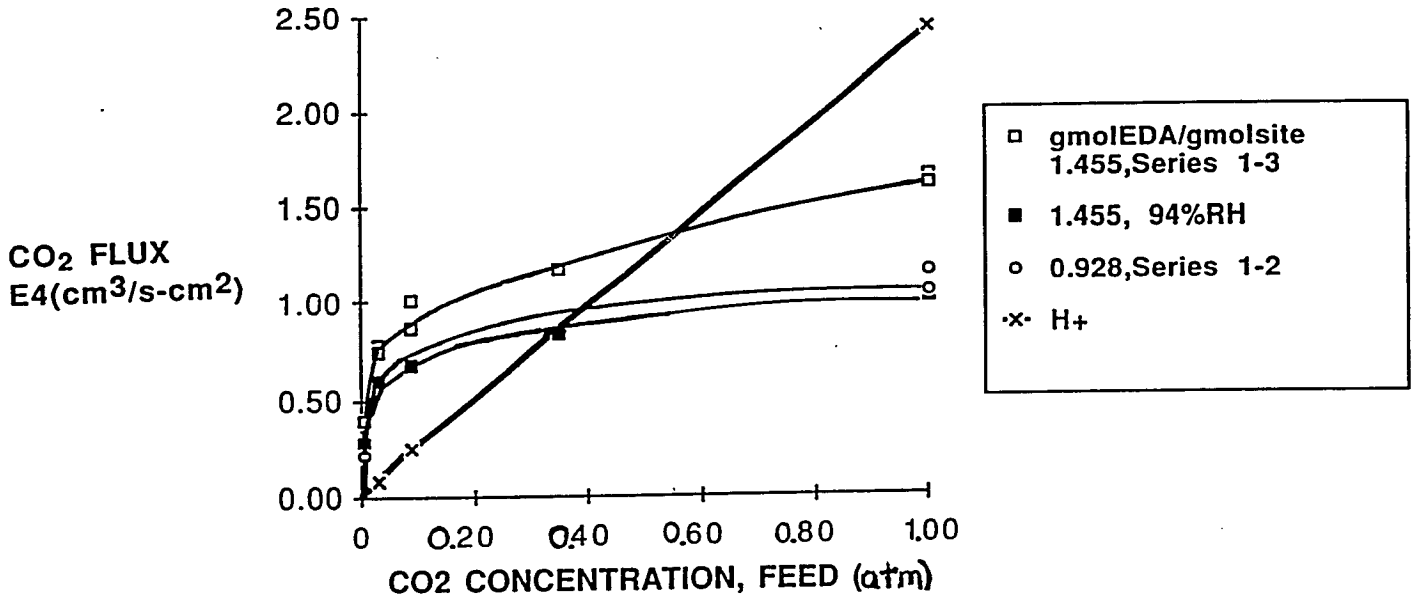

Figure 4-4: Effect of CO_2 Concentration, Loading and Series on Flux in Nafion 117, H^+ Form and With EDA, 100% Relative Humidity, 25°C, 1 atm

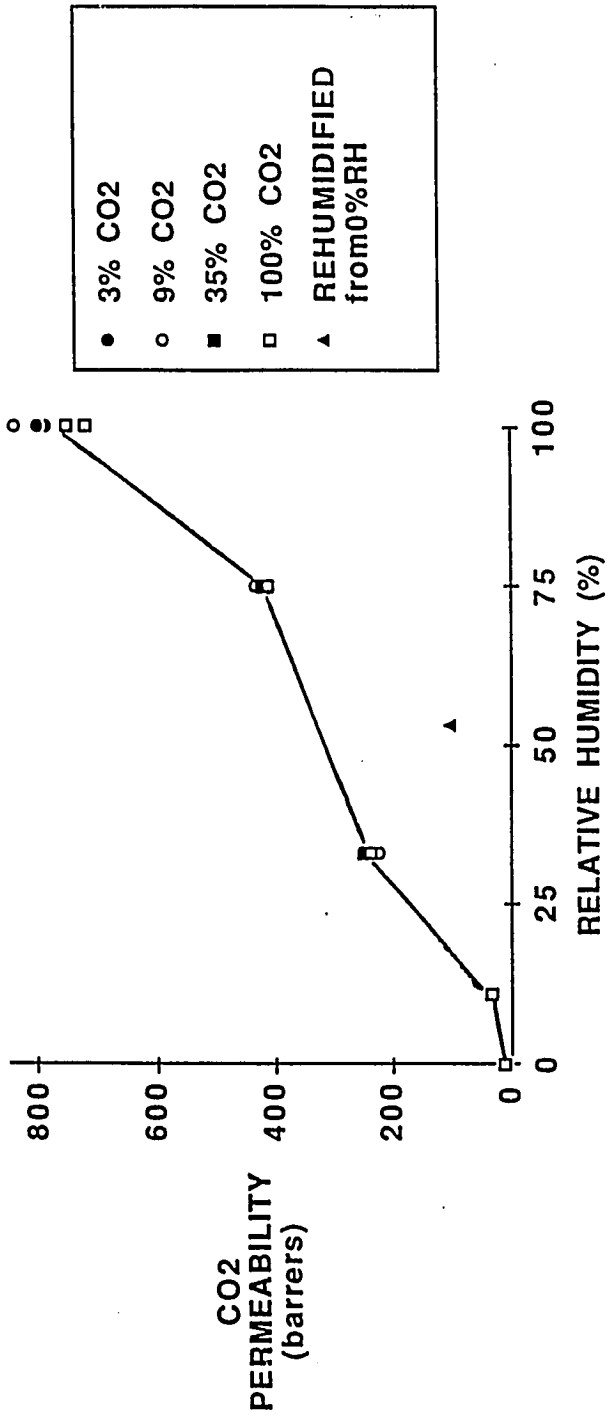

Figure 4-5: Effect of Decreasing Relative Humidity on Permeability of Nafion 117, H^+, 25°C, 1 atm, 3-100% CO_2

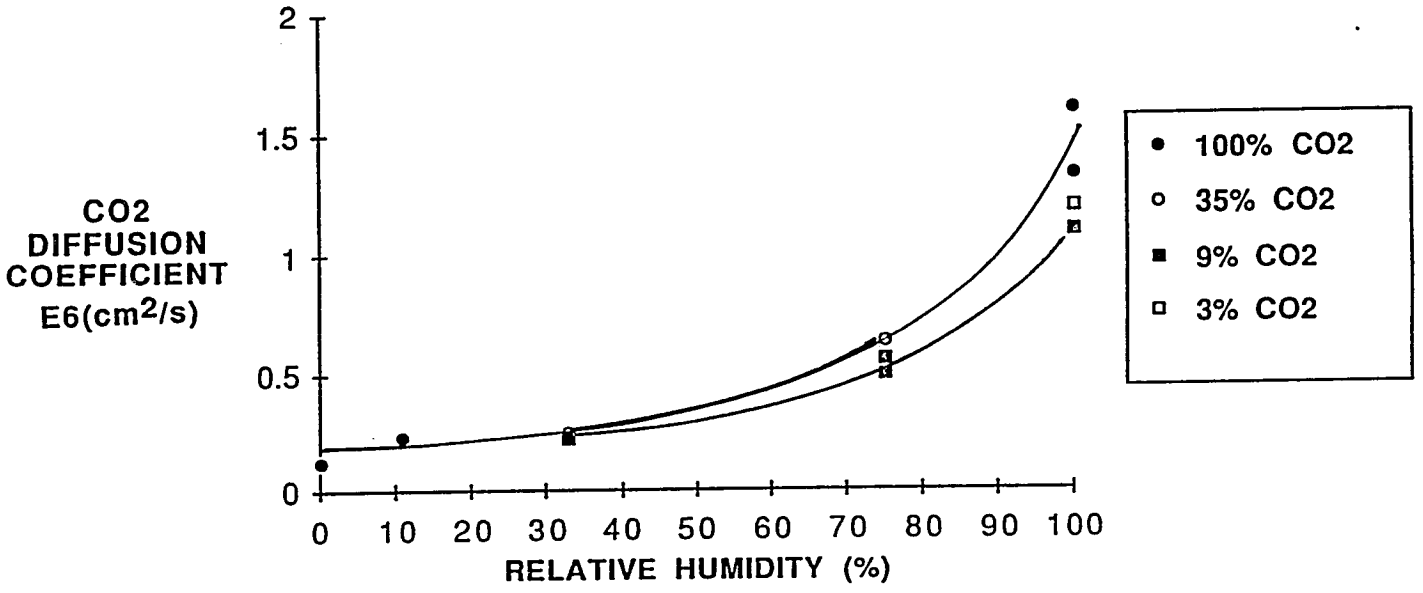

Figure 4-6: Effect of Decreasing Relative Humidity on CO_2 Diffusion Coefficient in Nafion 117, H^+, 25°C, 1 atm, 3-100% CO_2

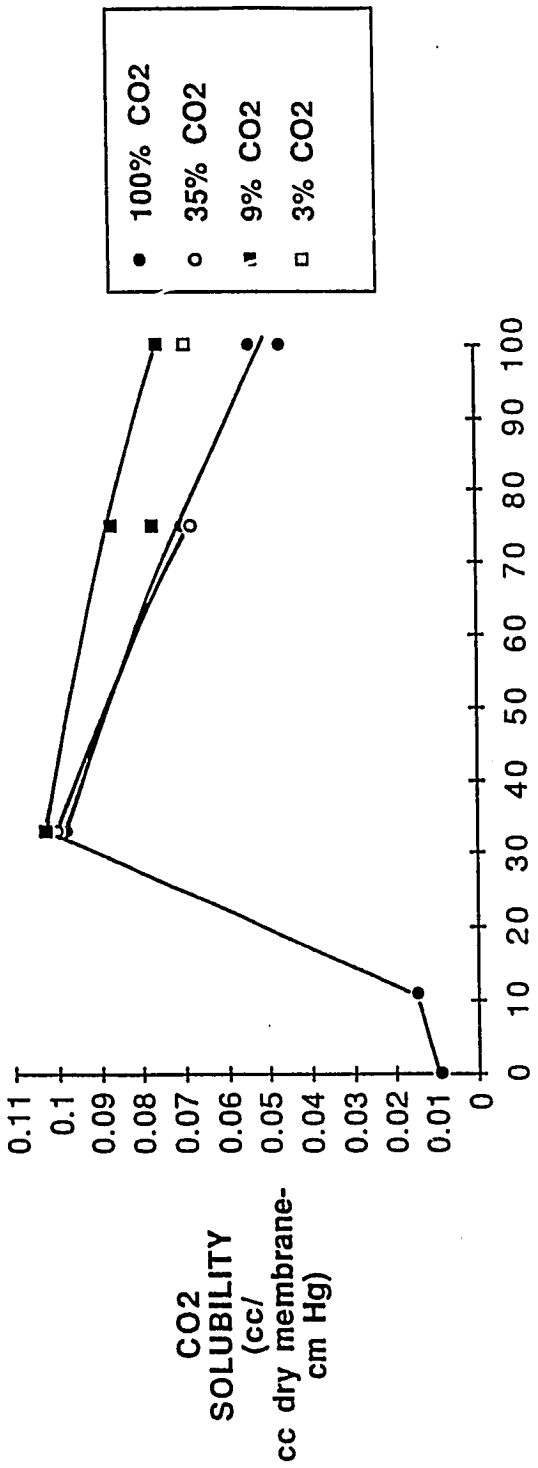

Figure 4-7: Effect of Decreasing Relative Humidity on CO_2 Solubility in Nafion 117, Hr, 25°C, 1 atm, 3-100% CO_2

Table 4-2. Permeability, Diffusion and Solubility Data for CO_2, O_2 and H_2 in Nafion, H^+-form and in water at 25°C

Gas_i	Permeability (barrers)		Diffusion Coefficient $*10^6(cm^2/s)$		Gas Solubility $*10^4(scc/cm^3\text{-cm Hg})$	
	Nafion	Water	Nafion	Water[e]	Nafion[d]	Water[f]
CO_2[a]	897	2090	1.5	20.7	607.0	101.0
O_2[b]	23	88	2.6	22.0	9.0	4.0
H_2[c]	45	149	----	59.5	------	2.5

[a]This study. 34 wt% water, Nafion 117, H+
[b]Sakai et al. (1986). 35 wt% water, Nafion 117, H+
[c]Sakai et al. (1986). 35 wt% water, Nafion 125, H+
[d]$S_i = (P_i/D)$ measured
[e]Published data, Bolz and Tuve (eds.) (1973)
[f]Published data, Weast (ed.) (1974)

concentration. This behaviour is consistent with Fickian diffusion and with well-behaved linear solubility of the CO_2 in the membrane.

4.4.2 Effect of Relative Humidity

At 100% relative humidity, the CO_2 permeability was about 750 barrers (1 barrer = 10^{-10} (scc-cm)/(cc-cm^2-ΔcmHg)). This value is five times greater than 160 barrers measured in the Na^+ form of Nafion 117 by Way et al. (1987). Permeabilities in the H^+ form twice that in the K^+ form of Nafion have been measured for O_2 and H_2 (Sakai et al., 1985, 1986) under comparable conditions. K^+ is similar to Na^+ in its physical properties. The larger increase seen for CO_2 in the H^+ form versus Na^+ suggests a greater affinity (solubility) of the polar CO_2 with the sulfonic acid form of Nafion versus that of H_2 or O_2. Therefore, the H^+ form should be more appropriate for gas separations.

The permeability in the fully hydrated (34 wt% water) membrane was 900 barrers. This is much higher than in vacuum dried Nafion (1.74 barrers, 25°C, Paul and Chiou, 1987). Typical CO_2 permeability in other glassy polymers varies from 0.2 to 80 barrers (35°C) (Chern et al., 1984).

In the fully hydrated membrane, the effective CO_2 diffusion coefficient was 1.48 *10^{-6} cm^2/s, about ten times less than that in water. As shown in Table 2, the CO_2 diffusion coefficient is comparable to that of O_2 and H_2 (Sakai et al., 1986) measured in Nafion at similar conditions (see Table 4-2). Several self diffusion

coefficients of cations such as Na^+, K^+ and Cs^+ are also reduced by about a factor of 10 in Nafion membranes (Yeager, 1982). Escoubes and Pineri (1982) showed by NMR that water mobility within the hydrated spheres of the ions in Nafion is on the order of the observed mobility in water. Therefore, the effective diffusion coefficients are smaller probably because of membrane tortuosity.

The CO_2 permeability and diffusion coefficient decrease with decreasing relative humidity. This effect follows the same trend as swelling of the membrane by water absorption. Therefore, decreased diffusion coefficients probably result from increased tortuosity at reduced swelling. The value of D over the entire range of relative humidities is quite large.

Even at 0% relative humidity, Nafion gave a relatively large diffusion coefficient of $0.121 * 10^{-6}$ cm^2/s compared to $0.0115 * 10^{-6}$ cm^2/s determined for dry Nafion 117 (Paul and Chiou, 1987). This behaviour suggests that some water is contained in the membrane at 0% relative humidity and that this water is separated from the fluorocarbon phase. Although no water was detectable by weighing, NMR studies by Escoubes and Pineri (1982) showed that Nafion does not desorb all of its water until the membrane is heated and vaccuum dried above its glass transition temperature, 220°C. Studies by Gierke et al. (1981), using small-angle x-ray diffraction on Nafion, support the existence of phase separation at 0% relative humidity.

The effective diffusion coefficient decreased only slightly with decreasing relative humidity below about 55% relative humidity. This would suggest that the diffusion pathway is remaining relatively constant. Escoubes and Pineri (1982) have proposed that the ionic clusters in the acid form of 1200 EW Nafion remain of constant size from 0 to 9 wt% water content based on NMR studies. They propose that expansion of clusters inside the organic phase is occurring above 9 wt% water .

The implied CO_2 solubility in the fully hydrated Nafion was six times that in water (25°C) (Weast , 1974) and four times that in vacuum dried Nafion 117, H^+ (25°C) (Paul and Chiou, 1987). The hydrated form may allow for mobile polar interactions that are not possible in dry Nafion.

The implied CO_2 solubility in fully hydrated Nafion is 67 to 87 times that of O_2 and H_2 (Table 4-2), respectively. Therefore, CO_2 permeability is 39 to 64 times that of the non-polar gases. Selectivity for CO_2 over other non-polar gases, such as CH_4, should also be good. These selectivities are much greater than the 16 to 24 selectivity of CO_2/CH_4 achieved in the commercially used ester hollow fiber membrane (Parro and Hamaker, 1985). Other CO_2/CH_4 selectivities of solid polymer membranes are 26 to 30 for asymmetric, cellulose esters (Coady and Davis, 1982; Mazur and Chan, 1982; Schell and Houston, 1982; Berry,1981), 17 to 24 for polysulfone/silicone rubber (Henis and Tripodi, 1980), 18 for polyetherimide (Browall, 1979) and 10 for silicone rubber/polycarbonate (Ward, 1976).

The implied CO_2 solubility increased from 100 to 33% relative humidity. Below 33 and 11% relative humidity, the implied CO_2 solubility decreased. At 11% relative humidity, Nafion gave a CO_2 solubility of 0.014 scc/cc-cmHg which compares with 0.0157 scc/cc-cmHg determined for vacuum dried Nafion 117 (25°C) (Paul and Chiou, 1987).

The observed increase in CO_2 solubility coincided with decreasing membrane water content. Since the CO_2 solubility in water is less than that in dry Nafion, an increase may be expected with decreasing water content. However, because the CO_2 solubility in hydrated Nafion is 4 times greater than that in dry Nafion, a decrease would be observed at the relative humidity at which Nafion loses all of it water, 11% relative humidity.

4.5 Transport Measurements in EDA Form of Nafion

The flux, permeability and diffusion coefficient of CO_2 in Nafion 117 loaded with 0.928 and 1.455 gmol EDA/gmol site was measured at 0 to 100% relative humidity and 0.005 to 1 atm CO_2 in the feed gas (Figures 4-4, 4-8, 4-9, 4-10 and Table 4-3) at 25°C. The implied solubility derived from these measurements is given in Figures 4-11 and 4-12 and Table 4-3. The arrows in the figures designate the direction in which the CO_2 concentration was varied for a series of experiments 1 to 3, for a given membrane.

4.5.1 Effect of CO_2 Concentration

The CO_2 flux was a non-linear increasing function of the CO_2 concentration with 1.455 gmol EDA/gmol site. This behaviour indicates that a reaction is taking place, which is consistent with the facilitated transport mechanism. A discussion of carrier saturation at the gas-membrane interface will be presented in the section on reaction chemistry.

At 100% relative humidity, the CO_2 flux in the membrane with 1.455 gmol EDA/gmol site was approximately twice that with 0.928 gmol EDA/gmol site. The fluxes with both membranes were greater than in the H^+ form below 35 to 55% CO_2. Above these concentrations, the flux in the H^+ form was greater. Meldon et al. (1985) also measured lower permeability of CO_2 in a liquid membrane with MEA, DEA and or TEA in a solution of polyethyleneglycol (PEG) below that with

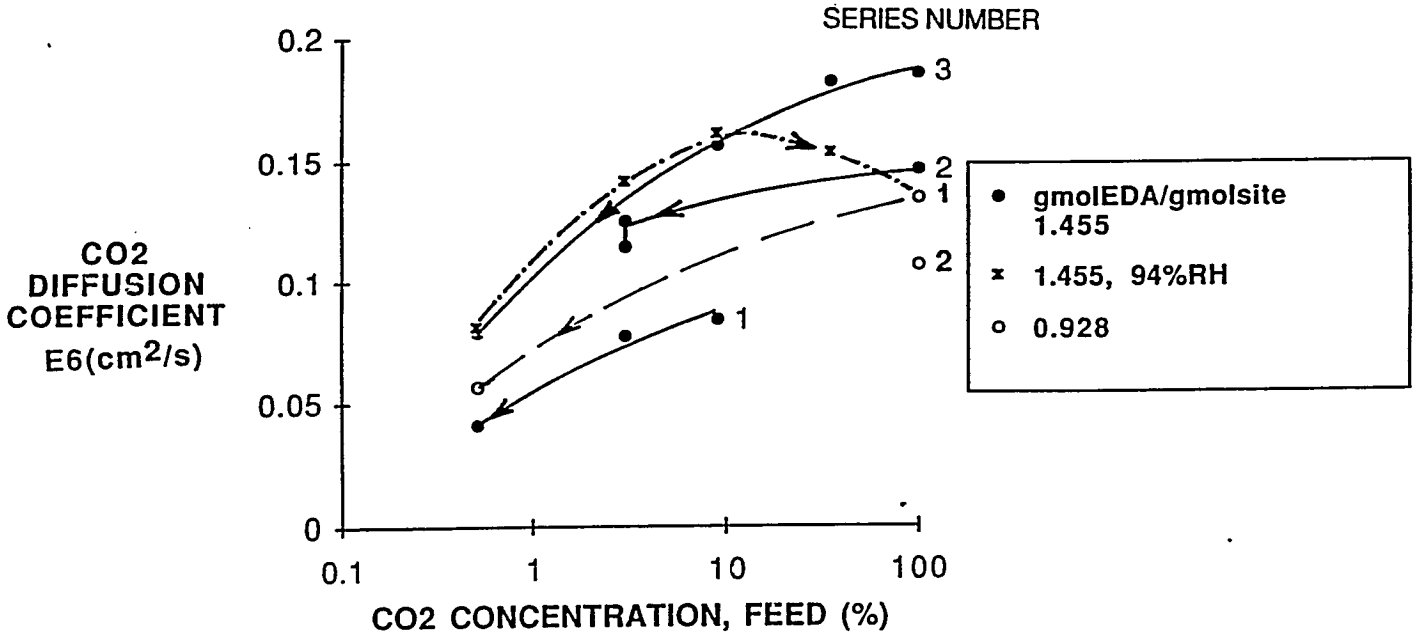

Figure 4-8: Effect of CO_2 Concentration, Loading and Series on CO_2 Diffusion Coefficient with Nafion 117 With EDA, 100% Relative Humidity, 25°C, 1 atm

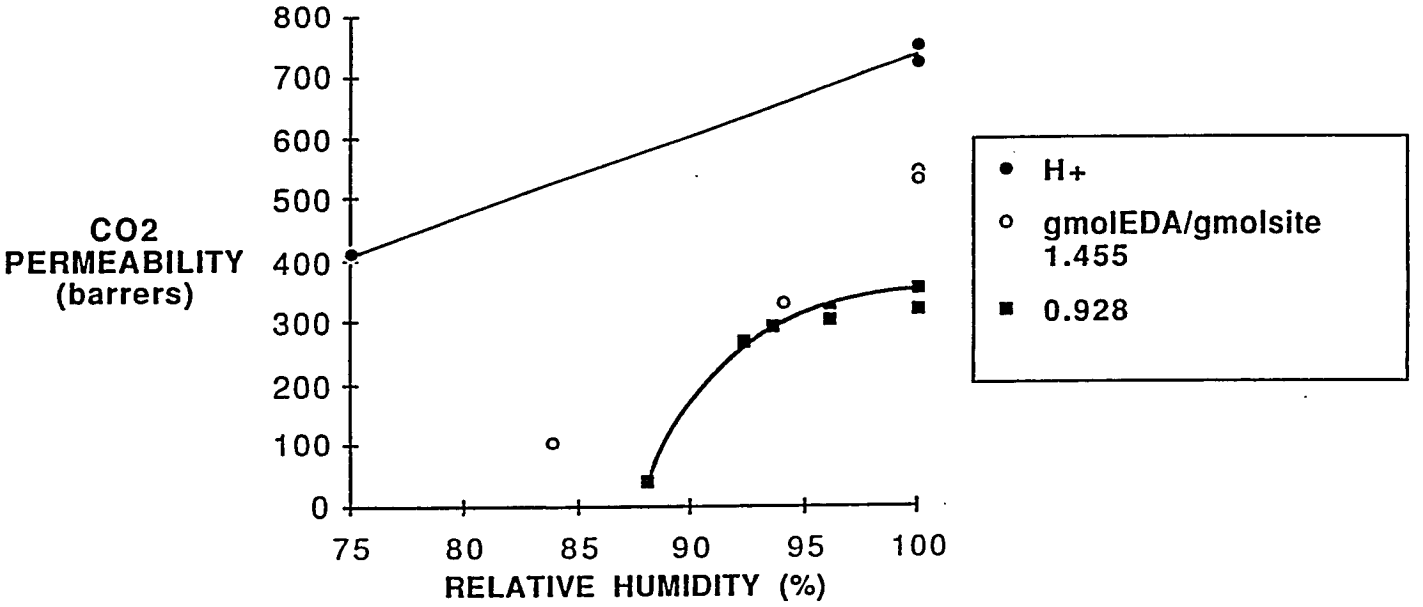

Figure 4-9: Effect of Decreasing Relative Humidity and Loading on Permeability of Nafion 117, H+ Form andWith EDA 25°C, 1 atm, 100% CO_2

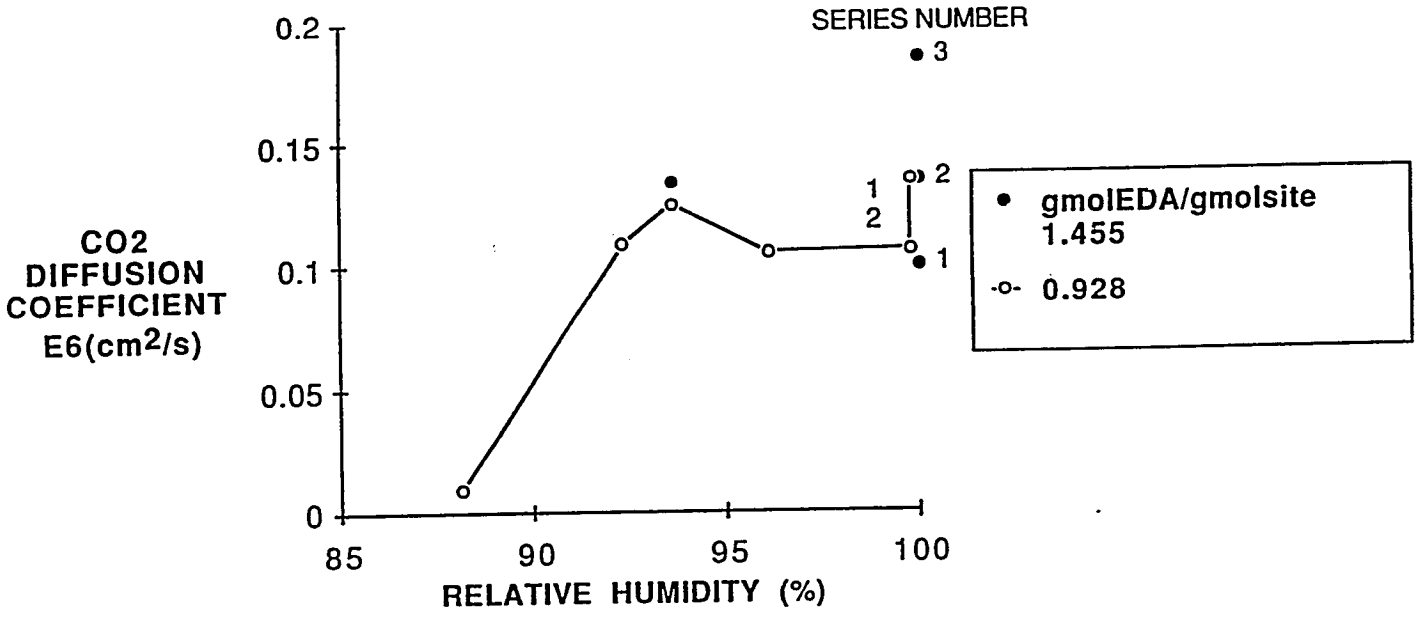

Figure 4-10: Effect of Decreasing Relative Humidity and Loading on CO_2 Diffusion Coefficient with Nafion 117 With EDA, 25°C, 1 atm, 100% CO_2

Table 4-3. Normalized CO_2 Solubility in Nafion 117

Sequence	Relative Humidity (%)	Membrane Thickness $*10^4$(cm)	CO_2 feed (%)	Permeability (barrers)	Diffusion Coefficient $*10^6(cm^2/s)$	Normalized CO_2 Solubility (gmol/ gmol site)	(gmol/ gmol EDA)
0.928 gmol EDA/gmol site							
1	100	198	100	356	0.134	0.429	0.46
2	100	198	0.5	13400	0.057	0.235	0.25
3	100	198	100	320	0.106	0.501	0.54
4	96	196	100	303	0.105	0.475	0.51
5	94	183	100	295	0.125	0.374	0.40
6	92	181	100	269	0.108	0.397	0.43
7	88	180	100	43	0.009	0.846	0.91
1.455 gmol EDA/gmol site							
1	100	206	9	3690	0.084	0.790	0.54
2	100	206	3	8710	0.077	0.678	0.47
3	100	206	0.5	29180	0.041	0.709	0.49
4	100	206	100	547	0.146	0.664	0.46
5	100	206	3	8760	0.124	0.422	0.29
6	100	206	3	8360	0.114	0.438	0.30
7	100	206	100	530	0.185	0.488	0.34
8	100	206	9	3200	0.156	0.368	0.25
9	100	206	0.5	21000	0.079	0.266	0.18
10	100	206	35	1100	0.181	0.240	0.17
11	94	200	0.5	19400	0.081	0.240	0.17
12	94	200	3	6700	0.141	0.287	0.20
13	94	200	9	2470	0.161	0.277	0.19
14	94	200	35	768	0.153	0.351	0.24
15	94	200	100	330	0.134	0.409	0.28
16	84	197[b]	100	180-100	-------	-------	------

Table 4-3 (continued)

Sequence	Relative Humidity (%)	Membrane Thickness *10^4(cm)	CO_2 feed (%)	Permeability (barrers)	Diffusion Coefficient *10^6(cm^2/s)	Normalized CO_2 (gmol/ gmol/site)	Solubility (gmol/ gmol/EDA)
H+ Form							
1	100	208	3	853	1.440	0.003	N/A
2	100	195	9	839	1.100	0.012	"
3	100	195	100	749	1.600	0.085	"
4	100	202	3	835	1.200	0.004	"
5	100	195	100	720	1.330	0.098	"
6	75	183	9	431	0.493	0.014	"
7	75	183	35	425	0.628	0.043	"
8	75	183	9	434	0.561	0.013	"
9	75	183	100	415	0.587	0.130	"
10	75	183	100	414	0.590	0.128	"
11	33	177	100	240	0.250	0.179	"
12	33	177	9	224	0.218	0.017	"
13	33	177	35	245	0.243	0.065	"
14	11	175	100	33	0.229	0.027	"
15	0	174	100	12	0.121	0.019	"

[a]Linear extrapolation between L at 84% relative humidity, 178cmE-4, and 94% relative humidity
[b]Linear extrapolation between L at 75% relative humidity, 194cmE-4, and 94% relative humidity
[c]Water content, 34 wt%, patted dry

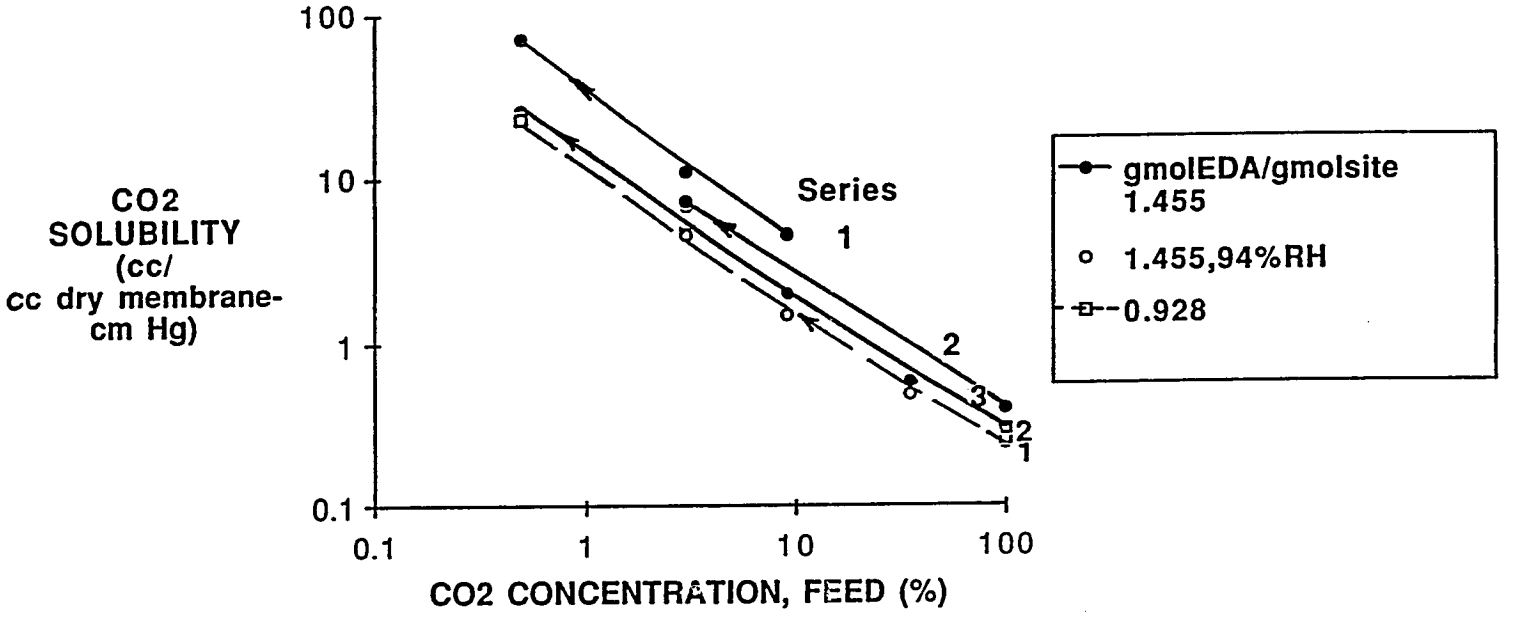

Figure 4-11: Effect of CO_2 Concentration, Loading and Series on CO_2 Solubility in Nafion 117 With EDA, 25°C, 1 atm, 100% Relative Humidity

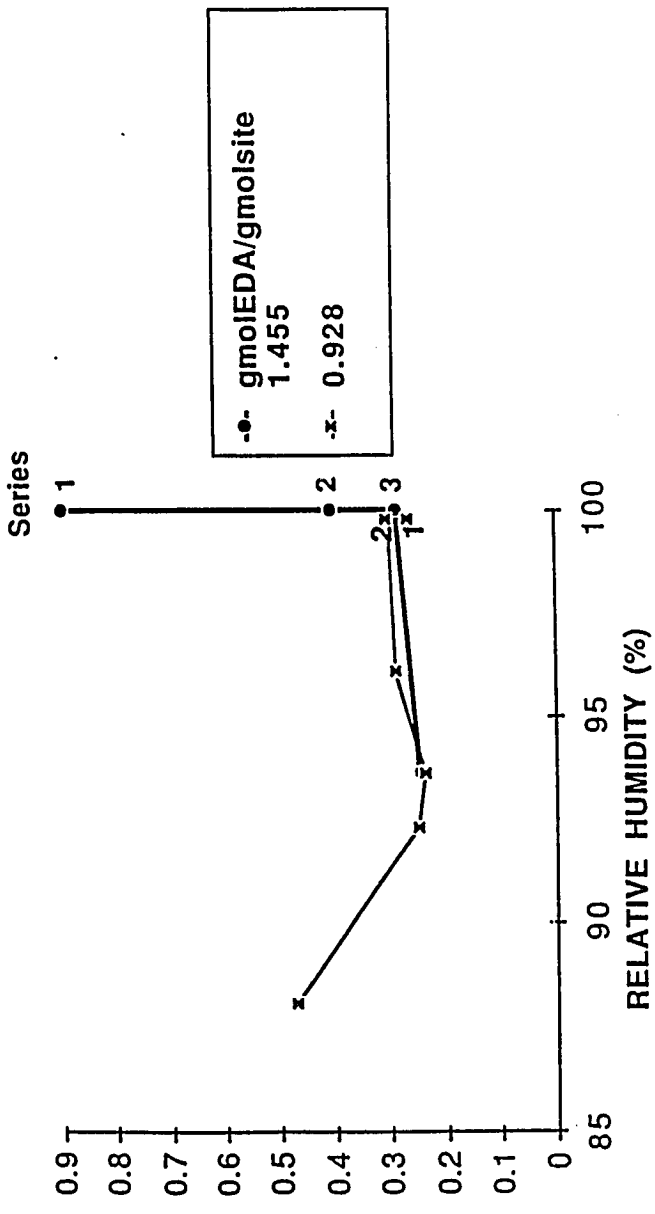

Figure 4-12: Effect of Decreasing Relative Humidity and Loading on CO_2 Solubility in Nafion 117 With EDA, 25°C, 1 atm, 100% CO_2

PEG alone. This effect was attributed to the higher viscosity of the amines over that of PEG.

Different behaviour of EDA loaded membranes at 100% CO_2 has been reported in the literature. Way et al. (1987) in studies with Nafion 117 loaded with ≤1.0 gmol EDA/gmol site at 100% relative humidity showed that the CO_2 flux in the EDA form decreased linearly with decreasing EDA loading and equalled the flux in the Na^+ form at 0 loading. LeBlanc et al. (1980) performed similar studies with sulfonated polystyrene grafted to a polyethylene backbone with 11% water content and 5 meq/g. They showed that the CO_2 flux in the Na+ form was equal to the flux in the EDA loaded membrane (1 gmol EDA/gmol site).

The permeability at 100% relative humidity of membranes loaded with EDA increased with decreasing CO_2 concentration. At 0.01 atm CO_2, the permeability was 12,000 barrers with 0.928 gmol EDA/gmol site. This is three times greater than that of 4,190 barrers achieved with 1 gmol EDA/gmol site at 0.01atm CO_2 (Way et al., 1987) under similar conditions. The most probable reason for this difference is that we prepared the EDA loaded membrane from the H^+ form, whereas Way et al. (1987) used the Na^+ form. The same logic that applied in the case of higher permeabilities in the H^+ form versus the Na+ form applies here.

A second reason for the difference observed is that Way et al. (1987) rinsed the EDA loaded membrane repeatedly before using it. In a separate experiment, we rinsed the 0.928 gmol EDA/gmol site in 25 ml of distilled water. A rapid

equilibration of the membrane with the water resulted in a final loading of 0.78 gmol EDA/gmol site.

Upon continuing the experiments at 100% relative humidity (series 2 and 3), the permeabilities decreased only slightly at high CO_2 concentrations. At lower CO_2 concentrations, the permeabilities decreased by up to 28% at 0.5% CO_2 with 1.455 gmol EDA/gmol site. This behaviour suggests that EDA is being lost by side reactions or other mechanisms. A discussion of EDA loss will be presented in the section on reaction chemistry.

The diffusion coefficient at 100% relative humidity for both EDA loaded membranes increased with increasing CO_2 concentration. This behaviour was expected based on a reaction occurring. Put more simply, the free CO_2 diffuses faster than the bulkier CO_2-EDA molecule. The self diffusion coefficients of cations have been found to follow the order $Na^+ > K^+ > Cs^+$ in Nafion membranes (Yeager, 1982), in the order of increasing size.

At 100% relative humidity, the diffusion coefficients with 0.928 gmol EDA/gmol site are approximately 50% greater than with 1.455 gmol EDA/gmol site. This behaviour is also consistent with the idea that free CO_2 diffuses faster than the CO_2-EDA molecule. The EDA membrane with less loading will have a lesser fraction of EDA-CO_2 molecules diffusing.

The diffusion coefficients in both EDA loaded membranes at 100% relative humidity are approximately an order of magnitude less than the effective diffusion coefficient in the H^+ form membrane. An estimate of diffusion coefficients in the "effective" membrane EDA concentrations was determined from the data of Weiland and Trass (1971) who studied the absorption of CO_2 into aqueous EDA solutions of varying carbonation ratio and EDA concentration at 25°C. They showed that the diffusion coefficient of CO_2 (simulated by N_2O) decreased with increasing carbonation ratio and amine concentration and attributed this to increasing solution viscosity. A 4.5 fold decrease and a 36 fold decrease in the diffusion coefficient of CO_2 in 3.4 M EDA and 5.33 M EDA, respectively, at a carbonation ratio of 0.5, from that in water was extrapolated from their data. The 10 fold decrease observed in the membrane is higher than the 4.5 fold decrease in the diffusion of CO_2 in 3.4 M EDA probably because of the obstructing effects of the matrix (Lagos and Kitchener, 1960) on the diffusion of the bulkier CO_2-EDA molecule.

The overprediction for the 5.33 m EDA "effective" concentration suggests that the diffusion of the CO_2-EDA molecule of the "free" EDA present (Table 4-1) is governed by additional effects. The unassociated complex would probably be less obstructed by interaction with the polymer chains of the membrane, travelling more through the center of the ionic clusters and channels instead of near the ionic sites of the surrounding "walls". This behaviour would have some similarity to that of co-ions (ions whose charge is opposite that of the counter-ion) whose diffusion coefficient is generally larger than that of the counter-ion because they avoid contact with the polymer chains by which they are electrostatically repelled (Meares, 1983).

In the estimation of the diffusion coefficient, as done in the preceding paragraph, it is important to consider the carbonation ratio of the amine. Failure to do so results in an over prediction of the diffusion coefficients of CO_2 by 2 to 5 times for the 3.4 M and 5.33 M EDA solutions, respectively.

For the same reason, it would be inappropriate to estimate the diffusion coefficient of CO_2 in the given system as similar to that of EDA in water-EDA solutions. Although, in the case where carbonation ratio is zero, the diffusion coefficients of EDA (Hikita et al., 1981) and CO_2 (Weiland and Trass, 1971) are similar in varying concentrations of EDA.

Finally, the Stokes-Einstein relation that diffusion coefficients vary inversely with solution viscosity (Bolz and Tuve, 1973) is not followed by the water-EDA system. Hikita et al. (1981) found that this relation greatly overpredicted the observed decrease in the EDA diffusion coefficient with increasing EDA concentration. However, Despic (1956) and Despic and Hills (1957) found that this dependence on viscosity was followed by the self-diffusion coefficients of such ions as Na^+ in ion exchange resins.

Because of these effects of solution viscosity and carbonation ratio, a more appropriate comparison of fluxes in a chemically unreacting environment to a reacting one would involve determining the flux of N_2O, which is physically similar to CO_2, in each of the EDA loaded membranes with appropriate carbonation ratios.

Upon continuing the experiments at 100% relative humidity, the diffusion coefficients with 1.455 gmol EDA/gmol site approximately doubled while those with 0.928 gmol EDA/gmol site decreased by 20%. This behaviour suggests that the EDA is being lost by side reactions or other mechanisms. A discussion of possible EDA loss will be presented in the section on reaction chemistry.

The implied CO_2 solubility, at 100% relative humidity, increased as the CO_2 concentration decreased. This behaviour indicates the chemical solubility of CO_2.

At 100% relative humidity, the implied CO_2 solubility with 1.455 gmol EDA/gmol site was initially 2 to 3 times higher than with 0.928 gmol EDA/gmol site because of the greater concentration of EDA. These increases are much greater than that which would be estimated based on the additional stoichiometry of CO_2 with the free EDA in the higher loaded membrane. This behaviour implies that the "free" EDA has a greater affinity for CO_2 than the "attached" EDA cations.

The implied CO_2 solubility at 100% relative humidity in the EDA loaded membranes was 10 to 1000 times greater than that in the H+ form. This behaviour, combined with the decrease in diffusion coefficient, explains why the permeability of the EDA loaded membranes exceeds that of the H+ form only below a certain CO_2 concentration. At lower CO_2 concentrations, the increased solubility has compensated for the reduction in diffusion coefficient.

At 100% relative humidity, upon continuing the experiments, the implied CO_2 solubility with 1.455 gmol EDA/gmol site decreased to the level with 0.928 gmol EDA/gmol site. The CO_2 solubility in the membrane with the lesser loading did not change significantly upon continuing the experiments. This difference in behaviour between the membranes suggests that the "free" EDA with 1.455 gmol EDA/gmol site is being lost. A discussion of possible EDA loss will be presented in the section on reaction chemistry.

4.5.2 Effect of Relative Humidity

The permeability and diffusion coefficient were a stronger function of relative humidity with EDA than without EDA. With 100% CO_2 and 0.928 gmol EDA/gmol site, the permeability decreased from 320 barrers at 100% relative humidity to 43 barrers at 88% relative humidity. A similar dramatic effect did not occur with no EDA until the relative humidity was reduced from 33% to 11% relative humidity. The drop in permeability coincides with a water/CO_2 mole ratio of 25 in the EDA loaded membranes and 12.5 in the H+ form.

The permeability and diffusion coefficient were practically the same with 0.928 and 1.455 gmol EDA/gmol site at 92% relative humidity. This observation would be consistent with loss of the free EDA in the higher loaded membrane.

The permeability and diffusion coefficient with 0.928 gmol EDA/gmol site did not vary from 100 to 92% relative humidity. The water content in the

membranes loaded with EDA decreased by 50% over this range which would double the "effective" EDA concentration. If the viscosity argument presented earlier were to apply here, a decreasing coefficient would be expected.

The implied solubility of CO_2, at 100% CO_2, from 100 to 92% relative humidity was practically constant and equal in the membranes with 0.928 and 1.455 gmol EDA/gmol site. The equality is consistent with the loss of free EDA with 1.455 gmol EDA/gmol site. The constancy suggests saturation of the EDA over the range of relative humidity. A detailed discussion on the saturation of EDA is presented in the following section.

4.6 Reaction Chemistry

The stoichiometry of CO_2 reaction with EDA can be estimated from the data on CO_2 solubility. The solubility of free CO_2 was estimated from data without EDA and subtracted from the total solubility with EDA to give an effective solubility resulting from interaction with EDA. The stoichiometry given in Table 4-3 is then estimated by normalizing with the EDA loading (Equation 3-18).

The maximum stoichiometry appears to be about 0.5 moles CO_2 per mole EDA. This stoichiometry is consistent with the reversible reaction shown in Equation 1-2. This is a reasonable reaction for the lower loaded membrane because the EDA probably exists in its monoprotonated form and is unlikely to form the dicarbamate species (Jensen and Christensen,1955; Swick et al.,1952). LeBlanc et

al. (1980) also supported this reaction mechanism. However, Way et al. (1987) supported the reaction shown in Equation 1-1.

With the higher loaded membrane, the maximum stoichiometry was about 0.54 moles CO_2 per mole EDA. Modeling (Section 4.7) of the equilibrium reactions involved shows that the stoichiometry at 1 atm CO_2 should be about 0.568 based on an equilibrium constant evaluated at 0.03 atm CO_2. This value is within experimental error of the measured value. Therefore, the experimental value of 0.54 is reasonable.

The lowest values of the stoichiometry were observed at lowest CO_2 pressures. With 0.928 gmol EDA/gmol site, a strong effect of decreasing stoichiometry with decreasing CO_2 was observed. This behaviour is consistent with a lack of complete reaction of CO_2 with the EDA at lower CO_2. This behaviour differed from that with 1.455 gmol EDA/gmol site for which stoichiometry was relatively independent of CO_2 concentration. This behaviour suggests that the EDA is saturated for all CO_2 concentrations. Based on this suggestion, the "flattening" out of the flux versus CO_2 concentration is not necessarily an indication of carrier saturation.

As the series of experiments were continued, the stoichiometry varied, especially with 1.455 gmol EDA/gmol site. The stoichiometry with 1.455 gmol EDA/gmol site in the later runs are 30% to 65% below those of the initial runs. However, if the stoichiometries are calculated assuming 1 gmol EDA/gmol site, the

stoichiometries are in the range of 0.25 to 0.50 and are consistent with measured stoichiometries using 0.928 gmol EDA/gmol site. The experiments in series two (5-7) and three (8-10) with 1.455 gmol EDA/gmol site gave lower solubility and greater diffusion coefficients. This observation is consistent with the loss of the free EDA in the higher loaded membrane. Less total EDA would reduce solubility but would reduce viscosity and therefore increase diffusion coefficients. With 0.928 gmol EDA/gmol site, a slight increase in stoichiometry was observed upon continuing the series.

The stoichiometry decreased with decreasing relative humidity. With 0.928 gmol EDA/gmol, as the relative humidity was dropped to 92% relative humidity, the stoichiometry decreased by about 15 to 20%. A much stronger effect of relative humidity was observed with 1.455 gmol EDA/gmol site. At 94% relative humidity, the stoichiometry decreased by 65% from the initial 0.5. This behaviour suggests that the completion of the reaction is dependent on the availability of water. The experiment at 84% relative humidity gave a maximum permeability of 180 barrers which then decreased gradually to 100 barrers over a period of several hours. This behaviour suggests that EDA may be lost through irreversible reactions in the membrane when contacted with 100% CO_2 and that these reactions are not instantaneous. This explanation would also be consistent with the dramatic change in behaviour observed with 1.455 gmol EDA/gmol site after the first exposure to 100% CO_2.

The observations with 1.455 gmol EDA/gmol site are consistent with the loss of free EDA by vaporization or other mechanisms, whereas those with 0.928 gmol EDA/gmol site are consistent with no loss. An estimate of maximum loss of EDA in the membrane equilibrated in 1.5 M EDA was made based on the relative volatility, 0.001, of EDA to water in a 1.5 M EDA solution (25°C) (Schmelzer et al., 1973). A maximum of 10% loss of total EDA per day was determined. A typical experiment (one point) lasted for one day. A series of experiments was generally 5 days. We expect that an estimate of the actual loss in the membrane would be much less because of gas phase mass transfer limitations. Secondly, the presence of CO_2 should reduce the EDA volatility. If the free EDA is lost, however, the remaining EDA will have a lower volatility. Finally, evaporative loss of EDA would tend to be continuous and therefore affect the performance of the membrane at each run. However, no effect was observed for runs 1 through 4.

We expect that no loss occurs for loadings < 1 because the relative volatility is at least an order of magnitude less and because EDA is in the form of an attatched cation. The experimental results with 0.928 gmol EDA/gmol site support this.

Runs 5-16 with 1.455 gmol EDA/gmol site appear to have significant effects occur after the membrane was exposed to high CO_2 concentrations. The marked effects observed after exposure to high concentrations of CO_2 suggest EDA loss through side reactions. To evaluate this hypothesis, the membrane used in the experiments where EDA loss was suspected was analyzed for nitrogen. The kjeldahl method was employed by Huffman Laboratories in Golden, Colorado. The

analysis was 2.96± 0.20 weight percent nitrogen. This value corresponds to an EDA loading of 1.234 to 1.423 gmol EDA/gmol site. The higher value is within experimental accuracy of the calculated initial loading of 1.455 gmol EDA/gmol site. The lower value suggests a loss of 15 weight percent of the total EDA present initially or 50 weight percent of the free EDA present initially. At the point where the membrane was removed from the cell, it had been continuously used in experiments for 33 days. Based on the aforementioned estimation of evaporation rate of 10% of the total EDA per day, a loss of at least all of the free EDA would be expected after the tenth day. This was not the case as evidenced by the continued high degree of facilitation observed. This suggests that the loss of EDA during the experiments was due to degradation rather than evaporation.

A second determination of possible EDA loss was accomplished by sparging 10 ml of 1.5 M EDA with 50 scc/m of 100% CO_2 at 100% relative humidity for three days. The solution at the end of this period was determined by acid titration with HCl to be 1.2 M EDA and was of the same volume. This result is consistent with loss of EDA through side reactions.

The experiment with 0.928 gmol EDA/gmol site at 100% CO_2 and 88% relative humidity gave a much higher stoichiometry of 0.91 moles CO_2 /mole EDA. This result was obtained at conditions giving the lowest values of permeability and diffusion coefficient observed in any of our experiments.

4.7 Modeling

4.7.1 Flux with $EDAH^+$

The flux of CO_2 with the monopositive form of EDA (0.928 gmol EDA/gmol site) at 0.5% CO_2 and 100% relative humidity was modeled (Figure 4-13) based on the equilibrium of Equation 1-2:

$$CO_2+2(H_2N\text{-}(CH_2)_2\text{-}NH_3^+) \Leftrightarrow (^+H_3N\text{-}(CH_2)_2\text{-}COO^-)^\circ + (+H_3N\text{-}(CH_2)_2\text{-}NH_3^+)^{+2} \quad (1\text{-}2)$$

An equilibrium constant of 50 atm^{-1} was calculated based on the solubility of CO_2 of 0.25 gmol CO_2/gmol EDA at 0.005 atm CO_2. Using this constant, the value of chemical CO_2 solubility was obtained over the range of 0.001 atm to 10 atm using the following equilibrium equation:

$$Keq_2=\frac{[^+H_3N(CH_2)_2NHCOO^-][EDAH_2^+]}{[EDAH^+]^2[p_{CO2}]} \quad (3\text{-}19)$$

or $Keq_2=\frac{X^2}{[1-X]^2[p_{CO2}]}$ where X is equivalent to the chemical CO_2 solubility. A total solubility (gmol CO_2/gmol EDA) for use in the relation P=DS was obtained by adding the contribution due to physical solubility using a Henry's constant, H, of 49 l-atm/gmol:

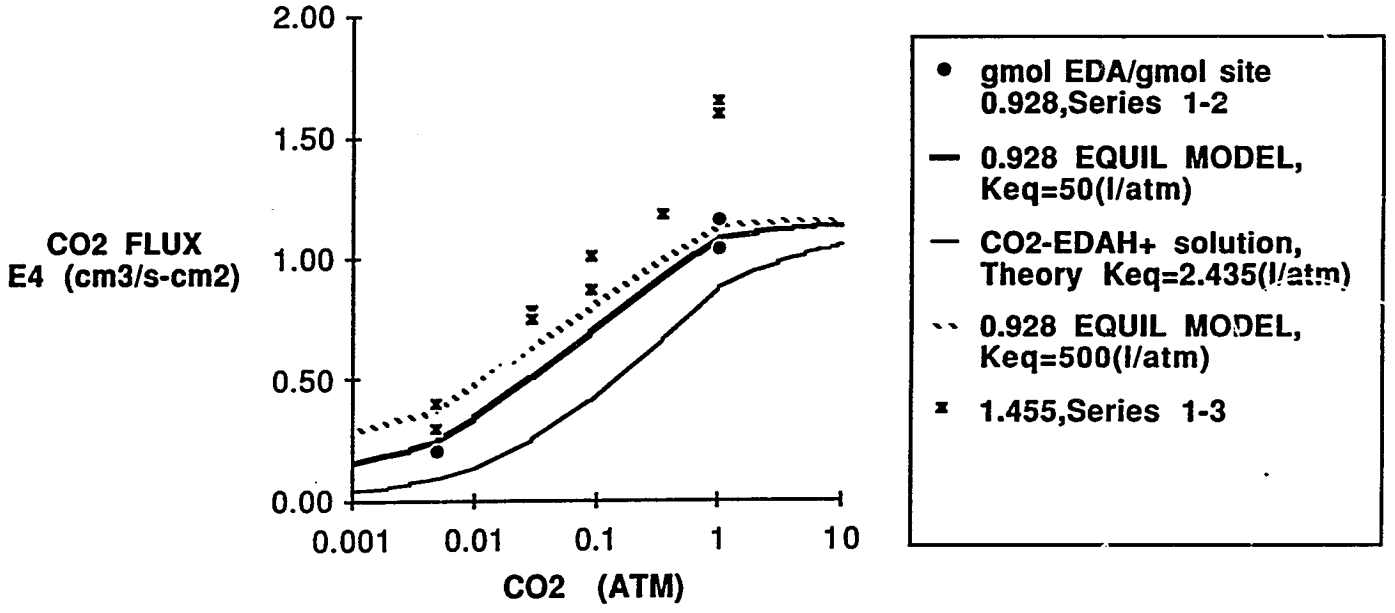

Figure 4-13: Modeling of CO_2 Flux With EDA Loaded Membranes. Membrane Loading = 0.928 gmol EDA/gmol site

$$\text{Total Solubility} = (\text{Normalized S at } p_{CO2,2} - \text{Normalized S at } p_{CO2,1}) + \frac{(p_{CO2,2} - p_{CO2,1})(0.06)}{H} \quad (4\text{-}3)$$

where the chemical and physical solubility at $p_{CO2,1}$ is set equal to zero and 0.06 is a conversion factor for gmol CO_2/liter EDA to gmol CO_2/gmol EDA. The value of H corresponds to a 3.4 M EDA solution with a carbonation ratio of 0.25 (Weiland and Trass, 1971). The following relation between the partial pressure of CO_2 and the diffusion coefficient between 0.005 atm and 1 atm was used in the calculations:

$$D*10^6 = [(0.0335)(\log p_{CO2(atm)})] + 0.134 \quad (0.005 \text{ atm} < p_{CO2} < 1 \text{atm}) \quad (4\text{-}4)$$

The value of the diffusion coefficient below 0.005 atm was assumed equal to the value at 0.005 atm CO_2 and that above 1 atm was set equal to the value at 1 atm.

The model fits the two extremes of the data shown which supports equilibrium of the reaction in the membrane phase. This result supports the use of the time lag method to obtain the values of the diffusion coefficients at these conditions. Furthermore, this model should apply equally well at conditions of relative humidity between 100 to 90% because the solubility and diffusion coefficient of CO_2 did not vary significantly over this range.

Figure 4-13 also shows that the equilibrium model predicts a maximum flux of CO_2 at 1 atm CO_2. This result is due to carrier saturation based on the reaction of

0.5 gmol CO_2 per gmol $EDAH^+$. The data with 1.455 gmol EDA/gmol site is shown for comparison only.

The value of the equilibrium constant is 20 times greater than that for CO_2 in a dilute liquid solution of $EDAH^+$. The value of the latter constant was calculated from the equilibrium data of Jensen and Christensen (1955). The greater value of the equilibrium constant for the membrane phase says that the equilibrium is shifted in the direction of formation of carbamate and $EDAH_2^{+2}$ in the ion exchange environment. A possible explanation for this behaviour is that the formation of greater valency species, i. e. $EDAH_2^{+2}$, which form ionic pairs with the SO_3^- groups improves the stability of the membrane and is, therefore, thermodynamically favored.

A second reason for the larger equilibrium constant is that the effective concentration of the amine is 3.4 M, not dilute, as in the case for the constant calculated for the liquid solution. A more concentrated solution would have smaller activity coefficients associated with the species, thereby improving the thermodynamics of their formation. The overall effect would be to shift the equilibrium of Equation 1-2 to the right, increasing the equilibrium constant.

The value of the equilibrium constant was obtained with one solubility value. Therefore, its accuracy may be questionable. However, boundaries on the value, assuming an exaggerated error of $\pm$ 5% in the value of the solubility, are 43 to 59 l-atm/gmol. Although at first glance this variation may appear significant, the

overall effect on the prediction of the flux is insignificant (Table 4-4). Even a ten fold increase in the constant results in insignificant variations (Figure 4-13) of predicted flux at CO_2 concentrations greater than approximately 0.1 atm.

Secondly, a further check on this constant was made by applying the constant to the equilibrium reaction of CO_2 with monopositive EDA for the membrane with 1.455 gmol EDA/gmol site, as explained in Section 4.7.2.

4.7.2 Flux with $EDAH^+$ and EDA

The flux obtained for Series 1 at 100% relative humidity with 1.455 gmol EDA/gmol site was modeled (Figure 4-14) based on the equilibrium of the reactions represented by the following two equations:

$$CO_2 + H_2N\text{-}(CH_2)_2\text{-}NH_2 \overset{Keq1}{\Longleftrightarrow} ({}^+H_3N\text{-}(CH_2)_2\text{-}NHCOO^-)^0 \qquad (4\text{-}5)$$

$$CO_2 + 2(H_2N\text{-}(CH_2)_2\text{-}NH_3^+) \overset{Keq2}{\Longleftrightarrow} ({}^+H_3N\text{-}(CH_2)_2\text{-}COO^-)^0 + (+H_3N\text{-}(CH_2)_2\text{-}NH_3^+)^{+2} \qquad (4\text{-}6)$$

Keq_2 was assumed equal to 50 atm^{-1} from the experiment with 0.928 gmol EDA/gmol site. The equilibrium constant varied from 245 atm^{-1} at 0.03 atm CO_2 to 3.8 atm^{-1} at 1 atm CO_2. The data was modeled based on the equilibrium constant, 245 atm^{-1}. The resulting variance of the predictions at higher CO_2 concentrations

Table 4-4: Effect of ± 5% Experimental Error on The Prediction of CO_2 Flux From Equilibrium Theory. Membrane Loading=0.928 gmol EDA/gmol site

p_{CO_2} (atm)	Flux * 10^4 Keq=50 atm^{-1}	Flux * 10^4 Keq=43 atm^{-1} (-5% Error)	Flux * 10^4 Keq=59 atm^{-1} (+5% Error)
0.001	0.15	0.14	0.16
0.002	0.19	0.18	0.20
0.003	0.21	0.20	0.22
0.004	0.23	0.22	0.24
0.005	0.25	0.24	0.26
0.01	0.29	0.28	0.30
0.03	0.36	0.35	0.37
0.09	0.44	0.44	0.45
0.35	0.65	0.64	0.65
0.65	0.85	0.85	0.86
1	1.09	1.08	1.09
2	1.11	1.10	1.11
3	1.12	1.11	1.12
4	1.12	1.12	1.13
5	1.13	1.12	1.13
6	1.13	1.13	1.13
7	1.13	1.13	1.13
8	1.13	1.13	1.14
9	1.14	1.13	1.14
10	1.14	1.14	1.14

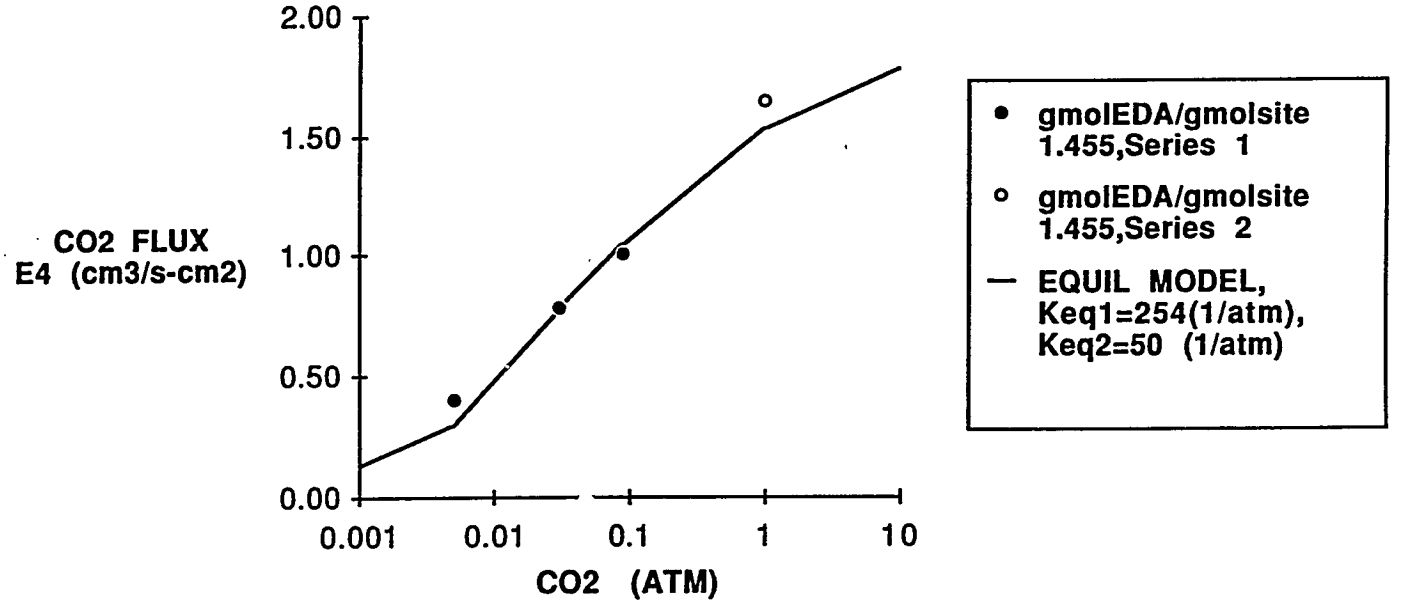

Figure 4-14: Modeling of CO_2 Flux With EDA Loaded Membranes. Membrane Loading = 1.455 gmol EDA/gmol site

with 3.8 atm^{-1} was within experimental accuracy (Figure 4-15), decreasing the solubility and, therefore, flux at 1 atm CO_2 by only 10%. Using this constant, the value of chemical CO_2 solubility was obtained over the range of 0.001 atm to 10 atm using the same method as described in Section 3.10. The value of the Henry's Law constant used was 49 l-atm/gmol. The following relation between the partial pressure of CO_2 and the diffusion coefficient between 0.005 atm and 1 atm was used in the calculations:

$$D*10^6 = [(0.0256)(\log p_{CO2(atm)})] + 0.10 \quad (0.005 \text{ atm} < p_{CO2} < 1 \text{atm}) \qquad (4\text{-}7)$$

The value of the diffusion coefficient below 0.005 atm was assumed equal to the value at 0.005 atm CO_2 and that above 1 atm was set equal to the value at 1 atm.

The model fits the data reasonably well. This result supports the equilibrium of the two reactions in the membrane phase and lends a second support to the value of Keq_2. Further, the use of the time lag method to obtain the values of the diffusion coefficients at these conditions is supported. Finally, this model should apply equally well at conditions of relative humidity between 100 to 90% because the solubility and diffusion coefficient of CO_2 did not vary significantly over this range.

The only area in which the model's accuracy declined was in predicting flux at 0.005 atm CO_2. At this low CO_2, the model underpredicted the flux by about 40%. The most probable reason for this is that Keq_1 is much greater than 245 atm^{-1}.

The data obtained at this point was not accurate enough to give a defined value of Keq_1. Therefore, the data at 0.005 atm CO_2 may be in error by about 20%.

Figure 4-14 also shows that the equilibrium model predicts a flattening out of the CO_2 flux at 10 atm CO_2. This result is due to carrier saturation based on the simultaneous reactions of CO_2 with $EDAH^+$ and EDA.

The value of Keq_1 is only 5 times greater than that for Keq_2. In a dilute liquid solution of EDA, the value of the equilibrium constant for Equation 4-5 is 2273 atm^{-1} and 2.345 atm^{-1} for Equation 4-6 (Jensen and Christensen, 1955; Weiland and Trass, 1971). The first reaction is therefore more strongly favored in the liquid than in the membrane phase. Conversely, the second reaction is more strongly favored in the membrane phase than in the liquid. This result lends support to the previously mentioned hypothesis that the formation of $EDAH_2^{+2}$ is thermodynamically favored because it improves the stability of the membrane by forming ionic pairs with the SO_3^- groups. Likewise, a reaction which did not result in further stabilization of the membrane would not be expected to be thermodynamically favored in the membrane phase versus the liquid phase, as in the case of reaction 1.

4.7.3 Predicting Effect of Sweep Side Concentration

The effect of increasing sweep side CO_2 concentration on the performance of the membrane with EDA can be obtained from a plot of CO_2 solubility versus

CO_2 partial pressure (Figure 4-15). The resultant driving force of solubility in the equation defining permeability is the difference in the solubility between the upstream and downstream pressures. The effect on the driving force for the H^+ form is a linear function of the CO_2 partial pressure difference. This behaviour contrasts with the behaviour with EDA present. Shown are the predicted values of CO_2 solubility with 0.928 gmol EDA/gmol site and 1.455 gmol EDA/gmol site from the models described in Sections 4.7.1 and 4.7.2. The driving force is a strong decreasing function of the sweep side partial pressure. Industrial operations must consider the negative effect of sweep side pressures above zero when determining the applicability of the membrane to their process. The extent of this effect could be lessened by choosing an amine for which the increase in solubility with CO_2 partial pressure would be more gradual, i. e. an amine with a lower equilibrium constant for the reaction with CO_2 such as the monopositive form of monoethanolamine.

The data presented in this report assumed that the CO_2 solubilities in the membranes at the downstream conditions were negligible. This assumption was supported by gas phase mass transfer resistance studies for both the H^+ forms and the EDA loaded forms of the membranes (Appendix A). All data was taken at the point where no significant changes in flux occurred after increasing the sweep side or feed side flow rates.

The accuracy of the model can be estimated by comparing its prediction of CO_2 solubility in the membrane with that measured based on the assumption of

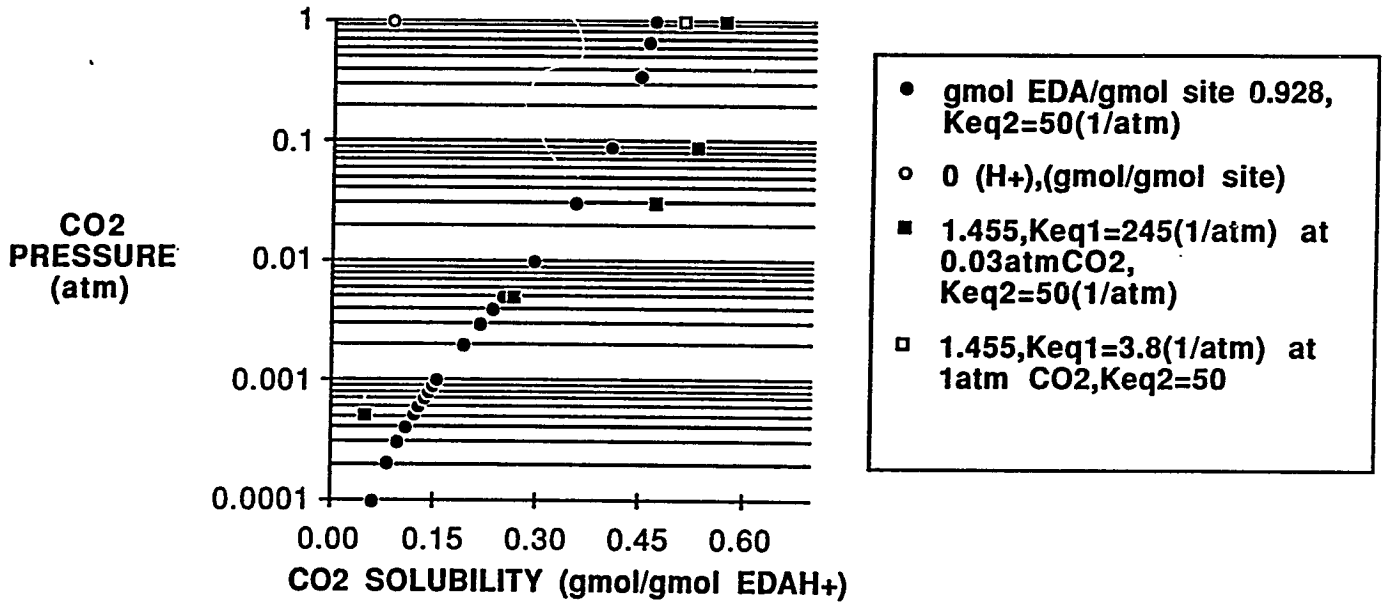

Figure 4-15: Prediction of Equilibrium CO_2 Solubility in EDA Loaded Membranes: A Means To Determine Driving Force. Keq_1=245 atm^{-1} , Keq_2 = 50 atm^{-1}

negligible solubility at the downstream conditions. Table 4-5 shows the CO_2 concentration in the sweep gas with the CO_2 solubilities in the EDA loaded membranes at the downstream side as predicted from the equilibrium models. The model with 0.928 gmol EDA/gmol site predicted a 30% less CO_2 driving force across the membrane at 0.005 atm CO_2 and at 1 atm CO_2 compared to that actually measured. The model with 1.455 gmol EDA/gmol site showed a better agreement at low CO_2 concentrations, underpredicting the CO_2 driving force by only 10%. Therefore, both models give a reasonable prediction of the data in the entire range of CO_2 pressures studied.

Table 4-5: Accuracy of Equilibrium Model: Prediction versus Actual Driving Force

$p_{CO2,2}$ (atm)	$X_{2\text{-}1,actual}$ gmol CO_2 / gmol EDA	$p_{CO2,1}$ (atm)	$X_{1,model}$ gmol CO_2 / gmol EDA	$X_{2\text{-}1,model}$ gmol CO_2 / gmol EDA
Loading=0.928 gmol EDA/gmol site Keq2=50 (1/atm) at 0.005 atm CO_2				
0.005	0.25	0.0002	0.08	0.17
1	0.50	0.0012	0.15	0.35
Loading=1.455 gmol EDA/gmol site Keq1=245 (1/atm) at 0.03 atm CO_2 Keq2=50 (1/atm)				
0.005	0.49	0.0004	0.04	0.45
1	0.51	0.0018	0.14	0.37

Chapter 5

Conclusions and Recommendations

5.1 Conclusions

CO_2 permeabilities in Nafion 117 were 750 barrers for the H^+ form and 500 to 29,200 barrers with EDA. The high values were shown to be due to the increased solubility of the CO_2 in the membrane. The permeabilities in the EDA form were up to 37 times greater that those measured for the H^+ form. CO_2 permeabilities in the fully hydrated H^+ form, compared to those in the literature for O_2 and H_2 for Nafion 117, H^+ under similar conditions, imply selectivities for CO_2 over nonpolar gases of 39 to 64. Selectivities in the EDA form should be even greater. Up to four fold increases in CO_2 permeability are obtained in the H^+ form versus the Na^+ form or the K^+ form. This difference continues to exist for the EDA loaded membranes from each type and suggests that the H^+ form is best used for gas separations.

EDA promoted transport occurred at less than 0.5 atm CO_2. Above this CO_2 concentration, higher permeabilities were achieved with the H+ form.

Diffusion coefficients of CO_2 measured for the fully hydrated H^+ form were 10 times less than that in water and compared with those in the literature for O_2 and H_2 for Nafion 117, H^+ under similar conditions. Those measured in the EDA form of Nafion were an order of magnitude lower than that of the fully hydrated H^+ form. This difference was shown to be due to increased solution viscosity in the membranes.

The permeability and diffusion coefficient decreased with decreasing relative humidity, especially with the EDA loaded membranes. This behaviour correlated with a decrease in water content and volume decrease with decreasing relative humidity.

The reaction stoichiometry was 0.2 to 0.5 gmol CO_2 per gmol EDA. The most probable reactions with EDA and $EDAH^+$ were supported. With no free EDA in the membrane, saturation occurred at high CO_2. With free EDA present, different behaviour was exhibited in that carrier saturation was suggested at all CO_2 concentrations.

Some loss of EDA may have occurred in the membrane with free EDA (1.455 gmol EDA/gmol site). No loss was observed with loadings less than 1 gmol EDA/gmol site, where no free EDA was present.

Modeling of the data with 0.928 gmol EDA/gmol site at 100% relative humidity supported the equilibrium reaction of 0.5 gmol CO_2 per gmol $EDAH^+$.

Secondly, modeling of the data with 1.455 gmol EDA/gmol site for the first series at 100% relative humidity supported the simultaneous equilibrium reactions of CO_2 with EDA and $EDAH^+$. These results supported the use of the time lag method to obtain the diffusion coefficients. The models should apply equally well at conditions of relative humidity between 100 to 90%.

The performance of the membrane is predicted to decrease with increasing sweep side concentration, especially with EDA. Amines with a lower equilibrium constant for the reaction with would lessen this effect.

5.2 Recommendations

The permeability of free CO_2 in the EDA loaded membranes was estimated from estimated values of the diffusion coefficient based on viscosity considerations and estimated solubilities based on solubilities in pure solution. Interactions between the membrane and the solvent was shown to alter these values in the case of the water swollen membrane. Therefore, such interactions may also alter these values in the membranes loaded with aqueous EDA. N_2O has similar interaction parameters amd molecular weight to that of CO_2 and should be measured in the EDA loaded membranes to provide a closer estimate of the free CO_2 permeability.

The literature supports the existence of two regions in the Nafion structure. All evidence points to gas diffusion in the ionic cluster region. Previous researchers have measured reactive gas diffusion when only the sites of the clusters have a

carrier. The inner portion of the clusters have, heretofore, not contained carrier. If the full potential of the membrane is to be utilized, further clarification of the diffusion when both free amine and associated amine is present needs to be addressed. This work represents the first attempt in this area and showed significant additional performance could be achieved under some conditions by adding free amine. A specific recommendation for further research would be to measure the diffusion and permeability with diethanolamine (DEA) and the monopositive form of diethanolamine (DEAH+). The free DEA would diffuse as a complex with CO_2, whereas the DEA^+ would not react. An estimate of the diffusion coefficient of the complex unassociated with the sites would be achieved.

Potential also exists for using the ion exchange membrane as a combined "drier" and separator. The permeability of water in the fully hydrated ion exchange membrane is at least twice that of most gases. The effects of drying a feed stream in combination with gas separation should be investigated. This could be achieved by using a lower relative humidity or dry gas for the sweep gas.

The balance of the CO_2 gas mixture was N_2 in these experiments. Previous researchers (Way et al., 1986) have shown that the presence of H_2S and CH_4 alter the permeabilities of H_2S from that determined separately. More industrially significant gas mixtures should be investigated such as $CO_2/H_2/CO$, CO_2/O_2, N_2/O_2 and $CO_2/H_2S/C_1,C_2+$.

The present research was performed at 25°C and 1 atm pressure. Most industrial operations are at much higher temperatures and pressures. The effects of industrial conditions on the permeability and diffusion coefficients of industrially significant gas mixtures should be investigated.

Increasing sweep side CO_2 concentration was predicted to have a strong negative effect on the performance of membranes with EDA. The extent of this effect could be lessened by choosing an amine for which the increase in solubility with CO_2 partial pressure would be more gradual, i. e. an amine with a lower equilibrium constant for the reaction with CO_2 such as $MEAH^+$. Since industrial processes often have some pressure on the downstream side, the use of such amines should be investigated.

Appendix A.

Experimental Data

The experimental raw data is contained in this section except for the chart recordings of the unsteady state experiments. These charts are available from Dr. Rochelle. Half-times which were obtained from these charts can be obtained from the values of the diffusion coefficients contained in this section.

Table A-1 :Permeability of CO_2 in Nafion 117: Mass Transfer Studies and Effects of CO_2 Concentration, Relative Humidity and EDA Loading

Date	Elapsed Time (hr)	% RH Feed,Sweep	Feed (%CO_2)	Feed (scc/m)	Sweep (scc/m)	Sweep (%CO_2)	P (barrers)	D*(10^{-6}) (cm^2/s)	S (cc/cc-cm Hg)	% Water (g/100g)
Sheet B H+, #1										
teflon cross support										
1/13/87		100	3	135	100	0.0174	897			34
1/13/87		100	3	135	100	0.0167	853	1.44	0.0592	
1/13/87		100	9	110	100	0.0503	839	1.1	0.076	
1/13/87		100	100	100	100	0.502	749	1.6	0.0468	27
Sheet B H+,#2										
teflon cross support										
1/15/87		100	3	135	100	0.0169	835	1.2	0.0694	27
1/15/87		100	3	270	100	0.0163	802			
1/15/87		100	3	386	100	0.016	787			
1/15/87		100	100	100	100	0.493	720	1.33	0.0541	23
3/16/87	38	75	9	110	100	0.025	399			9
3/16/87	39	75	9	275	100	0.0258	411			
3/16/87	40	75	9	990	100	0.026	414			
3/18/87	20	75	9	110	100	0.0285	460			9
3/18/87	24	75	9	110	100	0.0267	431	0.493	0.0873	
3/19/87	46	75	35	140	100	0.105	425	0.628	0.0685	
3/20/87	69	75	9	110	100	0.0273	434	0.561	0.0773	
	70	75	9	275	100		436			

continued

Table A-1: (continued) p.2

	71	75	9	990	100		439			
3/20/87	73	75	100	100	100	0.286	415	0.587	0.0708	
3/23/87	143	75	100	100	200	0.144	418			
3/25/87	187	75	100	100	100	0.286	414	0.59	0.0702	
3/25/87	190	75	100	100	1000	0.0286	413			
3/27/87	25	33	100	100	100	0.2	246			2
3/30/87	86	33	100	100	100	0.196	240	0.25	0.0985	
4/2/87	155	33	9	110	100	0.0166	224	0.218	0.103	
4/3/87	178	33	35	140	100	0.0714	245	0.243	0.101	
5/5/87	96	11	100	100	100	0.0303	36			0
5/9/87	190	11	100	100	100	0.0275	33	0.229	0.0144	0
5/15/87	27	0	100	100	100	0.0094	12	0.121	0.0913	0
REHUMIDIFY IN SITU										
5/26/87	47	53	100	100	100	0.084	104	----------	----------	5

continued

Table A-1 (continued) p.3

1.455 gmol EDA/gmol site
Sheet A, #1

6/15/87	336	100	9	110	100	0.167	2540	---------	----------
6/15/87	338	100	9	220	100	0.176	2680	---------	----------
6/15/87	339	100	9	550	100	0.182	2760	---------	----------
6/15/87	340	100	9	770	100	0.192	2920	---------	----------
6/15/87	341	100	9	990	100	0.195	2960	---------	----------
6/15/87	342	100	9	990	75	0.257	2930	---------	----------
6/15/87	343	100	9	990	50	0.376	2850	---------	----------
6/15/87	344	100	9	990	25	0.711	2700	---------	----------
6/17/87	386	100	9	990	100	0.188	2870	0.0491	5.84
6/22/87	102	75	9	990	100	0.0893	1424	0.00436	32.7
6/24/87	151	75	100	980	100	0.0543	70	0.0174	0.401
6/26/87	195	75	9	990	100	0.024	340	0.0151	2.26
REHUMIDIFY IN SITU									
6/29/87	73	100	9	990	100	0.116	1761	0.0598	2.947
RESOAK IN 1.5 M EDA									
7/8/87	51	100	9	990	100	0.134	2160	0.0425	5.091

continued

Table A - 1 (continued) p.4

1.455 gmol EDA/gmol site
Sheet B#1

extrapolate		100	100	990	100	0.3701	580	0.1	
7/15/87	25	100	9	990	100	0.2138	3690	0.0775	4.75
7/16/87		100	3	980	100	0.1662	8710	0.077	11.3
7/16/87		100	3	722	100	0.1671	8760	---	---
7/16/87		100	3	515	100	0.167	8740	---	---
7/22/87		100	0.5	1000	100	0.0851	29180	0.041	70.9
7/23/87		100	0.5	1000	535	0.0168	28623	---	---
7/24/87		100	100	800	100	0.349	547	0.135	0.405
7/27/87		100	3	980	100	0.167	8760	0.124	7.05
7/29/87		100	3	980	100	0.1595	8360	0.114	7.31
7/30/87		100	100	980	100	0.338	530	0.185	0.287
8/3/87		100	9	990	100	0.185	3200	0.156	2.04
8/4/87		100	0.5	1000	100	0.0624	21000	0.079	26.6
8/5/87		100	35	950	100	0.249	1100	0.181	0.604
8/10/87		94	0.5	1000	100	0.0591	19400	0.081	24
8/11/87		94	3	980	100	0.13	6700	0.141	4.77
8/12/87		94	9	990	100	0.146	2470	0.161	1.54
8/13/87		94	35	950	100	0.178	768	0.153	0.501
8/14/87		94	100	980	100	0.214	330	0.134	0.246
8/18/87		84	100	980	100	0.122	182(max)	-------	---
8/18/87		84	100	980	100	0.0658	98(min)	---	---

continued

Table A - 1 (continued) p.5

0.928 gmol EDA/gmol site
Sheet B#2

8/24/87		100	100	980	100	0.246	356	0.134	0.265
8/25/87		100	0.5	1000	100	0.0442	13400	0.057	23.7
8/26/87		100	100	980	100	0.221	320	0.106	0.301
9/1/87		96	100	980	100	0.228	318	----------	----------
9/2/87		96	100	980	100	0.217	303	0.105	0.288
9/4/87		94	100	980	100	0.218	295	0.125	0.237
9/9/87		92	100	980	100	0.199	269	0.108	0.248
9/15/87		88	100	980	100	0.033	43	0.009	0.473

Table A-2 :Predicting Solubility and Flux From Equilibrium Constant.
Membrane Loading = 0.928 gmol EDA/gmol site

Keq(l/gmol)= 50 (1/atm)

	Quadratic Values			Roots To Quadratic Eqn. $\frac{\text{gmol CO2}}{\text{gmol EDA}}$		Solubility	Permeability(P)	Flux*E4
PCO2(atm)	a	b	c	Xr (+SQ RT)	Xr (-SQ RT)	S(cc/(cc-cmHg)	Dave*S (barrer)	$P*P_{CO2}/L$ $\frac{(\text{std cm}^3)}{(\text{s-cm}^2)}$
0.0001	-1	-0.02	0.005	-0.08	0.06	289	163359	0.06
0.0002	-1	-0.04	0.01	-0.13	0.08	194	109873	0.08
0.0003	-0.9	-0.06	0.015	-0.16	0.10	153	86472	0.10
0.0004	-0.9	-0.08	0.02	-0.20	0.11	129	72675	0.11
0.0005	-0.9	-0.1	0.025	-0.23	0.12	112	63354	0.12
0.0006	-0.9	-0.12	0.03	-0.27	0.13	100	56537	0.13
0.0007	-0.9	-0.14	0.035	-0.30	0.14	91	51286	0.13
0.0008	-0.8	-0.16	0.04	-0.33	0.14	83	47088	0.14
0.0009	-0.8	-0.18	0.045	-0.37	0.15	77	43639	0.15
0.001	-0.8	-0.2	0.05	-0.40	0.15	72	40743	0.15
0.002	-0.6	-0.4	0.1	-0.86	0.19	45	25541	0.19
0.003	-0.4	-0.6	0.15	-1.72	0.22	34	19183	0.21
0.004	-0.2	-0.8	0.2	-4.24	0.24	28	15563	0.23
0.005	0	-1	0.25	0.25	0.25	23.34	13276	0.25
0.01	1	-2	0.5	1.71	0.29	13.67	7830	0.29
0.03	5	-6	1.5	0.84	0.36	5.52	3251	0.36
0.09	17	-18	4.5	0.65	0.40	2.10	1333	0.44
0.35	69	-70	17.5	0.57	0.45	0.60	500	0.65
0.65	129	-130	32.5	0.55	0.46	0.33	354	0.85
1	199	-200	50	0.54	0.47	0.22	293	1.09
2	399	-400	100	0.53	0.48	0.11	149	1.11
3	599	-600	150	0.52	0.48	0.07	100	1.12
4	799	-800	200	0.52	0.48	0.06	76	1.12
5	999	-1000	250	0.52	0.48	0.05	61	1.13
6	1199	-1200	300	0.51	0.49	0.04	51	1.13
7	1399	-1400	350	0.51	0.49	0.03	44	1.13
8	1599	-1600	400	0.51	0.49	0.03	38	1.13
9	1799	-1800	450	0.51	0.49	0.03	34	1.14
10	1999	-2000	500	0.51	0.49	0.02	31	1.14

continued

Table A-2 Predicting Solubility and Flux From Equilibrium Constant. (continued) p.2
Membrane Loading=0.928 gmol EDA/gmol site

Keq(l/gmol)= 2.435(1/atm)

	Quadratic Values			Roots To Quadratic Eqn.		Solubility	Permeability(P)	Flux*E4(scc/s-cm^2)
p_{CO2}(atm)	a	b	c	Xr (+SQ RT)	Xr (-SQ RT)	S(cc/(cc-cmHg)	Dave*S(barrers)	P*p_{CO2}/L
0.001	-0.990	-0.0097	0.0024	-0.05	0.04	20.96	11843	0.04
0.002	-0.981	-0.0195	0.0049	-0.08	0.06	14.29	8074	0.06
0.003	-0.971	-0.0292	0.0073	-0.10	0.07	11.36	6416	0.07
0.004	-0.961	-0.039	0.0097	-0.12	0.08	9.62	5434	0.08
0.005	-0.951	-0.0487	0.0122	-0.14	0.09	8.44	4800	0.09
0.01	-0.903	-0.0974	0.0244	-0.23	0.12	5.55	3180	0.12
0.03	-0.708	-0.2922	0.0731	-0.59	0.18	2.73	1606	0.18
0.09	-0.123	-0.8766	0.22	-7.35	0.24	1.25	797	0.27
0.35	2.409	-3.409	0.85	1.09	0.32	0.43	363	0.47
0.65	5.331	-6.331	1.58	0.83	0.36	0.26	276	0.66
1	8.74	-9.74	2.44	0.74	0.38	0.18	238	0.88
2	18.48	-19.48	4.87	0.65	0.41	0.10	128	0.95
3	28.22	-29.22	7.31	0.61	0.42	0.07	88	0.98
4	37.96	-38.96	9.74	0.60	0.43	0.05	68	1.00
5	47.7	-48.7	12.175	0.58	0.44	0.04	55	1.02
6	57.44	-58.44	14.61	0.58	0.44	0.03	46	1.03
7	67.18	-68.18	17.045	0.57	0.45	0.03	40	1.04
8	76.92	-77.92	19.48	0.56	0.45	0.03	35	1.04
9	86.66	-87.66	21.915	0.56	0.45	0.02	31	1.05
10	96.4	-97.4	24.35	0.56	0.45	0.02	28	1.06

continued

TableA- 2Predicting Solubility and Flux From Equilibrium Constant. (continued) p.3
Membrane Loading=0.928 gmol EDA/gmol site

Keq(l/gmol)= 500(1/atm)

	Quadratic Values			Roots To Quadratic Eqn.		Solubility	Permeability(P)	Flux*E4(scc/s-cm^2)
p_{CO2}(atm)	a	b	c	Xr (+SQ RT)	Xr (-SQ RT)	S(cc/(cc-cmHg)	Dave*S(barrers)	P*PCO2/L
0.001	1	-2	0.5	1.71	0.29	137	77235	0.29
0.002	3	-4	1	1.00	0.33	78	43949	0.33
0.003	5	-6	1.5	0.84	0.36	55	31208	0.35
0.004	7	-8	2	0.77	0.37	43	24352	0.36
0.005	9	-10	2.5	0.73	0.38	35.46	20173	0.37
0.01	19	-20	5	0.64	0.41	19.07	10925	0.40
0.03	59	-60	15	0.57	0.44	6.89	4054	0.45
0.09	179	-180	45	0.54	0.47	2.41	1533	0.51
0.35	699	-700	175	0.52	0.48	0.64	539	0.70
0.5	999	-1000	250	0.52	0.48	0.45	433	0.80
0.65	1299	-1300	325	0.51	0.49	0.35	375	0.90
1	1999	-2000	500	0.51	0.49	0.23	307	1.14
2	3999	-4000	1000	0.51	0.49	0.11	154	1.14
3	5999	-6000	1500	0.51	0.49	0.08	103	1.15
4	7999	-8000	2000	0.51	0.49	0.06	78	1.15
5	9999	-10000	2500	0.51	0.50	0.05	62	1.15
6	11999	-12000	3000	0.50	0.50	0.04	52	1.15
7	13999	-14000	3500	0.50	0.50	0.03	44	1.15
8	15999	-16000	4000	0.50	0.50	0.03	39	1.15
9	17999	-18000	4500	0.50	0.50	0.03	35	1.15
10	19999	-20000	5000	0.50	0.50	0.02	31	1.15

Table A-2Predicting Solubility and Flux From Equilibrium Constant. (continued) p.4
Membrane Loading=0.928 gmol EDA/gmol site

Keq(l/gmol)= 59 (1/atm)

	Quadratic Values			Roots To Quadratic Eqn.		Solubility	Permeability(P)	Flux*E4(scc/s-cm^2)
p_{CO2}(atm)	a	b	c	Xr (+SQ RT)	Xr (-SQ RT)	S(cc/(cc-cmHg)	Dave*S(barrers)	P*PCO2/L
0.001	-0.764	-0.236	0.059	-0.47	0.163	76	43109	0.16
0.002	-0.528	-0.472	0.118	-1.10	0.204	48	26847	0.20
0.003	-0.292	-0.708	0.177	-2.65	0.228	36	20082	0.22
0.004	-0.056	-0.944	0.236	-17.1	0.246	29	16244	0.24
0.005	0.18	-1.18	0.295	6.30	0.26	24.30	13825	0.26
0.01	1.36	-2.36	0.59	1.43	0.30	14.13	8097	0.30
0.03	6.08	-7.08	1.77	0.80	0.36	5.65	3327	0.37
0.09	20.24	-21.24	5.31	0.64	0.41	2.13	1354	0.45
0.35	81.6	-82.6	20.65	0.56	0.45	0.60	504	0.65
0.65	152.4	-153.4	38.35	0.54	0.46	0.33	357	0.86
1	235	-236	59	0.53	0.47	0.22	294	1.09
2	471	-472	118	0.52	0.48	0.11	150	1.11
3	707	-708	177	0.52	0.48	0.07	101	1.12
4	943	-944	236	0.52	0.48	0.06	76	1.13
5	1179	-1180	295	0.51	0.49	0.05	61	1.13
6	1415	-1416	354	0.51	0.49	0.04	51	1.13
7	1651	-1652	413	0.51	0.49	0.03	44	1.13
8	1887	-1888	472	0.51	0.49	0.03	38	1.14
9	2123	-2124	531	0.51	0.49	0.03	34	1.14
10	2359	-2360	590	0.51	0.49	0.02	31	1.14

continued

Table A- 2: Predicting Solubility and Flux From Equilibrium Constant. (continued) p.5
Membrane Loading=0.928 gmol EDA/gmol site

Keq(l/gmol)= 43 (1/atm)

	Quadratic Values			Roots To Quadratic Eqn.		Solubility	Permeability(P)	Flux*E4(scc/s-cm^2)
p_{CO2}(atm)	a	b	c	Xr (+SQ RT)	Xr (-SQ RT)	S(cc/(cc-cmHg)	Dave*S(barrers)	P*PCO2/L
0.001	-0.828	-0.172	0.043	-0.35	0.15	68	38651	0.14
0.002	-0.656	-0.344	0.086	-0.71	0.18	43	24371	0.18
0.003	-0.484	-0.516	0.129	-1.28	0.21	33	18373	0.20
0.004	-0.312	-0.688	0.172	-2.43	0.23	26	14945	0.22
0.005	-0.14	-0.86	0.215	-6.38	0.24	22.46	12776	0.24
0.01	0.72	-1.72	0.43	2.11	0.28	13.24	7584	0.28
0.03	4.16	-5.16	1.29	0.89	0.35	5.40	3178	0.35
0.09	14.48	-15.48	3.87	0.67	0.40	2.07	1314	0.44
0.35	59.2	-60.2	15.05	0.57	0.44	0.59	496	0.64
0.65	110.8	-111.8	27.95	0.55	0.46	0.33	352	0.85
1	171	-172	43	0.54	0.46	0.22	291	1.08
2	343	-344	86	0.53	0.47	0.11	149	1.10
3	515	-516	129	0.52	0.48	0.07	100	1.11
4	687	-688	172	0.52	0.48	0.06	76	1.12
5	859	-860	215	0.52	0.48	0.05	61	1.12
6	1031	-1032	258	0.52	0.48	0.04	51	1.13
7	1203	-1204	301	0.51	0.49	0.03	44	1.13
8	1375	-1376	344	0.51	0.49	0.03	38	1.13
9	1547	-1548	387	0.51	0.49	0.03	34	1.13
10	1719	-1720	430	0.51	0.49	0.02	31	1.14

Table A- 2 :Predicting Solubility and Flux From Equilibrium Constant. (continued) p.6
Membrane Loading=1.455 gmol EDA/gmol site

$Keq_2 = 50\ atm^{-1}$ P_{CO2}(atm)	X_r	Solubility	Permeability (P)	Flux*E4
$Keq_1 = 245\ atm^{-1}$				
0.0005	0.05	70.91	29074	0.05
0.005	0.26	38.37	15731	0.29
0.03	0.47	11.41	6952	0.77
0.09	0.53	4.29	3138	1.05
1	0.57	0.41	414	1.53
10	0.66	0.05	48	1.79
$Keq_1 = 3.8\ atm^{-1}$				
1	0.51	0.37	371	1.38

Table A-3: Equilibrium Volume and Water Measurements: H^+ Form

	B*.length(cm)	B.width(cm)	B.thickness(in)	A*.length(cm)	A.width(cm)	A.thickness(in)
B#1 ,100%RH	9.05	1.35	0.0083	8.45	1.25	0.0077
	9.00	1.40	0.0084	8.40	1.20	0.0076
			0.0081			0.0078
			0.0080			0.0076
B = before equilibration (fully hydrated); A= after equilibration						
AVE. DIMENSION. (cm)	9.025	1.38	0.0208	8.425	1.225	0.0195
FRACTION DIMENSION DECREASE				0.066	0.109	0.064
VOLUME DECREASE						0.222
AVE. AREA (cm^2)	12.4			10.32		
FRACTION AREA DECREASE				0.168		
	B.water	A.water				
WATER(wt%)	37	21				
WT (g)	0.422	0.37				
Density(g/cc)	1.63	1.86				

(continued)

Table A-3 (continued) p.2

	B.length(cm)	B.width(cm)	B.thickness(in)	A.length(cm)	A.width(cm)	A.thickness(in)
B#1 ,93.3%RH	8.95	1.4	0.0082	8.25	1.25	0.0074
	8.95	1.3	0.0084	8.3	1.2	0.0074
			0.0081			0.0075
			0.0081			0.0074
AVE. DIMEN.(cm)	8.95	1.35	0.0208	8.275	1.225	0.0189
DIMENSION DECREASE				0.075	0.093	0.095
VOLUME DECREASE						0.24
AVE. AREA	12.1			10.14		
AREA DECREASE				0.161		

	B.water	A.water
WATER(wt%)	34	13
WT (g)	0.418	0.35
Density (g/cc)	1.66	1.82

	B.length	B.width	B.thickness	A.length	A.width	A.thickness
B#2 ,93.3%RH	9	1.75	0.0079	8.35	1.65	0.0072
	8.95	1.85	0.008	8.4	1.7	0.0072
			0.0081			0.0071
			0.0078			0.007
AVE. DIMEN.	8.975	1.8	0.0202	8.375	1.675	0.0181
DIMENSION DECREASE				0.067	0.069	0.104
VOLUME DECREASE						0.222
AVE. AREA	16.2			14.03		
AREA DECREASE				0.132		

	B.water	A.water
Water wt(%)	30	14

continued

Table A-3 (continued) p.3

	B.length	B.width	B.thickness	A.length	A.width	A.thickness
B#2 ,85%RH	9.05	1.8	0.0083	8.2	1.65	0.0072
	9.05	1.8	0.0081	8.2	1.6	0.0071
			0.0081			0.0071
			0.008			0.0071
AVE. DIMEN.	9.05	1.8	0.0206	8.2	1.625	0.0181
DIMENSION DECREASE				0.094	0.097	0.123
VOLUME DECREASE						0.283
AVE. AREA	16.3			13.33		
AREA DECREASE				0.182		

	B.water	A.water
WATER(wt%)	32	10
WT (g)	0.545	0.46
Density(g/cc)	1.62	1.89

continued

Table A-3 (continued) p. 4

	B.length	B.width	B.thickness	A.length	A.width	A.thickness
B#2 ,54%RH	8.95	1.85	0.0081	7.95	1.6	0.0069
	8.95	1.8	0.008	7.95	1.55	0.0069
			0.0082			0.007
			0.008			0.007
AVE. DIMEN.	8.95	1.83	0.0205	7.95	1.575	0.0177
DIMENSION DECREASE				0.112	0.137	0.139
VOLUME DECREASE						0.34
AVE. AREA	16.3			12.52		
AREA DECREASE				0.233		

	B.water	A.water
WATER(wt%)	30	4.6
WT (g)	0.535	0.43
Density(g/cc)	1.6	1.95

continued

Table A-3 (continued) p.3

	B.length	B.width	B.thickness	A.length	A.width	A.thickness
B#2 ,33%RH	9	1.8	0.008	7.9	1.55	0.007
	8.95	1.85	0.0079	7.9	1.6	0.0069
			0.0079			0.007
			0.0079			0.0069
AVE. DIMEN.	8.975	1.83	0.0201	7.9	1.575	0.0177
DIMENSION DECREASE				0.12	0.137	0.123
VOLUME DECREASE						0.334
AVE. AREA	16.4			12.44		
AREA DECREASE				0.24		

	B.water	A.water
WATER(wt%)	30	2
WT (g)	0.537	0.42
Density(g/cc)	1.63	1.91

continued

Table A-3 (continued) p.6

	B.length	B.width	B.thickness	A.length	A.width	A.thickness
B#1,75%RH	8.9	1.35	0.0082	8.05	1.15	0.0071
	8.95	1.35	0.0081	8	1.2	0.0072
			0.008			0.0073
			0.0082			0.0072
AVE. DIMEN.	8.925	1.35	0.0206	8.025	1.175	0.0183
DIMENSION DECREASE				0.101	0.13	0.114
VOLUME DECREASE						0.306
AVE. AREA	12			9.429		
AREA DECREASE				0.217		

	B.water	A.water
WATER(wt%)	33	9.1
WT (g)	0.411	0.34

	A.length	A.width	A.thickness
B#2,11%RH	7.75	1.55	0.0175
WATER(wt%) 0.15			
B#2,0%RH	7.7	1.533	0.0174
WATER(wt%) 0			

SAMPLE	Vol. Dry(cc)	Vol.Boiled(cc)	Wt Dry(g)	ccdry/gmolH+
B#2	0.2056344	0.326331	0.4084	553.9
B#1	0.15552(est.)	0.251316	0.3081	555.2

Table A-4: Equilibrium, Volume and Water Measurements: EDA Form

Sample A, 1.5M EDA	%RH	g sol./100g dry	length(cm)	width(cm)	thick(cm)	vol % increase
A#2, Blotted dry	- - - -	17.99	7.80	1.48	0.0208	45
A#1, Blotted dry	- - - -	17.97	7.48	1.60	0.0210	34
A#1, (Vdry=0.1852cm3)	100	27.65	7.36	1.60	0.0207	32
A#2,(Vdry=0.1656cm3)	97	16.19				
A#2	94	12.84	7.45	1.43	0.0201	29
A#2	84	6.74	7.30	1.38	0.0192	16
A#2	81	4.61	7.23	1.33	0.0189	10
A#2	75	3.08				
A#1	0	0	7.26	1.35	0.0189	0
A#2	0	0	7.00	1.30	0.0182	0
Sample B#1, 1.5M EDA	100	43.67gH2O/100gdry	8.80	1.33	0.0206	46
equil RH 1.5M EDA	96	19.2	8.58	1.30	0.0203	37
	93.6	16.1	8.43	1.26	0.02	29
	84.3	10.22	8.20	1.21	0.0194	17
(Vdry=0.1659cm3)	0	0	7.90	1.20	0.0175	0
H+ fully hydrated	100	34.79				
1.5MEDA, fully hydrated	96	26.35	8.80	1.35	0.0208	50
patted from 100%RH	100	36.93				
SampleB#2, 0.15MEDA	100	27.55	8.58	1.70	0.0198	38
equil RH 0.15M EDA	98	24.53	8.53	1.70	0.0196	36
	93.6	15.72	8.20	1.63	0.0183	17
	84.3	12.20	8.05	1.58	0.0178	8
	81	10.69	8.00	1.58	0.0177	7
	75.3	9.43	8.00	1.59	0.0175	7
	32.8	6.67	7.85	1.55	0.0173	1
(Vdry=0.2087cm3)	0	0.00	7.80	1.54	0.0174	0
H+, fuliy hydrated	100	37.11				
0.15MEDA, fully hydrated	98	28.38	8.60	1.73	0.0199	41

Table A-5: Desorption Rate Data, H+ Form
Sample B#2, 33%RH

hour	min	Total time (hours)	wt. (g)	corr.wt. including tare(g)	water wt%
0	32	0.00	0.517	0.537	30
0	34	0.03	0.512	0.532	29
0	36	0.07	0.506	0.526	28
0	38	0.10	0.5	0.52	26
0	40	0.13	0.494	0.514	25
0	42	0.17	0.489	0.509	24
0	45	0.22	0.482	0.502	22
0	48	0.27	0.473	0.493	20
0	51	0.32	0.467	0.487	18
0	55	0.38	0.457	0.477	16
1	0	0.47	0.446	0.466	13
1	5	0.55	0.437	0.457	11
1	10	0.63	0.428	0.448	9
1	15	0.72	0.422	0.442	7
1	26	0.90	0.413	0.433	5
1	40	1.13	0.411	0.431	5
2	30	1.97	0.408	0.428	4
3	57	3.42	0.404	0.424	3
9	20	8.80	0.401	0.421	2
29	10	28.63	0.4	0.42	2

continued

TableA-5 : Desorption Rate Data, H+ Form (continued) p.2
Sample B#2, 54%RH

hour	min	Total time (hours)	wt. (g)	corr.wt. including tare(g)	water wt%
0	59	0.00	0.515	0.535	30
1	0	0.02	0.519	0.539	31
1	1	0.03	0.517	0.537	30
1	2	0.05	0.515	0.535	30
1	4	0.08	0.51	0.53	29
1	7	0.13	0.507	0.527	28
1	10	0.18	0.493	0.513	25
1	12	0.22	0.484	0.504	22
1	15	0.27	0.475	0.495	20
1	19	0.33	0.47	0.49	19
1	26	0.45	0.453	0.473	15
1	30	0.52	0.445	0.465	13
1	35	0.60	0.438	0.458	11
1	45	0.77	0.429	0.449	9
2	1	1.03	0.424	0.444	8
2	58	1.98	0.412	0.432	5
3	55	2.93	0.41	0.43	4
5	10	4.18	0.411	0.431	5
6	4	5.08	0.411	0.431	5
7	6	6.12	0.411	0.431	5
27	0	26.02	0.411	0.431	5

(continued)

Table A-5: Desorption Rate Data, H+ Form (continued) p.3
Sample B#1, 75%RH

hour	min	Total time (hours)	wt. (g)	corr.wt. including tare(g)	water wt%
0	56	0.00	0.391	0.411	33
0	57	0.02	0.391	0.411	33
0	58	0.03	0.389	0.409	33
1	0	0.07	0.386	0.406	32
1	3	0.12	0.381	0.401	30
1	7	0.18	0.376	0.396	29
1	11	0.25	0.37	0.39	27
1	17	0.35	0.363	0.383	24
1	24	0.47	0.356	0.376	22
1	34	0.63	0.346	0.366	19
1	40	0.73	0.341	0.361	17
1	47	0.85	0.336	0.356	16
1	58	1.03	0.33	0.35	14
2	7	1.18	0.326	0.346	12
2	33	1.62	0.32	0.34	10
2	45	1.82	0.318	0.338	10
3	40	2.73	0.316	0.336	9
4	54	3.97	0.316	0.336	9
7	45	6.82	0.316	0.336	9
24	15	23.32	0.316	0.336	9
28	25	27.48	0.316	0.336	9

(continued)

Table A-5: Desorption Rate Data, H+ Form (continued) p.4
Sample B#2: 85%RH

hour	min	Total time (hours)	wt. (g)	corr.wt. including tare(g)	water wt%
0	48	0.00	0.525	0.545	32
0	49	0.02	0.52	0.54	31
0	50	0.03	0.519	0.539	31
0	51	0.05	0.518	0.538	31
0	53	0.08	0.515	0.535	30
0	55	0.12	0.513	0.533	29
1	1	0.22	0.508	0.528	28
1	10	0.37	0.5	0.52	26
1	25	0.62	0.49	0.51	24
1	40	0.87	0.48	0.5	21
1	55	1.12	0.472	0.492	19
2	18	1.50	0.461	0.481	17
2	45	1.95	0.451	0.471	14
3	13	2.42	0.444	0.464	13
4	1	3.22	0.438	0.458	11
5	0	4.20	0.435	0.455	10
7	27	6.65	0.434	0.454	10
10	11	9.38	0.436	0.456	11
24	2	23.23	0.435	0.455	10

(continued)

Table A-5: Absorption Rate Data, H+ Form (continued) p.5
Sample B#2, 85%RH to 100%RH

hour	min	Total time (hours)	wt. (g)	corr.wt. including tare(g)	water wt%
0	37	0.00	0.439	0.459	11
0	40	0.05	0.44	0.46	12
0	50	0.22	0.441	0.461	12
1	0	0.38	0.443	0.463	12
1	10	0.55	0.444	0.464	13
1	20	0.72	0.445	0.465	13
1	35	0.97	0.446	0.466	13
1	50	1.22	0.447	0.467	13
2	10	1.55	0.448	0.468	14
4	0	3.38	0.45	0.47	14
4	45	4.13	0.451	0.471	14
6	0	5.38	0.453	0.473	15
21	55	21.30	0.48	0.5	21
27	9	26.53	0.474	0.494	20

(continued)

Table A-5: Desorption Rate Data, H+ Form (continued) p.6
Sample B#1: 93.3%RH

hour	min	Total time (hours)	wt. (g)	corr.wt. including tare(g)	water wt%
0	17	0.00	0.403	0.4179	36
0	20	0.05	0.392	0.407	32
0	25	0.13	0.39	0.405	31
0	30	0.22	0.388	0.403	31
0	35	0.30	0.387	0.402	30
0	40	0.38	0.384	0.399	30
0	45	0.47	0.383	0.398	29
0	55	0.63	0.381	0.396	29
1	5	0.80	0.378	0.393	28
1	11	0.90	0.376	0.391	27
1	20	1.05	0.374	0.389	26
1	32	1.25	0.371	0.386	25
1	43	1.43	0.368	0.383	24
1	50	1.55	0.366	0.381	24
2	0	1.72	0.364	0.379	23
2	10	1.88	0.361	0.376	22
2	20	2.05	0.359	0.374	21
2	31	2.23	0.356	0.371	20
2	40	2.38	0.355	0.37	20
2	52	2.58	0.353	0.368	19
3	0	2.72	0.351	0.366	19
3	15	2.97	0.349	0.364	18
3	33	3.27	0.347	0.362	17
3	45	3.47	0.345	0.36	17
4	10	3.88	0.343	0.358	16
4	37	4.33	0.34	0.355	15
5	12	4.92	0.338	0.353	15
6	0	5.72	0.336	0.351	14
6	50	6.55	0.335	0.35	14
22	0	21.72	0.333	0.348	13
23	20	23.05	0.333	0.348	13
24	10	23.88	0.333	0.348	13
25	30	25.22	0.332	0.347	13
26	40	26.38	0.332	0.347	13

(continued)

Table A-5: Desorption Rate Data, H+ Form (continued) p.7
Sample B#2: 93.3%RH

hour	min	Total time (hours)	wt. (g)	corr.wt. including tare(g)	water wt%
0	13	0.00	0.545	0.545	32
0	15	0.03	0.54	0.54	31
0	16	0.05	0.54	0.54	31
0	20	0.12	0.538	0.538	31
0	26	0.22	0.537	0.537	30
0	30	0.28	0.537	0.537	30
0	35	0.37	0.528	0.528	28
0	40	0.45	0.526	0.526	28
0	45	0.53	0.525	0.525	27
0	50	0.62	0.523	0.523	27
1	0	0.78	0.519	0.519	26
1	6	0.88	0.517	0.517	25
1	10	0.95	0.516	0.516	25
1	20	1.12	0.514	0.514	25
1	48	1.58	0.504	0.504	22
1	58	1.75	0.501	0.501	22
2	4	1.85	0.5	0.5	21
2	15	2.03	0.5	0.5	21
2	29	2.27	0.494	0.494	20
2	37	2.40	0.492	0.492	19
2	52	2.65	0.491	0.491	19
3	5	2.87	0.488	0.488	18
6	33	6.33	0.473	0.473	15
18	50	18.62	0.469	0.469	14
20	5	19.87	0.468	0.468	14
21	35	21.37	0.466	0.466	13
23	50	23.62	0.462	0.462	12
26	22	26.15	0.459	0.459	11

(continued)

Table A-5: Desorption Rate Data, H+ Form (continued) p.8
Sample B#1, 100%RH

hour	min	Total time (hours)	wt. (g)	corr.wt. including tare(g)	water wt%
0	9	0.00	0.402	0.422	37
0	11	0.03	0.401	0.421	37
0	12	0.05	0.4	0.42	36
0	33	0.40	0.404	0.424	38
1	33	1.40	0.403	0.423	37
2	42	2.55	0.378	0.398	29
6	40	6.52	0.365	0.385	25
10	33	10.40	0.359	0.379	23
48	12	48.05	0.35	0.37	20
50	39	50.50	0.354	0.374	21

Appendix B.

Acid Titrations

Acid titration was used to analyze the content of EDA in the membranes and the EDA content in a carbonated solution. For the first case, the analysis consisted of leaching the membrane in 25 mL of distilled water, removing the membrane after the solution reached equilibrium and titrating the remaining solution with a known concentration of HCl to the equivalence point as determined with a pH probe/meter.

The chemistry involved in the analysis is given by:

$$H_2N\text{-}\ C_2H_4\text{-}\ NH_2 + HCl \rightarrow {}^{+}H_3N\text{-}\ C_2H_4\text{-}\ NH_2{}^{+} + Cl^{-}$$

$${}^{+}H_3N\text{-}\ C_2H_4\text{-}\ NH_2 + HCl \rightarrow {}^{+}H_3N\text{-}\ C_2H_4\text{-}\ NH_3{}^{+} + Cl^{-}$$

The second acidification occurs at a pH of about 4. The amount of EDA titrated at the equivalence point is given by:

$$\text{EDA (gmol)} = \frac{[\text{ x(ml) titrant} * \text{y(ml) N HCl}]*[1 \text{ mole EDA}]}{1000*[2 \text{ mole acid}]}$$

The amount of EDA in the membrane was determined by adding the amount of EDA which remained in the membrane to the amount leached. The amount remaining in the membrane was determined from an experimental determination of the amount of EDA in a membrane equilibrated from the H^+ form into a known amount of EDA at the same final solution concentration. The same solution analysis procedure as described for the leached solution was used to determine the amount of EDA in the membrane.

For the second case, acid titration was performed on a concentrated solution of 10 mL of EDA which had been sparged with 1atm CO_2 for several days. The solution was titrated with a known concentration of NaOH to the equivalence point as determined with a pH probe.

The chemistry involved in the analysis is given by:

$$^{+}H_3N\text{-}\ C_2H_4\text{-}\ NHCOO^{-} + HCl \rightarrow {}^{+}H_3N\text{-}\ C_2H_4\text{-}\ NH_2 + CO_2$$

$$^{+}H_3N\text{-}\ C_2H_4\text{-}\ NH_2 + HCl \rightarrow {}^{+}H_3N\text{-}\ C_2H_4\text{-}\ NH_3^{+} + Cl^{-}$$

The second reaction occurs at a pH of about 4. The amount od EDA titrated at the equivalence point is given by:

$$\text{EDA (gmol)} = \frac{[\text{a (ml) titrant} * \text{b (ml) N HCl}] * [1 \text{ mole EDA}]}{1000 * [2 \text{ mole acid}]}$$

Appendix C.

Cell Design

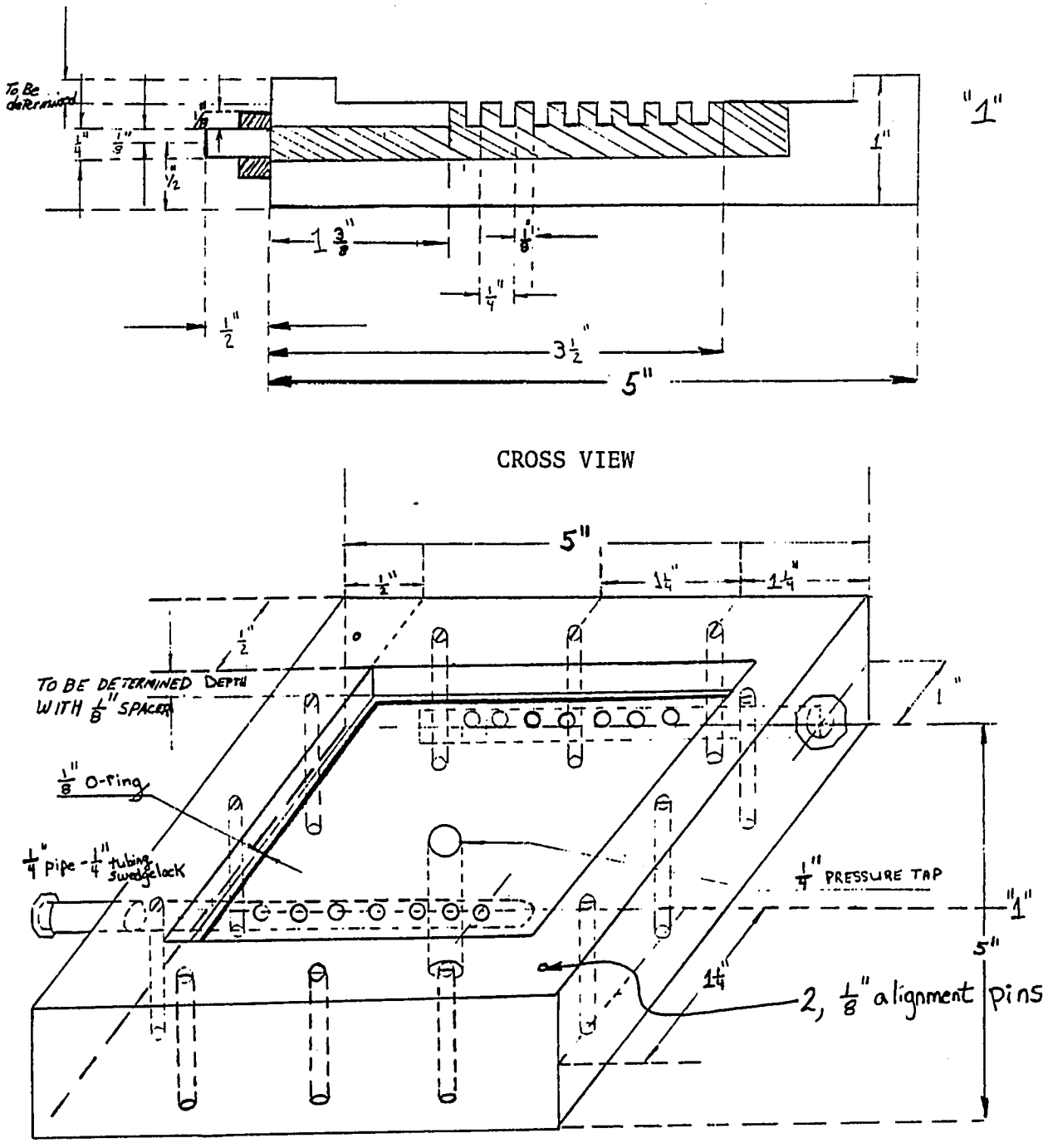

Figure C-1: Top View of Permeation Cell and Dimensions

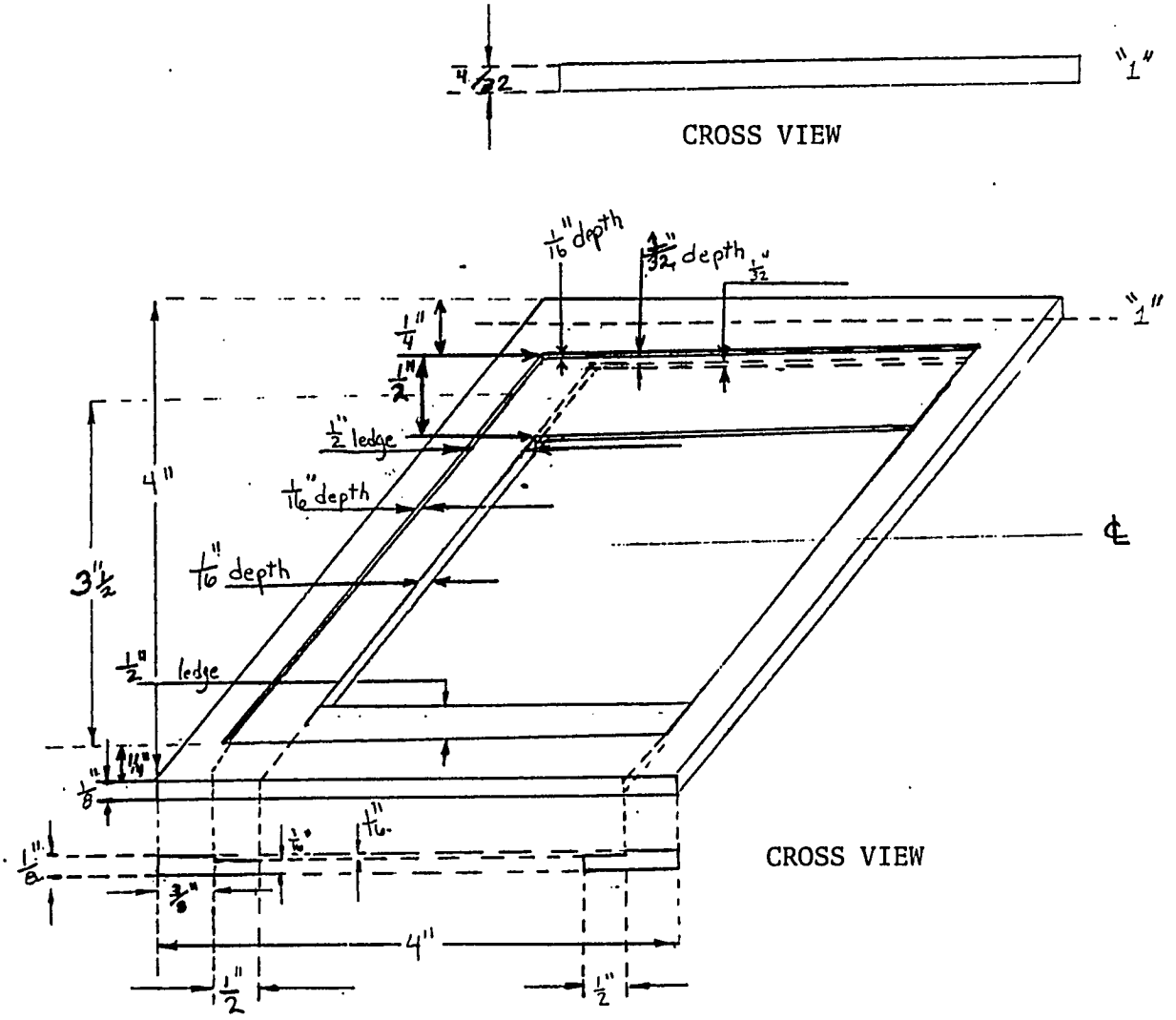

Figure C-2: Schematic of Spacer and Dimensions

Appendix D.

Sample Calculations

The following calculations were performed for the run at 100% relative humidity with 0.928 gmol EDA/gmol site, 0.005 atm CO_2 feed pressure and 100 std cm^3/ min sweep gas flowrate. The same procedure for calculations were performed for each run.

D.1 $$\text{Flux} = \frac{(\%\ CO_2)\ \text{sweep} * (\text{Flowrate std } cm^3/\text{min})\ \text{sweep}}{A\ (cm^2) \quad * \quad (60\ \text{s/min})}$$

$$= \frac{(0.0442\%) * (100\ \text{std } cm^3/\text{min})}{31.99\ cm^2 * 60\ \text{s/min}}$$

$$\text{Flux} = 2.303 * 10^{-5}\ \text{std } cm^3/\text{s-}cm^2$$

D.2 $$\text{Permeability} = \frac{NL}{\Delta P}$$

$$= \frac{(2.303 * 10^{-5}\ \text{std } cm^3/\text{s-}cm^2) * (0.0198\ \text{cm}) * 10^{10}}{[0.005 - (0.000442/2)] * 73.4\ \text{cm Hg}^*}$$

where 10^{10} is a conversion factor from std cm^3-cm/(s-cm^2-cm Hg) to barrers and * refers to 100% relative humidity, p_{H2O} = 2.6 cm Hg

Permeability = 13,400 barrers

D.3 $$\text{Diffusion Coefficient} = \frac{L^2}{7.199 * t_{1/2}}$$

$$= \frac{(0.0204\ \text{cm})^2}{7.199 * (17.05\ \text{min}) * (60\text{s/min})}$$

$$D = 0.0565^* * 10^{-6}\ cm^2/s$$

D.4 $$CO_2\ \text{Solubility} = \frac{P}{D}$$

$$= \frac{1.3380^* * 10^{-6}\ \text{std } cm^3\text{-cm}/cm^2\text{-s-cm Hg}}{0.0565^* * 10^{-6}\ cm^2/s}$$

$$CO_2\ \text{Solubility} = 23.7 \frac{\text{std } cm^3}{cm^3\text{-cm Hg}}$$

D.5 Stoichiometry , $X_{total} = \frac{P^*(p_2)^* EW}{D^* \rho_p * V_{ID} L_m}$

$$= \frac{1.3400^* 10^{-6} \frac{\text{std cm}^3\text{-cm}}{\text{cm}^2\text{-s- cmHg}} * (0.005)^*(73.4 \text{ cm Hg})^*(1100 \frac{\text{g}}{\text{gmolsite}})}{0.0565 * 10^{-6} \frac{\text{cm}^2}{\text{s}} * (1.9 \frac{\text{g}}{\text{cm}^3})^*(\frac{22400 \text{ std cm}^3}{\text{gmol CO}_2})^*(0.928 \frac{\text{gmol EDA}}{\text{gmol site}})}$$

$$= 0.25 \frac{\text{gmol CO2}}{\text{gmol EDA}}$$

D.6 Equilibrium Constant, $Keq_2 = \frac{X_r^2}{pCO2.2^*(1-2X_r)^2}$

where Xr = X total - X physical

$$= \frac{[0.25 \frac{\text{gmol CO2}}{\text{gmol EDA}} - (\frac{0.005 \text{ atm}}{49 \text{ L-atm/gmol}})^*\frac{0.06 \text{ L EDA}}{\text{gmol EDA}}]\ 2}{(0.005 \text{ atm})^*[1-2(0.25 \frac{\text{gmol CO2}}{\text{gmol EDA}} - (\frac{0.005 \text{ atm}}{49 \text{ L-atm/gmol}})^*\frac{0.06 \text{ L EDA}}{\text{gmol EDA}})]\ 2}$$

$Keq_2 = 50 \text{ atm}^{-1}$

D.7 Equilibrium Constant, Keq_1, for 0.03 atm CO_2, X total = $0.47 \frac{\text{gmol CO2}}{\text{gmol EDA}}$,

$$Xr = 0.47 \frac{\text{gmol CO2}}{\text{gmol EDA}}$$

$$Keq_2 = \frac{X_r * (X_r - e_1)}{(pCO2.2)^*[0.66-2(X_r-e_1)]^2}$$

$$50 = \frac{0.47 \frac{\text{gmol CO2}}{\text{gmol EDA}} * (0.47 \frac{\text{gmol CO2}}{\text{gmol EDA}} - e_1)}{(0.03 \text{ atm})^*[0.66 \frac{\text{gmol CO2}}{\text{gmol EDA}} - 2^*(0.47 - e_1) \frac{\text{gmol CO2}}{\text{gmol EDA}}]^2}$$

1. (+SQRT) $e_1 = 0.266 \frac{\text{gmol CO2}}{\text{gmol EDA}}$ $\quad e_2^* = 0.204 \frac{\text{gmol CO2}}{\text{gmol EDA}}$

2. (-SQRT) $e_1 = -0.065 \frac{\text{gmol CO2}}{\text{gmol EDA}}$ $\quad e_2^* = 0.535 \frac{\text{gmol CO2}}{\text{gmol EDA}}$

*$e_2 = 0.47 - e_1$

1. is correct since 0.66 - 2 e_2 must be positive.

$$Keq_1 = \frac{X_r}{(pCO2.2)^*(0.34 - e_1)}$$

$$= \frac{0.47 \frac{\text{gmol CO2}}{\text{gmol EDA}}}{(0.03 \text{ atm})^*(0.34 - 0.266) \frac{\text{gmol CO2}}{\text{gmol EDA}}}$$

$Keq_1 = 245 \text{ atm}^{-1}$

Appendix E.

Error Analysis and Equipment Calibration

The permeation results were presented as flux, permeability, diffusion coefficient, CO_2 solubility and stoichiometry. The main uncertainties involved in these calculations are the gas flow rate, the CO_2 concentration in the sweep stream, the membrane area of permeation, the half time and the membrane EDA content. The gas flowrate was measured with 0.1% precision and 0.5% accuracy by electronic mass flow controllers/meters (Brooks) calibrated with nitrogen and a soap film meter. The CO_2 concentration was measured with 0.1% precision and 2% accuracy using an infrared absorption CO_2 analyzer calibrated weekly with a CO_2/N_2 standard gas ($\pm$1%). The membrane area was measured with 0.5% precision and 2% accuracy with a ruler marked in 0.1 cm divisions. The half time was measured with 0.2% precision and 1% accuracy using a variable speed chart recorder which was calibrated for speed accuracy and reproducibility to within 0.1%. The EDA content was measured with 1% precision and 2% accuracy by solution analysis with acid titration. The following accuracies are calculated: flux, $\pm$2.5%; permeability, $\pm$4%; diffusion coefficient, $\pm$0.5%; solubility, $\pm$4.5% and stoichiometry, $\pm$5%.

The performance of the membrane is a strong function of relative humidity. Relative humidity was controlled by sparging the gases through saturated salt solutions with liquid height at least $4\frac{1}{2}$". The relative humidity was measured with a precision of 1% and an accuracy of 2% using a capacitance type probe (Vaisala). The probes were calibrated every month with standard salt solutions, for at least six relative humidities.

During actual operation of the apparatus, when multiple experiments at identical conditions were performed, the deviation from the average was below ±6%. The maximum deviation between experiments was below 12%.

Glossary

A = membrane permeation area, cm^2

C_1 = steady state sweep gas CO_2 concentration, mol%

C_2 = feed gas CO_2 concentration, mol%

C_m = "effective" EDA concentration in the membrane, gmol/Liter water

C_s = solution EDA concentration, gmol/L

D = "effective" diffusion coefficient, cm^2/s

EDA_m = EDA in the membrane, gmol

EW = equivalent weight, g dry membrane/gmol exchange sites

IEC = ion exchange capacity, milliequivalents/g dry membrane

L = "effective" membrane thickness, cm

L_m = membrane loading, gmol EDA/gmol ion exchange sites

Δm = water gain of the membrane from the dry state, g

N = flux of CO_2, $cm^3/s\text{-}cm^2$ (standard conditions)

p_1 = upstream partial pressure of CO_2, cm Hg

p_2 = downstream partial pressure of CO_2, cm Hg

P = membrane permeability, barrers (1 barrer=10^{-10} cm^3-cm/s-cm^2-Δcm Hg)

Q_s = volumetric flowrate of the sweep gas, cm^3/s (standard conditions)

S = CO_2 solubility in the membrane, cm^3 (gas)/cm^3 dry membrane-cm Hg

S_{EDA} = normalized CO_2 solubility per gmol of EDA in the membrane, gmol/gmol EDA

S_{site} = normalized CO_2 solubility per ion exchange site in the membrane, gmol/gmol site

$t_{1/2}$ = half-time, s

ΔV = volume change of the membrane from the dry state, cm^3

V_{ID} = molar volume of CO_2, cm^3/gmol (standard conditions)

W_p = weight of dry membrane in H^+ form, g

Greek Letters

ρ_p = density of the dry membrane, g/cm^3

ρ_w = density of water, g/cm^3

Bibliography

Anon., "Membranes Simplify Catalytic Reactions," *Chem. and Eng. News*, 58, (July 28, 1980).

Astarita, G., D. W. Savage and A. Bisio, *Gas Treating with Chemical Solvents*, New York : John Wiley & Sons. Inc., 1983.

Astarita, G., G. Marrucci and F. Gioia, "The influence of carbonation ratio and total amine concentration on carbon dioxide absorption in aqueous monoethanolamine solutions," *Chem. Eng. Sci.*, 19, 95 (1964).

Bolz, R. E. and G. L. Tuve, eds., *Handbook of Tables for Applied Engineering Science*, 2nd Ed., Cleveland: The Chemical Rubber Co., 1973.

Brunauer, S., *The Adsorption of Gases and Vapors. Vol. I. Physical Adsorption*, Princeton: Princeton University Press, 1943.

Chern, R. T., W. J. Koros, H. B. Hopfenberg and V. T. Stannett, "Material Selection For Membrane-Based Gas Separations," *Polym. Mater. Sci. Eng.*, 50, 88 (1984).

Chowdhury, J., "Membranes Set to Tackle Larger Separation Tasks," *Chemical Engineering*, 94 (13), 14 (1987).

Cooley, T. E. and W. L. Dethloff, "Field Tests Show Membrane Processing Attractive," *Chem. Eng. Prog.*, 81 (10), 45 (1985).

Crank, J. and G. S. Park (eds.), *Diffusion in Polymers*, New York: Academic Press, 1968.

Danckwerts, P. V., *Gas-Liquid Reactions*, San Francisco, CA: McGraw-Hill Book Company, 1970.

Despic, A. and G. J. Hills, "Electrochemical Properties of Ion Exchange Resins (II) Ionic Conductance In Cross-Linked Polymethacrylic Acid," *Trans. Faraday Soc.*, 51, 1260 (1955).

Despic, A., "Ionic Self-Diffusion Coefficients in Ion Exchange Resins," *Trans. Faraday Soc.*, 53, 1262 (1957).

Donaldson, T. L. and Y. N. Nguyen, "Carbon Dioxide Reaction Kinetics and Transport in Aqueous Amine Membranes," *Ind. Eng. Chem. Fundam.*, 19, 260 (1980).

Donaldson, T. L., and J. A. Quinn, "Carbon Dioxide Transport Through Enzymatically Active Synthetic Membranes," *Chem. Engr. Sci.*, 30, 103 (1975).

Emmert, R. E. and R. C. Pigford, "Gas Absorption Accompanied by Chemical Reaction: A Study of the Absorption of Carbon Dioxide in Aqueous Solutions of Monoethanolamine," *AIChE J.*, 8, 171 (1962).

Enns, T., "Facilitation by Carbonic Anhydrase of Carbon Dioxide Transport," *Science*, 155, 44 (1967).

Escoubes, M. and M. Pineri, "Thermodynamic Studies of the Water-Perfluorosulfonated Polymer Interactions: Experimental Results," *Perfluorinated Ionomer Membranes*, ACS Symposium Series 180, 2, A. Eisenberg and H. L. Yeager, eds., Washington, D.C.: ACS, 1982.

Falk, M., "Infrared Spectra of Perfluorosulfonated Polymer and of Water in Perfluorosulfonated Polymer," *Perfluorinated Ionomer Membranes*, ACS Symposium Series 180, 8, A. Eisenberg and H. L. Yeager, eds., Washington, D.C.: American Chemical Society, 1982.

Gierke, T. D. and W. Y. Hsu, "The Cluster Network Model of Ion Clustering in Perfluorosulfonated Membranes," *Perfluorinated Ionomer Membranes*, ACS Symposium Series 180, 13, A. Eisenberg and H.L. Yeager, eds., Washington, D.C.: American Chemical Society, 1982.

Gierke, T. D., G. E. Munn and F. C. Wilson, "The Morphology in Nafion Perfluorinated Membrane Products, As Determined by Wide- and Small-Angle X-Ray Studies," *J. Polym. Sci., Polym. Phys. Ed.*, 19 (11), 1687 (1981).

Grey, N. R. and W. H. Mazur, "Membrane Separation of CO_2 and H_2S From Natural Gas-Field Experience," Paper 9d, 1984 AIChE Spring National Meeting, Anaheim, CA, May 20-23, 1984.

Grot, W. G. F., "Perfluorinated Cation Exchange Polymers," *Chemie-Ing.-Techn.*, 47, 617 (1975).

Grot, W. G. F., "Perfluorinated Ion Exchange Membranes of High Chemical and Thermal Stability," *Chem. Ing. Tech.*, 44, 167 (1972).

Hashimoto, T., M. Fujimara and H. Kawai, "Structure of Sulfonated and Carboxylated Perfluorinated Ionomer Membranes: Small-Angle and Wide-Angle X-Ray Scattering and Light Scattering," *Perfluorinated Ionomer Membranes*, ACS Symposium Series 180, 11, A. Eisenberg and H. L. Yeager, eds., Washington, D.C.: ACS, 1982.

Hikita, H., Ishikawa, H., Murakami, T., and Ishii, T., "Densities, Viscosities and Amine Diffusivities of Aqueous MIPA, DIPA, DGA and EDA Solutions," *J. of Chem. Eng. of Japan,* 14 (5), 411 (1981).

Jeffreys, G. V. and A. F. Bull, "Effect of Glycine Additive on the Rate of Absorption of CO_2 in Na_2CO_3 Solutions," *Trans. Inst. Chem. Engrs.*, 42 (3), T118 (1964).

Jensen, A., and R. Christensen, "Studies on Carbamates. XI: The Carbamate of Ethylenediamine," *Acta Chemica Scand.*, 9, 486 (1955).

Kawami, M. Y. Yamashita, M. Yamasaki, M. Iwamoto and S. Kagawa, "Effects of Dissolved Inorganic Salts on Gas Permeabilities of Immobilized Liquid Polyethylene glycol Membranes," *J. Polym. Sci. Polym. Lett. Ed.*, 20, 251 (1982).

Kimura, S. G., "Membrane CO_2 Scrubbing of Sewage Digester Gas," *Report No. 332CRD002,* General Electric Company, Schenectady, New York, 1982.

Kimura, S. G., S. L. Matson, and W. J. Ward III, "Industrial Applications of Facilitated Transport," *Recent Developments in Separation Science*, N. N. Li (ed.), Cleveland, Ohio: CRC Press, 1979.

King, C. J., "Recovery of Polar Organics from Aqueous Solution by Regenerable Adsorption Processes," Louis T. Pirkey Centennial Lecture, The University of Texas at Austin, February 10, 1988.

Komoroski, R.A., and K.A. Mauritz, "Nuclear Magnetic Resonance Studies and the Theory of Ion Pairing in Perfluorosulfonate Ionomers," *Perfluorinated Ionomer Membranes,* ACS Symposium Series 180, 7, A. Eisenberg and H.L. Yeager, eds., Washington, D.C.: ACS, 1982.

Lagos, A. E. and J. A. Kitchener, "Diffusion in Poly(styrenesulfonic acid) Ion Exchange Resins," *Trans. Faraday Soc.*, 56, 1245 (1960).

LeBlanc, Oliver H., Jr., W. J. Ward, S. L. Matson and S. G. Kimura, "Facilitated Transport in Ion Exchange Membranes," *J. Membr. Sci.*, 6, 339 (1980).

Leiber, C. M. and N. S. Lewis, "Probing Polymer Effects on Chemical Reactivity: Ligand Substitution Kinetics of $Ru(NH_3)_5(H_2O)^{2+}$ in Nafion Films," *J. Am. Chem. Soc.*, 107, 7190 (1985).

Matson, S. L., J. Lopez and J. A. Quinn, "Review Article Number 13. Separation of Gases with Synthetic Membranes," *Chem. Eng. Sci.*, 38, 503 (1983).

Matson, S. L., C. S. Herrick, and W. J. Ward, III., "Progress on the Selective Removal of H_2S from Gasified Coal Using an Immobilized Liquid Membrane," *Ind. Eng. Chem., Process Des. Dev.*,16 , 370 (1977).

Meares, P., "Transport in Ion Exchange Polymers," *Diffusion in Polymers*, 10, J. Crank and G. S. Park, eds., New York: Academic Press, 1968.

Meldon, J. H., K. A. Smith and C. K. Colton, "The Effect of Weak Acids Upon the Transport of Carbon Dioxide in Alkaline Solutions," *Chem. Eng. Sci.*, 32, 939 (1977).

Meldon, J. H., P. Stroeve, and C. K. Gregoire, "Facilitated Transport of Carbon Dioxide: A Review ," *Chem. Eng. Commun.*, 16 (1-6), 263 (1982).

Meldon, J. H., Paboojian, A. and G. Rajangam, "Selective Carbon Dioxide Permeation in Immobilized Liquid Membranes," *AIChE Symp. Ser.*, 82 (248), 114 (1986).

Miller, B. D., R. Richards and M. E. Schott, "Separex System Makes Hydrocarbon Recovery Feasible," *Energy Progress*, 5 (1), 25 (1985).

Moy, P. and F. E. Karasz, "Epoxy-Water Interactions," *Polym. Eng. Sci.*, 20(4), 315 (1980).

Onda, K., T. Kobayashi and T. Nagase, "Rate of Absorption of Carbon Dioxide by Sodium Carbonate Solutions Containing Amino Acids or Arsenious Acid," *International Chemical Engineering*, 8, 520-526 (1968).

Otto, N. C. and J. A. Quinn, "The Facilitated Transport of Carbon Dioxide through Bicarbonate Solutions," *Chemical Engineering Science*, 26, 949 (1971).

Parro, D. and B. Hamaker, "CO_2 Hydrocarbon Membrane Separation Systems from Laboratory to Commercial Success," *Paper 42b*, AIChE Spring Nat. Meet., Houston (Mar., 1985).

Paul, D. R. and J. S. Chiou, Interdepartmental communication, The University of Texas at Austin, 1987, to be published.

Perry, R. H. and C. H. Chilton, eds., *Chemical Engineer's Handbook*, 5th. N. Y.: McGraw Hill, 1973.

Sakai, T., H. Takenaka and E. Torikai, "Gas Diffusion in the Dried and Hydrated Nafions," *J. Electrochem. Soc.: Electrochemical Science and Technology*, 133, 88 (1986).

Sakai, T., H. Takenaka, N. Wakabayashi, Y. Kawami and E. Torikai, "Gas Permeation Properties of Solid Polymer Electrolyte (SPE) Membranes," *J. Electrochem. Soc.: Electrochemical Science and Technology*, 132, 1328 (1985).

Sata, T., K. Motani and Y. Ohashi, "Perfluorinated Ion Exchange Membrane, Neosepta-F and its Properties," *Ion Exchange Membranes,* 9, D. S. Flett, ed., Chinchester, London: Ellis Horwood Limited, 1983.

Schell, W. J., "Commercial Applications for Gas Permeation Membrane Systems," *J. Membr. Sci.*, 22, 217 (1985).

Schendel, R. L., "Using Membranes For The Separation of Acid Gases and Hydrocarbons," *Chem. Eng.. Progress*, 80(5), 39 (1984).

Schmelzer, J. and K. Quitzsch, "Isobare Flussigkeit-Dampfgleichgewichte der Binaren Systeme Benzol-Athylendiamin und Wasser-Athylendiamin," *Z. Phys. Chemie, Leipzig*, 252, 280 (1973).

Scholander, P. F., "Oxygen Transport Through Hemoglobin Solutions," *Science*, 131, 585 (1960).

Sharma, M. M., and P. V. Danckwerts, "Catalysis by Bronsted Bases of the Reaction between CO_2 and Water," *Trans. Faraday Soc.*, 59, 386 (1963).

Sondheimer, S.J., N.J. Bunce, and C.A. Fyfe, "Structure and Chemistry of Nafion-H: A Fluorinated Sulfonic Acid Polymer," *JMS-Rev. Macromol. Chem. Phys.*, C26-(3), 353 (1986).

Stookey, D.J., T.E. Graham, "Natural Gas Processing with Prism Separators," *Acid and Sour Gas Treating Processes,* 20, S.A. Newman, (ed.), Houston, Texas: Gulf Publishing Co. Book Division, 1985.

Swick, R. W., D. L. Buchanan and A. Nakao, "Ethylenediamine A Carbonate-Free Alkali For Carbon Dioxide Absorption," *Anal. Chem.*, 24, 2000 (1954).

Ward, W. J., III., and C. K. Neulander, "Immobilized Liquid Membranes For Sulfur Dioxide Separation," *U. S. Govt. Res. Develop. Rep.*, 70 (14), 59 (1970).

Ward, W. J., III., "Immobilized Liquid Membranes," *Recent Developments in Separation Science*, 1, N. N. Li (ed.), Cleveland, Ohio: CRC Press, 1972.

Ward, W. J., III., and W. L. Robb, "Carbon Dioxide-Oxygen Separation: Facilitated Transport of Carbon Dioxide Across a Liquid Film," *Science*, 156, 1481 (1967).

Way, J. D., Noble, R. D. Noble and L. A. Powers, "Gas Separation Using Ion Exchange Membranes," U. S. Department of Energy, Office of Fossil Energy, Report under Contract No. DE-AI21-84MC21271, May 1986.

Way, J. D., R. D. Noble, D. L. Reed and G. M. Ginley, "Facilitated Transport of CO_2 in Ion Exchange Membranes," *AIChE J.*, 33 (3), 480 (1987).

Weast, R. C., ed., *CRC Handbook of Chemistry and Physics*, 60th. Boca Raton, Florida: CRC Press, Inc., 1974.

Weiland, R. H. and O. Trass, "Absorption of Carbon Dioxide in Ethylenediamine Solutions. I: Absorption Kinetics and Equilibrium," *Can. J. Chem. Eng.*, 49, 767 (1971).

Wittenburg, J. B., "The Molecular Mechanism of Hemoglobin-facilitated Oxygen Diffusion," *J. Biol. Chem.*, 241, 104 (1966).

Yeager, H. L, "Transport Properties of Perfluorosulfonate Polymer Membranes," *Perfluorinated Ionomer Membranes*, ACS Symposium Series 180, 4, A. Eisenberg and H.L. Yeager, eds., Washington, D.C.: ACS, 1982.

Ziegel, K. D., H. K. Frensdorff and D. E. Blair, "Measurement of Hydrogen Isotope Transport in Poly(vinylfluoride) Films by the Permeation Rate Method," *J. Polym. Sci.*, Part A-2, 7, 809 (1969).

VITA

Terry Dunkley-Timmerman was born on February 5, 1959 in San Antonio, Texas, the daughter of Mary Louise Dunkley and John Daniel Dunkley, Jr. She graduated as Valedictorian of her class at Robert E. Lee High School in 1977. During the fall of 1977 and the spring of 1978, she attended Trinity University in San Antonio with a full tuition scholarship. She entered the University of Texas at Austin in the fall of 1978. During the summer of 1979, spring of 1980 and summer of 1981, she worked as a cooperative education student with IBM, Burlington, Vt. and IBM, Tucson, Az. She received the degree of Bachelor of Science in Chemical Engineering from the University of Texas in December of 1981. In January of 1982, she joined Exxon Production Company in Houston, Texas, where she worked as a project engineer until December of 1983. In January of 1984, she entered the Graduate School of The University of Texas. The primary sponsor of her research was the Separations Research Program. She married Scott Edward Timmerman in June of 1987.

Permanent Address: 2000 Whitis, Apt. 201
Austin, Texas 78705

This dissertation was typed by the author and Judith Searcy.